0. Introduction to lectures 1–4

Please read this introduction before the start of the summer school.

It would also be very helpful if you would read through and familiarize yourself with the contents of section 1.1 (Lecture 1) before the start of the lectures.

0.1 General outline

These written notes which accompany the lectures are quite detailed and comprehensive. In the lectures, there will not be time to go over all the topics which are described in the notes. Rather, we will go slowly through the key ideas and the most important points. Later, after the summer school, you may wish to study the notes in greater detail and look at those parts we will not have time to go through.

The lectures will follow the notes closely and I recommend most strongly that during the lectures you do not take any notes, but listen and follow the presentation. The lecture notes provided here are so comprehensive that you will not really miss anything by not taking notes.

There will be exercise classes following the lectures, and I hope that by working through the problems you will deepen your understanding. Again, there may not be time to work through all the exercises.

0.2 Scheme of the lectures

Lecture 2 Product Operators will be given first. It sets out a straightforward theory which is well suited to analysing multiple-pulse NMR experiments, and which will be used in the other lectures. Although this theory has a sound base in quantum mechanics, it is quite easy to use as much of it can be interpreted geometrically.

Lecture 3 Basic concepts for two-dimensional NMR will be given next. In this lecture, the key ideas behind two-dimensional NMR will be introduced, and several important experiments will be analysed using the product operator approach introduced in lecture 1.

Lecture 1 Introduction to quantum mechanics introduces the theory which is used to describe NMR experiments and from which the product operator approach is developed. All of the basic ideas in quantum mechanics are introduced, but these are developed in relation to NMR rather than using the examples most commonly found in books about elementary quantum mechanics.

Finally, Lecture 4 Coherence selection: phase cycling and gradient pulses describes a very practical part of multiple-pulse NMR, which is how to select the signals we want and reject those we do not. Two methods – phase cycling and gradient pulses – are described in theory and many examples will be given of how to devise and analyse coherence selection schemes.

0.3 General matters

Lectures 1 and 2 have been prepared specially for this summer school. The first half of Lecture 3 is based in part of a third-year undergraduate course NMR Spectroscopy which I gave in Cambridge in association with Dr Melinda Duer; I thank her for invaluable advice and assistance . Lecture 4 was prepared for the EMBO sponsored course held in Turin, Italy, in 1995. The section on phase cycling was based in part on a lecture given at a NATO ASI Workshop in Italy in 1990. The section on field gradient pulses is based on an article published in Methods in Enzymology volume 239C (1994) which I co-authored with Robin Clowes, Adrian Davis and Ernest Laue. I thank the organisers of this and other meetings for the opportunity to prepare and present this material.

You are welcome to make copies of these lecture notes for your own use, and to supply copies to colleagues, provided that due acknowledgement of their origin is given. If you wish to make large numbers of copies, I would appreciate being consulted first.

James Keeler Cambridge 1998

University of Cambridge,
Department of Chemistry
Lensfield Rd
Cambridge, CB2 1EW
U.K.
EMAIL: James.Keeler@ch.cam.ac.uk

1 Introduction to quantum mechanics

Quantum mechanics is the basic tool needed to describe, understand and devise NMR experiments. Fortunately for NMR spectroscopists, the quantum mechanics of nuclear spins is quite straightforward and many useful calculations can be done by hand, quite literally "on the back of an envelope". This simplicity comes about from the fact that although there are a very large number of molecules in an NMR sample they are interacting very weakly with one another. Therefore, it is usually adequate to think about only one molecule at a time. Even in one molecule, the number of spins which are interacting significantly with one another (*i.e.* are coupled) is relatively small, so the number of possible quantum states is quite limited.

The discussion will begin with revision of some mathematical concepts frequently encountered in quantum mechanics and NMR.

1.1 Mathematical concepts

1.1.1 Complex numbers

An ordinary number can be thought of as a point on a line which extends from minus infinity through zero to plus infinity. A *complex number* can be thought of as a point in a plane; the *x*-coordinate of the point is the *real part* of the complex number and the *y*-coordinate is the *imaginary part*.

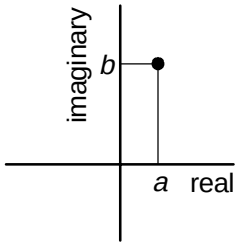

A complex number can be though of as a point in the complex plane with a real part (*a*) and an imaginary part (*b*).

If the real part is *a* and the imaginary part is *b*, the complex number is written as ($a + ib$) where i is the square root of –1. The idea that $\sqrt{-1}$ (or in general the square root of any negative number) might have a "meaning" is one of the origins of complex numbers, but it will be seen that they have many more uses than simply expressing the square root of a negative number.

i appears often and it is important to get used to its properties:

$$i^2 = \sqrt{-1} \times \sqrt{-1} = -1$$
$$i^3 = i \times i^2 = -i$$
$$i^4 = i^2 \times i^2 = +1$$
$$\frac{1}{i} = \left(\frac{1}{i}\right)\left(\frac{i}{i}\right) \quad \{\text{multiplying top and bottom by } i\}$$
$$= \frac{i}{i^2} = \frac{i}{-1} = -i$$

The *complex conjugate* of a complex number is formed by changing the sign of the imaginary part; it is denoted by a *

$$(a + ib)^* = (a - ib)$$

The square magnitude of a complex number C is denoted $|C|^2$ and is found by multiplying C by its complex conjugate; $|C|^2$ is always real

$$\begin{aligned} \text{if } C &= (a+ib) \\ |C|^2 &= C \times C^* \\ &= (a+ib)(a-ib) \\ &= a^2 + b^2 \end{aligned}$$

These various properties are used when manipulating complex numbers:

addition: $(a+ib)+(c+id) = (a+c)+i(b+d)$

multiplication: $(a+ib)\times(c+id) = (ac-bd)+i(ad+bc)$

division:

$$\frac{(a+ib)}{(c+id)} = \frac{(a+ib)}{(c+id)} \times \frac{(c+id)^*}{(c+id)^*} \quad \{\text{multiplying top and bottom by } (c+id)^*\}$$

$$= \frac{(a+ib)(c+id)^*}{\left(c^2+d^2\right)} = \frac{(a+ib)(c-id)}{\left(c^2+d^2\right)} = \frac{(ac+bd)+i(bc-ad)}{\left(c^2+d^2\right)}$$

Using these relationships it is possible to show that

$$(C \times D \times E \times \ldots)^* = (C^* \times D^* \times E^* \times \ldots)$$

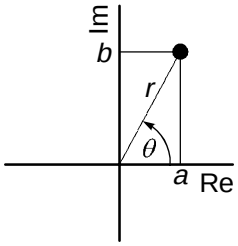

An alternative representation of a complex number is to specify a distance, r, and an angle, θ.

The position of a number in the complex plane can also be indicated by the distance, r, of the point from the origin and the angle, θ, between the real axis and the vector joining the origin to the point (see opposite). By simple geometry it follows that

$$\begin{aligned} \text{Re}\left[(a+ib)\right] &= a & \text{Im}\left[(a+ib)\right] &= b \\ &= r\cos\theta & &= r\sin\theta \end{aligned} \qquad [1.1]$$

Where Re and Im mean "take the real part" and "take the imaginary part", respectively.

In this representation the square amplitude is

$$\begin{aligned} \left|(a+ib)\right|^2 &= a^2 + b^2 \\ &= r^2\left(\cos^2\theta + \sin^2\theta\right) = r^2 \end{aligned}$$

where the identity $\cos^2\theta + \sin^2\theta = 1$ has been used.

1.1.2 Exponentials and complex exponentials

The exponential function, e^x or $\exp(x)$, is defined as the power series

$$\exp(x) = 1 + \tfrac{1}{2!}x^2 + \tfrac{1}{3!}x^3 + \tfrac{1}{4!}x^4 + \ldots$$

The number e is the base of natural logarithms, so that ln(e) = 1.

Exponentials have the following properties

$$\exp(0) = 1 \qquad \exp(A)\times\exp(B) = \exp(A+B) \qquad \left[\exp(A)\right]^2 = \exp(2A)$$

$$\exp(A)\times\exp(-A) = \exp(A-A) = \exp(0) = 1$$

$$\exp(-A) = \frac{1}{\exp(A)} \qquad \frac{\exp(A)}{\exp(B)} = \exp(A)\times\exp(-B)$$

The *complex exponential* is also defined in terms of a power series:

$$\exp(i\theta) = 1 + \tfrac{1}{2!}(i\theta)^2 + \tfrac{1}{3!}(i\theta)^3 + \tfrac{1}{4!}(i\theta)^4 + \ldots$$

By comparing this series expansion with those for $\sin\theta$ and $\cos\theta$ it can easily be shown that

$$\exp(i\theta) = \cos\theta + i\sin\theta \qquad [1.2]$$

This is a very important relation which will be used frequently. For negative exponents there is a similar result

$$\begin{aligned}\exp(-i\theta) &= \cos(-\theta) + i\sin(-\theta)\\ &= \cos\theta - i\sin\theta\end{aligned} \qquad [1.3]$$

where the identities $\cos(-\theta) = \cos\theta$ and $\sin(-\theta) = -\sin\theta$ have been used.

By comparison of Eqns. [1.1] and [1.2] it can be seen that the complex number ($a + ib$) can be written

$$(a + ib) = r\exp(i\theta)$$

where $r = a^2 + b^2$ and $\tan\theta = (b/a)$.

In the complex exponential form, the complex conjugate is found by changing the sign of the term in i

$$\text{if} \quad C = r\exp(i\theta)$$
$$\text{then} \quad C^* = r\exp(-i\theta)$$

It follows that

$$\begin{aligned} |C|^2 &= CC^* \\ &= r\exp(i\theta) r\exp(-i\theta) \\ &= r^2\exp(i\theta - i\theta) = r^2\exp(0) \\ &= r^2 \end{aligned}$$

Multiplication and division of complex numbers in the (r,θ) format is straightforward

$$\text{let} \quad C = r\exp(i\theta) \quad \text{and} \quad D = s\exp(i\phi) \quad \text{then}$$
$$\frac{1}{C} = \frac{1}{r\exp(i\theta)} = \frac{1}{r}\exp(-i\theta) \qquad C \times D = rs\exp\left(i\left(\theta + \phi\right)\right)$$
$$\frac{C}{D} = \frac{r\exp(i\theta)}{s\exp(i\phi)} = \frac{r}{s}\exp(i\theta)\exp(-i\phi) = \frac{r}{s}\exp\left(i\left(\theta - \phi\right)\right)$$

1.1.2.1 Relation to trigonometric functions

Starting from the relation

$$\exp(i\theta) = \cos\theta + i\sin\theta$$

it follows that, as $\cos(-\theta) = \cos\theta$ and $\sin(-\theta) = -\sin\theta$,

$$\exp(-i\theta) = \cos\theta - i\sin\theta$$

From these two relationships the following can easily be shown

$$\exp(i\theta) + \exp(-i\theta) = 2\cos\theta \quad \text{or} \quad \cos\theta = \tfrac{1}{2}\left[\exp(i\theta) + \exp(-i\theta)\right]$$
$$\exp(i\theta) - \exp(-i\theta) = 2i\sin\theta \quad \text{or} \quad \sin\theta = \tfrac{1}{2i}\left[\exp(i\theta) - \exp(-i\theta)\right]$$

1.1.3 Circular motion

In NMR basic form of motion is for magnetization to precess about a magnetic field. Viewed looking down the magnetic field, the tip of the magnetization vector describes a circular path. It turns out that complex exponentials are a very convenient and natural way of describing such motion.

Consider a point *p* moving in the *xy*-plane in a circular path, radius *r*, centred at the origin. The position of the particle can be expressed in terms of the distance *r* and an angle θ. The *x*–component is $r \cdot \cos\theta$ and the *y*-component is $r \cdot \sin\theta$. The analogy with complex numbers is very compelling (see section 1.1.1); if the *x*- and *y*-axes are treated as the real and imaginary parts, then the position can be specified as the complex number $r \cdot \exp(i\theta)$.

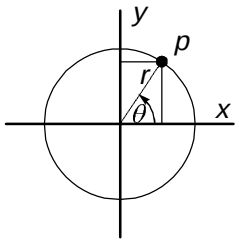

A point p moving on a circular path in the *xy*-plane.

In this complex notation the angle θ is called the *phase*. Points with different angles θ are said to have different phases and the difference between the two angles is called the *phase difference* or *phase shift* between the two points.

If the point is moving around the circular path with a constant speed then the phase becomes a function of time. In fact for a constant speed, θ is simply proportional to time, and the constant of proportion is the angular speed (or frequency) ω

$$\theta = \omega t$$

where θ is in radians, *t* is in seconds and ω is in radians s^{-1}. Sometimes it is convenient to work in Hz (that is, revolutions per second) rather than $rad \cdot s^{-1}$; the frequency in Hz, ν, is related to ω by $\omega = 2\pi\nu$.

The position of the point can now be expressed as $r \exp(i\omega t)$, an expression which occurs very frequently in the mathematical description of NMR. Recalling that $\exp(i\theta)$ can be thought of as a phase, it is seen that there is a strong connection between phase and frequency. For example, a phase shift of $\theta = \omega t$ will come about due to precession at frequency ω for time *t*.

Rotation of the point *p* in the opposite sense is simply represented by changing the sign of ω: $r \exp(-i\omega t)$. Suppose that there are two particles, *p* and *p*', one rotating at $+\omega$ and the other at $-\omega$; assuming that they both start on the *x*-axis, their motion can be described by $\exp(+i\omega t)$ and $\exp(-i\omega t)$ respectively. Thus, the *x*- and *y*-components are:

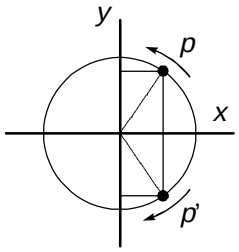

The *x*-components of two counter-rotating points add, but the *y*-components cancel. The resultant simply oscillates along the *x*-axis.

	x - comp.	*y* - comp.
p	$\cos\omega t$	$\sin\omega t$
p'	$\cos\omega t$	$-\sin\omega t$

It is clear that the *x*-components add, and the *y*-components cancel. All that is

left is a component along the *x*-axis which is oscillating back and forth at frequency ω. In the complex notation this result is easy to see as by Eqns. [1.2] and [1.3], $\exp(i\omega t) + \exp(-i\omega t) = 2\cos\omega t$. In words, a point oscillating along a line can be represented as two counter-rotating points.

1.2 Wavefunctions and operators

In quantum mechanics, two mathematical objects – wavefunctions and operators – are of central importance. The wavefunction describes the system of interest (such as a spin or an electron) completely; if the wavefunction is known it is possible to calculate all the properties of the system. The simplest example of this that is frequently encountered is when considering the wavefunctions which describe electrons in atoms (atomic orbitals) or molecules (molecular orbitals). One often used interpretation of such electronic wavefunctions is to say that the square of the wavefunction gives the probability of finding the electron at that point.

Wavefunctions are simply mathematical functions of position, time *etc.* For example, the 1s electron in a hydrogen atom is described by the function $\exp(-ar)$, where r is the distance from the nucleus and a is a constant.

In quantum mechanics, operators represent "observable quantities" such as position, momentum and energy; each observable has an operator associated with it.

Operators "operate on" functions to give new functions, hence their name

$$\text{operator} \times \text{function} = \text{(new function)}$$

An example of an operator is $\left(\mathrm{d}/\mathrm{d}x\right)$; in words this operator says "differentiate with respect to x". Its effect on the function $\sin x$ is

$$\frac{\mathrm{d}}{\mathrm{d}x}(\sin x) = \cos x$$

the "new function" is $\cos x$. Operators can also be simple functions, so for example the operator x^2 just means "multiply by x^2".

It is clear from this discussion that operators and functions *cannot be re-ordered* in the same way that numbers or functions can be. For example

$$2 \times 3 \text{ is the same as } 3 \times 2$$

$$x \times \sin(x) \text{ is the same as } \sin(x) \times x$$

$$\text{but } \left(\frac{\mathrm{d}}{\mathrm{d}x}\right) \times \sin(x) \text{ is not the same as } \sin(x) \times \left(\frac{\mathrm{d}}{\mathrm{d}x}\right)$$

Generally operators are thought of as acting on the functions that appear to their right.

1.2.1 Eigenfunctions and eigenvalues

Generally, operators act on functions to give another function:

$$\text{operator} \times \text{function} = \text{(new function)}$$

However, for a given operator there are some functions which, when acted upon, are regenerated, but multiplied by a constant

$$\text{operator} \times \text{function} = \text{constant} \times \text{(function)} \qquad [1.4]$$

Such functions are said to be *eigenfunctions* of the operator and the constants are said to be the associated *eigenvalues.*

If the operator is $\hat{Q}$ (the hat is to distinguish it as an operator) then Eqn. [1.4] can be written more formally as

$$\hat{Q}f_q = qf_q \qquad [1.5]$$

where f_q is an eigenfunction of $\hat{Q}$ with eigenvalue q; there may be more that one eigenfunction each with different eigenvalues. Equation [1.5] is known as the *eigenvalue equation.*

For example, is $\exp(ax)$, where a is a constant, an eigenfunction of the operator $(\mathrm{d}/\mathrm{d}x)$? To find out the operator and function are substituted into the left-hand side of the eigenvalue equation, Eqn. [1.5]

$$\left(\frac{\mathrm{d}}{\mathrm{d}x}\right)\exp(ax) = a\exp(ax)$$

It is seen that the result of operating on the function is to generate the original function times a constant. Therefore $\exp(ax)$ is an eigenfunction of the operator $(\mathrm{d}/\mathrm{d}x)$ with eigenvalue a.

Is $\sin(ax)$, where a is a constant, an eigenfunction of the operator $(\mathrm{d}/\mathrm{d}x)$? As before, the operator and function are substituted into the left-hand side of the eigenvalue equation.

$$\left(\frac{\mathrm{d}}{\mathrm{d}x}\right)\sin(ax) = a\cos(ax)$$
$$\neq \text{constant} \times \sin(ax)$$

As the original function is not regenerated, sin(*ax*) is not an eigenfunction of the operator $\left(\mathrm{d}/\mathrm{d}x\right)$.

1.2.2 Normalization and orthogonality

A function, ψ, is said to be *normalised* if

$$\int \left(\psi^*\right) \psi \, \mathrm{d}\tau = 1$$

where, as usual, the * represents the complex conjugate. The notation $\mathrm{d}\tau$ is taken in quantum mechanics to mean integration over the full range of all relevant variables *e.g.* in three-dimensional space this would mean the range $-\infty$ to $+\infty$ for all of *x*, *y* and *z*.

Two functions ψ and ϕ are said to be *orthogonal* if

$$\int \left(\psi^*\right) \phi \, \mathrm{d}\tau = 0$$

It can be shown that the eigenfunctions of an operator are orthogonal to one another, provided that they have different eigenvalues.

$$\text{if } \hat{Q} f_q = q f_q \text{ and } \hat{Q} f_{q'} = q' f_{q'}$$
$$\text{then } \int \left(f_q{}^*\right) f_{q'} \, \mathrm{d}\tau = 0$$

1.2.3 Bra-ket notation

This short-hand notation for wavefunctions is often used in quantum mechanics. A wavefunction is represented by a "ket" $|\ldots\rangle$; labels used to distinguish different wavefunctions are written in the ket. For example

$$f_q \text{ is written } |q\rangle \text{ or sometimes } \left| f_q \right\rangle$$

It is a bit superfluous to write f_q inside the ket.

The complex conjugate of a wavefunction is written as a "bra" $\langle\ldots|$; for example

$$\left(f_{q'}\right)^* \text{ is written } \langle q'|$$

The rule is that if a bra appears on the *left* and a ket on the *right*, integration over $d\tau$ is implied. So

$$\langle q' \| q \rangle \text{ implies } \int \left(f_{q'} * \right) f_q \, d\tau$$

sometimes the middle vertical lines are merged: $\langle q' | q \rangle$.

Although it takes a little time to get used to, the bra-ket notation is very compact. For example, the normalization and orthogonality conditions can be written

$$\langle q | q \rangle = 1 \qquad \langle q' | q \rangle = 0$$

A frequently encountered integral in quantum mechanics is

$$\int \psi_i^* \hat{Q} \psi_j \, d\tau$$

where ψ_i and ψ_j are wavefunctions, distinguished by the subscripts *i* and *j*. In bra-ket notation this integral becomes

$$\langle i | \hat{Q} | j \rangle \qquad [1.6]$$

as before, the presence of a bra on the left and a ket on the right implies integration over $d\tau$. Note that in general, it is not allowed to re-order the operator and the wavefunctions (section 1.2). The integral of Eqn. [1.6] is often called a *matrix element*, specifically the *ij* element, of the operator $\hat{Q}$.

In the bra-ket notation the eigenvalue equation, Eqn. [1.5], becomes

$$\hat{Q} | q \rangle = q | q \rangle$$

Again, this is very compact.

1.2.4 Basis sets

The position of any point in three-dimensional space can be specified by giving its *x*-, *y*- and *z*-components. These three components form a complete description of the position of the point; two components would be insufficient and adding a fourth component along another axis would be superfluous. The three axes are orthogonal to one another; that is any one axis does not have a component along the other two.

In quantum mechanics there is a similar idea of expressing a wavefunction in terms of a set of other functions. For example, ψ may be expressed as a linear combination of other functions

$$\left|\psi\right\rangle = a_1|1\rangle + a_2|2\rangle + a_3|3\rangle + \ldots$$

where the $|i\rangle$ are called the *basis functions* and the a_i are coefficients (numbers).

Often there is a limited set of basis functions needed to describe any particular wavefunction; such a set is referred to as a *complete basis set*. Usually the members of this set are orthogonal and can be chosen to be normalized, *i.e.*

$$\left\langle i \middle| j \right\rangle = 0 \quad \langle i|i\rangle = 1$$

1.2.5 Expectation values

A postulate of quantum mechanics is that if a system is described by a wavefunction ψ then the value of an observable quantity represented by the operator $\hat{Q}$ is given by the expectation value, $\left\langle \hat{Q} \right\rangle$, defined as

$$\left\langle \hat{Q} \right\rangle = \frac{\int \psi^* \hat{Q} \psi \, \mathrm{d}\tau}{\int \psi^* \psi \, \mathrm{d}\tau}$$

or in the bra-ket notation

$$\left\langle \hat{Q} \right\rangle = \frac{\left\langle \psi \middle| \hat{Q} \middle| \psi \right\rangle}{\left\langle \psi \middle| \psi \right\rangle}$$

1.3 Spin operators

1.3.1 Spin angular momentum

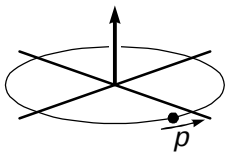

A mass going round a circular path possesses angular moment, represented by a vector which points perpendicular to the plane of rotation.

A mass going round a circular path (an orbit) possesses *angular momentum*; it turns out that this is a vector quantity which points in a direction perpendicular to the plane of the rotation. The *x*-, *y*- and *z*-components of this vector can be specified, and these are the angular momenta in the *x*-, *y*- and *z*-directions. In quantum mechanics, there are operators which represent these three components of the angular momentum.

Nuclear spins also have angular momentum associated with them – called *spin angular momentum*. The three components of this spin angular momentum (along *x*, *y* and *z*) are represented by the operators $\hat{I}_x$, $\hat{I}_y$ and $\hat{I}_z$ (from now on the hats will be dropped unless there is any possibility of ambiguity).

These operators are extremely important in the quantum mechanical description of NMR, indeed just about all of the theory in these lectures uses these operators. It is therefore very important to understand their properties.

1.3.2 Eigenvalues and eigenfunctions

From now on the discussion is restricted to nuclei with nuclear spin quantum number, I, = $\frac{1}{2}$. For such a spin, it turns out that there are just $(2I + 1) = 2$ eigenfunctions of any one of the operators I_x, I_y and I_z. As it is traditional to define the direction of the applied magnetic field as *z*, the eigenfunctions of the I_z operator are the ones of most interest. These two eigenfunctions are usually denoted $|\alpha\rangle$ and $|\beta\rangle$; they have the properties

$$I_z|\alpha\rangle = \tfrac{1}{2}\hbar|\alpha\rangle \qquad I_z|\beta\rangle = -\tfrac{1}{2}\hbar|\beta\rangle$$

where $\hbar$ is Planck's constant divided by 2π. These properties mean that $|\alpha\rangle$ and $|\beta\rangle$ are indeed eigenfunctions, with eigenvalues $\frac{1}{2}\hbar$ and $-\frac{1}{2}\hbar$ respectively. These functions are normalized and orthogonal to one another

$$\langle\alpha|\alpha\rangle = 1 \quad \langle\beta|\beta\rangle = 1 \quad \langle\alpha|\beta\rangle = 0$$

The interpretation of these two states rests on the idea of angular momentum as a vector quantity. It turns out that angular momentum of size I (here $I = \frac{1}{2}$) can be represented by a vector of length $\hbar\sqrt{I(I+1)}$; for spin $\frac{1}{2}$ the length of the vector is $\left(\sqrt{3}/2\right)\hbar$. This vector can orient itself with respect to a fixed axis, say the z-axis, in only $(2I + 1)$ ways such that the *projection* of the vector I onto the z-axis is $I\hbar,(I-1)\hbar,\ldots -I\hbar$, *i.e.* integer steps between I and $-I$. In the case of $I = \frac{1}{2}$, there are only two possible projections, $+\frac{1}{2}\hbar$ and $-\frac{1}{2}\hbar$. These projections are labelled with a quantum number m_I, called the magnetic quantum number. It has values $+\frac{1}{2}$ and $-\frac{1}{2}$.

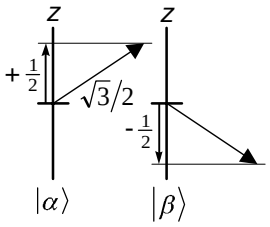

Vector representation of the spin angular momentum of a spin half and its projections onto the *z*-axis.

An alternative way of denoting the two eigenfunctions of the operator I_z is to label them with the m_I values

$$I_z\left|m_I\right\rangle = m_I\hbar\left|m_I\right\rangle$$
$$i.e.\quad I_z\left|\tfrac{1}{2}\right\rangle = \tfrac{1}{2}\hbar\left|\tfrac{1}{2}\right\rangle \qquad I_z\left|-\tfrac{1}{2}\right\rangle = -\tfrac{1}{2}\hbar\left|\tfrac{1}{2}\right\rangle$$

So $\left|\frac{1}{2}\right\rangle$ and $\left|-\frac{1}{2}\right\rangle$ correspond to $|\alpha\rangle$ and $|\beta\rangle$ which can be thought of as "spin up" and "spin down".

The functions $|\alpha\rangle$ and $|\beta\rangle$ are not eigenfunctions of either I_x or I_y.

1.3.3 Raising and lowering operators

The raising operator, I_+, and the lowering operator, I_-, are defined as

$$I_+ = I_x + iI_y \quad I_- = I_x - iI_y \qquad [1.7]$$

These operators have the following properties

$$\begin{aligned} I_+\left|-\tfrac{1}{2}\right\rangle &= \hbar\left|\tfrac{1}{2}\right\rangle \quad I_+\left|\tfrac{1}{2}\right\rangle = 0 \\ I_-\left|\tfrac{1}{2}\right\rangle &= \hbar\left|-\tfrac{1}{2}\right\rangle \quad I_-\left|-\tfrac{1}{2}\right\rangle = 0 \end{aligned} \qquad [1.8]$$

Their names originated from these properties. The raising operator acts on the state $\left|-\frac{1}{2}\right\rangle$, which has $m_I = -\frac{1}{2}$, in such a way as to increase m_I by one unit to give $m_I = +\frac{1}{2}$. However, if I_+ acts on the state $\left|\frac{1}{2}\right\rangle$ there is no possibility of further increasing m_I as it is already at its maximum value; thus I_+ acting on $\left|\frac{1}{2}\right\rangle$ gives zero.

The same rationalization can be applied to the lowering operator. It acts on $\left|\frac{1}{2}\right\rangle$, which has $m_I = +\frac{1}{2}$, and produces a state on which m_I has been lowered by

one i.e. $m_I = -\frac{1}{2}$. However, the m_I value can be lowered no further so I_- acting on $\left|-\frac{1}{2}\right\rangle$ gives zero.

Using the definitions of Eqn. [1.7], I_x and I_y can be expressed in terms of the raising and lowering operators:

$$I_x = \tfrac{1}{2}\left(I_+ + I_-\right) \quad I_y = \tfrac{1}{2i}\left(I_+ - I_-\right)$$

Using these, and the properties given in Eqn. [1.8], it is easy to work out the effect that I_x and I_y have on the states $|\alpha\rangle$ and $|\beta\rangle$; for example

$$\begin{aligned} I_x|\alpha\rangle &= \tfrac{1}{2}\left(I_+ + I_-\right)|\alpha\rangle \\ &= \tfrac{1}{2} I_+|\alpha\rangle + \tfrac{1}{2} I_-|\alpha\rangle \\ &= 0 + \tfrac{1}{2}\hbar|\beta\rangle \\ &= \tfrac{1}{2}\hbar|\beta\rangle \end{aligned}$$

By a similar method it can be found that

$$I_x|\alpha\rangle = \tfrac{1}{2}\hbar|\beta\rangle \quad I_x|\beta\rangle = \tfrac{1}{2}\hbar|\alpha\rangle \quad I_y|\alpha\rangle = \tfrac{1}{2}i\hbar|\beta\rangle \quad I_y|\beta\rangle = -\tfrac{1}{2}i\hbar|\alpha\rangle \quad [1.9]$$

These relationships all show that $|\alpha\rangle$ and $|\beta\rangle$ are not eigenfunctions of I_x and I_y.

1.4 Hamiltonians

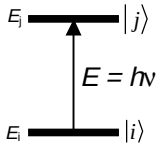

A spectroscopic transition takes place between two energy levels, E_i and E_j, which are eigenvalues of the Hamiltonian; these levels correspond to eigenfunctions of the Hamiltonian.

The Hamiltonian, H, is the special name given to the operator for the *energy* of the system. This operator is exceptionally important as its eigenvalues and eigenfunctions are the "energy levels" of the system, and it is transitions between these energy levels which are detected in spectroscopy. To understand the spectrum, therefore, it is necessary to have a knowledge of the energy levels and this in turn requires a knowledge of the Hamiltonian operator.

In NMR, the Hamiltonian is seen as having a more subtle effect than simply determining the energy levels. This comes about because the Hamiltonian also affects how the spin system evolves in time. By altering the Hamiltonian the time evolution of the spins can be manipulated and it is precisely this that lies at the heart of multiple-pulse NMR.

The precise mathematical form of the Hamiltonian is found by first writing down an expression for the energy of the system using classical mechanics and then "translating" this into quantum mechanical form according to a set of rules. In this lecture the form of the relevant Hamiltonians will simply be stated rather than derived.

In NMR the Hamiltonian changes depending on the experimental situation.

There is one Hamiltonian for the spin or spins in the presence of the applied magnetic field, but this Hamiltonian changes when a radio-frequency pulse is applied.

1.4.1 Free precession

Free precession is when the spins experience just the applied magnetic field, B_0, traditionally taken to be along the *z*-axis.

1.4.1.1 One spin

The free precession Hamiltonian, H_{free}, is

$$H_{\text{free}} = \gamma B_0 \hbar I_z$$

where γ is the gyromagnetic ratio, a constant characteristic of a particular nuclear species such as proton or carbon-13. The quantity $\gamma B_0 \hbar$ has the units of energy, which is expected as the Hamiltonian is the operator for energy. However, it turns out that it is much more convenient to write the Hamiltonian in units of angular frequency (radians s^{-1}), which is achieved by dividing the expression for H_{free} by $\hbar$ to give

$$H_{\text{free}} = \gamma B_0 I_z$$

To be consistent it is necessary then to divide *all* of the operators by $\hbar$. As a result all of the factors of $\hbar$ disappear from many of the equations given above *e.g.* they become:

$$I_z|\alpha\rangle = \tfrac{1}{2}|\alpha\rangle \qquad I_z|\beta\rangle = -\tfrac{1}{2}|\beta\rangle \qquad [1.10]$$

$$I_+|\beta\rangle = |\alpha\rangle \qquad I_-|\alpha\rangle = \hbar|\beta\rangle \qquad [1.11]$$

$$I_x|\alpha\rangle = \tfrac{1}{2}|\beta\rangle \quad I_x|\beta\rangle = \tfrac{1}{2}|\alpha\rangle \quad I_y|\alpha\rangle = \tfrac{1}{2}i|\beta\rangle \quad I_y|\beta\rangle = -\tfrac{1}{2}i|\alpha\rangle \quad [1.12]$$

From now on, the properties of the wavefunctions and operators will be used in this form. The quantity γB_0, which has dimensions of angular frequency (rad s^{-1}), is often called the Larmor frequency, ω_0.

Eigenfunctions and eigenvalues

The eigenfunctions and eigenvalues of H_{free} are a set of functions, $|i\rangle$, which

satisfy the eigenvalue equation:

$$H_{\text{free}}|i\rangle = \varepsilon_i|i\rangle$$
$$\omega_0 I_z|i\rangle = \varepsilon_i|i\rangle$$

It is already known that $|\alpha\rangle$ and $|\beta\rangle$ are eigenfunctions of I_z, so it follows that they are also eigenfunctions of any operator proportional to I_z:

$$\begin{aligned} H_{\text{free}}|\alpha\rangle &= \omega_0 I_z|\alpha\rangle \\ &= \tfrac{1}{2}\omega_0|\alpha\rangle \end{aligned}$$

and likewise $H_{\text{free}}|\beta\rangle = \omega_0 I_z|\beta\rangle = -\tfrac{1}{2}\omega_0|\beta\rangle$.

So, $|\alpha\rangle$ and $|\beta\rangle$ are eigenfunctions of H_{free} with eigenvalues $\tfrac{1}{2}\omega_0$ and $-\tfrac{1}{2}\omega_0$, respectively. These two eigenfunctions correspond to two energy levels and a transition between them occurs at frequency $\left(\tfrac{1}{2}\omega_0 - \left(-\tfrac{1}{2}\omega_0\right)\right) = \omega_0$.

1.4.1.2 Several spins

If there is more then one spin, each simply contributes a term to H_{free}; subscripts are used to indicate that the operator applies to a particular spin

$$H_{\text{free}} = \omega_{0,1} I_{1z} + \omega_{0,2} I_{2z} + \ldots$$

where I_{1z} is the operator for the first spin, I_{2z} is that for the second and so on. Due to the effects of chemical shift, the Larmor frequencies of the spins may be different and so they have been written as $\omega_{0,i}$.

Eigenfunctions and eigenvalues

As H_{free} separates into a *sum* of terms, the eigenfunctions turn out to be a *product* of the eigenfunctions of the separate terms; as the eigenfunctions of $\omega_{0,1}I_{1z}$ are already known, it is easy to find those for the whole Hamiltonian.

As an example, consider the Hamiltonian for two spins

$$H_{\text{free}} = \omega_{0,1} I_{1z} + \omega_{0,2} I_{2z}$$

From section 1.4.1.1, it is known that, for spin 1

$$\omega_{0,1} I_{1z} \left|\alpha_1\right\rangle = \tfrac{1}{2}\omega_0 \left|\alpha_1\right\rangle \quad \text{and} \quad \omega_{0,1} I_{1z} \left|\beta_1\right\rangle = -\tfrac{1}{2}\omega_{0,2} \left|\beta_1\right\rangle$$

likewise for spin 2

$$\omega_{0,2} I_{2z} \left|\alpha_2\right\rangle = \tfrac{1}{2}\omega_{0,2} \left|\alpha_2\right\rangle \quad \text{and} \quad \omega_{0,2} I_{2z} \left|\beta_2\right\rangle = -\tfrac{1}{2}\omega_{0,2} \left|\beta_2\right\rangle$$

Consider the function $|\beta_1\rangle|\alpha_2\rangle$, which is a product of one of the eigenfunctions for spin 1 with one for spin 2. To show that this is an eigenfunction of H_{free}, the Hamiltonian is applied to the function

$$\begin{aligned} H_{\text{free}} \left|\beta_1\right\rangle \left|\alpha_2\right\rangle &= \left(\omega_{0,1} I_{1z} + \omega_{0,2} I_{2z}\right) \left|\beta_1\right\rangle \left|\alpha_2\right\rangle \\ &= \omega_{0,1} I_{1z} \left|\beta_1\right\rangle \left|\alpha_2\right\rangle + \omega_{0,2} I_{2z} \left|\beta_1\right\rangle \left|\alpha_2\right\rangle \\ &= -\tfrac{1}{2}\omega_{0,1} \left|\beta_1\right\rangle \left|\alpha_2\right\rangle + \omega_{0,2} \left|\beta_1\right\rangle I_{2z} \left|\alpha_2\right\rangle \\ &= -\tfrac{1}{2}\omega_{0,1} \left|\beta_1\right\rangle \left|\alpha_2\right\rangle + \tfrac{1}{2}\omega_{0,2} \left|\beta_1\right\rangle \left|\alpha_2\right\rangle \\ &= \left(-\tfrac{1}{2}\omega_{0,1} + \tfrac{1}{2}\omega_{0,2}\right) \left|\beta_1\right\rangle \left|\alpha_2\right\rangle \end{aligned}$$

As the action of H_{free} on $|\beta_1\rangle|\alpha_2\rangle$ is to regenerate the function, then it has been shown that the function is indeed an eigenfunction, with eigenvalue $\left(-\tfrac{1}{2}\omega_{0,1} + \tfrac{1}{2}\omega_{0,2}\right)$. Some comment in needed on these manipulation needed between lines 2 and 3 of the above calculation. The order of the function $|\beta_1\rangle$ and the operator I_{2z} were changed between lines 2 and 3. Generally, as was noted above, it is not permitted to reorder operators and functions; however it is permitted in this case as the operator refers to *spin 2* but the function refers to *spin 1*. The operator has no effect, therefore, on the function and so the two can be re-ordered.

There are four possible products of the single-spin eigenfunctions and each of these can be shown to be an eigenfunction. The table summarises the results; in it, the shorthand notation has been used in which $|\beta_1\rangle|\alpha_2\rangle$ is denoted $|\beta\alpha\rangle$ *i.e.* it is implied by the order of the labels as to which spin they apply to

Eigenfunctions and eigenvalues for two spins

eigenfunction	$m_{\text{I},1}$	$m_{\text{I},2}$	M	eigenvalue
$\left\|\alpha\alpha\right\rangle$	$+\tfrac{1}{2}$	$+\tfrac{1}{2}$	1	$+\tfrac{1}{2}\omega_{0,1} + \tfrac{1}{2}\omega_{0,2}$
$\left\|\alpha\beta\right\rangle$	$+\tfrac{1}{2}$	$-\tfrac{1}{2}$	0	$+\tfrac{1}{2}\omega_{0,1} - \tfrac{1}{2}\omega_{0,2}$
$\left\|\beta\alpha\right\rangle$	$-\tfrac{1}{2}$	$+\tfrac{1}{2}$	0	$-\tfrac{1}{2}\omega_{0,1} + \tfrac{1}{2}\omega_{0,2}$
$\left\|\beta\beta\right\rangle$	$-\tfrac{1}{2}$	$-\tfrac{1}{2}$	1	$-\tfrac{1}{2}\omega_{0,1} - \tfrac{1}{2}\omega_{0,2}$

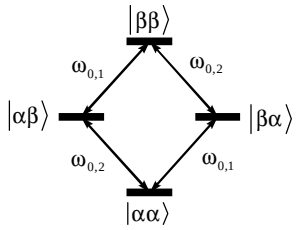

The four energy levels of a two-spin system. The allowed transitions of spin 1 are shown by dashed arrows, and those of spin 2 by solid arrows.

Also shown in the table are the m_I values for the individual spins and the total magnetic quantum number, M, which is simply the sum of the m_I values of the two spins.

In normal NMR, the allowed transitions are between those levels that differ in M values by one unit. There are two transitions which come out at $\omega_{0,1}$, $|\beta\alpha\rangle \leftrightarrow |\alpha\alpha\rangle$ and $|\alpha\beta\rangle \leftrightarrow |\beta\beta\rangle$; and there are two which come out at $\omega_{0,2}$, $|\beta\alpha\rangle \leftrightarrow |\beta\beta\rangle$ and $|\alpha\beta\rangle \leftrightarrow |\alpha\alpha\rangle$. The former two transitions involve a flip in the spin state of spin 1, whereas the latter pair involve a flip of the state of spin 2. The energy levels and transitions are depicted opposite.

1.4.1.3 Scalar coupling

The Hamiltonian for scalar coupling contains a term $2\pi J_{ij} I_{iz} I_{jz}$ for each coupled pair of spins; J_{ij} is the coupling constant, in Hz, between spins i and j. The terms representing coupling have to be added to those terms described in section 1.4.1.2 which represent the basic Larmor precession. So, the complete free precession Hamiltonian for two spins is:

$$H_{\text{free}} = \omega_{0,1} I_{1z} + \omega_{0,2} I_{2z} + 2\pi J_{12} I_{1z} I_{2z}$$

Eigenfunctions and eigenvalues for two spins

The product functions, such as $|\beta_1\rangle|\alpha_2\rangle$, turn out to also be eigenfunctions of the coupling Hamiltonian. For example, consider the function $|\beta_1\rangle|\alpha_2\rangle$; to show that this is an eigenfunction of the coupling part of H_{free}, the relevant operator is applied to the function

$$\begin{aligned} 2\pi J_{12} I_{1z} I_{2z} \left|\beta_1\right\rangle \left|\alpha_2\right\rangle &= 2\pi J_{12} I_{1z} \left|\beta_1\right\rangle I_{2z} \left|\alpha_2\right\rangle \\ &= 2\pi J_{12} I_{1z} \left|\beta_1\right\rangle \tfrac{1}{2} \left|\alpha_2\right\rangle \\ &= 2\pi J_{12} \left(-\tfrac{1}{2}\right) \left|\beta_1\right\rangle \tfrac{1}{2} \left|\alpha_2\right\rangle \\ &= -\tfrac{1}{2}\pi J_{12} \left|\beta_1\right\rangle \left|\alpha_2\right\rangle \end{aligned}$$

As the action of $2\pi J_{12} I_{1z} I_{2z}$ on $|\beta_1\rangle|\alpha_2\rangle$ is to regenerate the function, then it follows that the function is indeed an eigenfunction, with eigenvalue $\left(-\tfrac{1}{2}\pi J_{12}\right)$. As before, the order of operators can be altered when the relevant operator and function refer to different spins.

In a similar way, all four product functions can be show to be eigenfunctions of the coupling Hamiltonian, and therefore of the complete free precession Hamiltonian. The table shows the complete set of energy levels.

Eigenfunctions and eigenvalues for two coupled spins

number	eigenfunction	M	eigenvalue
1	$\lvert\alpha\alpha\rangle$	1	$+\frac{1}{2}\omega_{0,1}+\frac{1}{2}\omega_{0,2}+\frac{1}{2}\pi J_{12}$
2	$\lvert\alpha\beta\rangle$	0	$+\frac{1}{2}\omega_{0,1}-\frac{1}{2}\omega_{0,2}-\frac{1}{2}\pi J_{12}$
3	$\lvert\beta\alpha\rangle$	0	$-\frac{1}{2}\omega_{0,1}+\frac{1}{2}\omega_{0,2}-\frac{1}{2}\pi J_{12}$
4	$\lvert\beta\beta\rangle$	1	$-\frac{1}{2}\omega_{0,1}-\frac{1}{2}\omega_{0,2}+\frac{1}{2}\pi J_{12}$

There are two allowed transitions in which spin 1 flips, 1–3 and 2–4, and these appear at $\omega_{0,1} + \pi J_{12}$ and $\omega_{0,1} - \pi J_{12}$, respectively. There are two further transitions in which spin 2 flips, 1–2 and 3–4, and these appear at $\omega_{0,2} + \pi J_{12}$ and $\omega_{0,2} - \pi J_{12}$, respectively. These four lines form the familiar two doublets found in the spectrum of two coupled spins.

Transition 1–2 is one in which spin 2 flips *i.e.* changes spin state, but the spin state of spin 1 remains the same. In this transition spin 2 can be said to be *active*, whereas spin 1 is said to be *passive*. These details are summarized in the diagram below

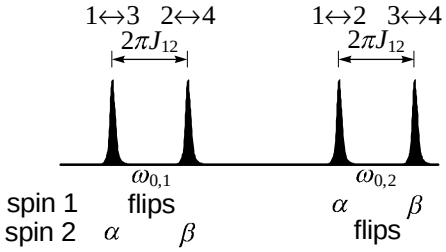

The spectrum from two coupled spins, showing which spins are passive and active in each transition. The frequency scale is in rad s^{-1}, so the splitting of the doublet is $2\pi J_{12}$ rad s^{-1}, which corresponds to J_{12} Hz.

Eigenfunctions and eigenvalues for several spins

For N spins, it is easy to show that the eigenfunctions are the 2^N possible products of the single spin eigenfunctions $|\alpha\rangle$ and $|\beta\rangle$. A particular eigenfunction can be labelled with the m_I values for each spin, $m_{I,i}$ and written as $\left|m_{I,1}m_{I,2}\ldots m_{I,i}\right\rangle$. The energy of this eigenfunction is

$$\sum_{i=1}^{N} m_{I,i}\omega_{0,i} + \sum_{i=1}^{N}\sum_{j>i}^{N} m_{I,i}m_{I,j}\left(2\pi J_{ij}\right)$$

The restricted sum over the index j is to avoid counting the couplings more than once.

1.4.2 Pulses

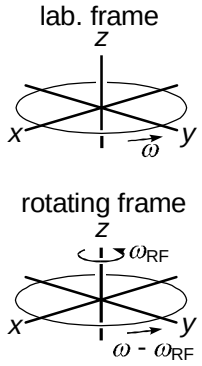

At object rotating at frequency ω in the *xy*-plane when viewed in the lab. frame (fixed axes) appears to rotate at frequency ($\omega - \omega_{RF}$) when observed in a frame rotating about the *z*-axis at ω_{RF}.

In NMR the nuclear spin magnetization is manipulated by applying a magnetic field which is (a) transverse to the static magnetic field *i.e.* in the *xy*-plane, and (b) oscillating at close to the Larmor frequency of the spins. Such a field is created by passing the output of a radio-frequency transmitter through a small coil which is located close to the sample.

If the field is applied along the *x*-direction and is oscillating at ω_{RF}, the Hamiltonian for one spin is

$$H = \omega_0 I_z + 2\omega_1 \cos\omega_{RF} t \; I_x$$

The first term represents the interaction of the spin with the static magnetic field, and the second represents the interaction with the oscillating field. The strength of the latter is given by ω_1.

It is difficult to work with this Hamiltonian as it depends on time. However, this time dependence can be removed by changing to a *rotating set of axes*, or a *rotating frame*. These axes rotate about the *z*-axis at frequency ω_{RF}, and in the same sense as the Larmor precession.

In such a set of axes the Larmor precession is no longer at ω_0, but at ($\omega_0 - \omega_{RF}$); this quantity is called the *offset*, Ω. The more important result of using the rotating frame is that the time dependence of the transverse field is removed. The details of how this comes about are beyond the scope of this lecture, but can be found in a number of standard texts on NMR.

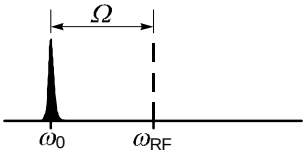

Illustration of the relationship between the Larmor frequency, ω_0, the transmitter frequency, ω_{RF}, and the offset, Ω.

In the rotating frame, the Hamiltonian becomes time independent

$$\begin{aligned} H &= \left(\omega_0 - \omega_{RF}\right) I_z + \omega_1 I_x \\ &= \Omega I_z + \omega_1 I_x \end{aligned}$$

Commonly, the strength of the radiofrequency field is arranged to be much greater than typical offsets: $\omega_1 >> |\Omega|$. It is then permissible to ignore the offset term and so write the pulse Hamiltonian as (for pulses of either phase)

$$H_{\text{pulse},x} = \omega_1 I_x \qquad \text{or} \qquad H_{\text{pulse},y} = \omega_1 I_y$$

Such pulses are described as *hard* or *non-selective*, in the sense that they affect spins over a range of offsets. Pulses with lower field strengths, ω_1, are termed *selective* or *soft*.

1.4.2.1 Several spins

For multi-spin systems, a term of the form $\omega_1 I_{ix}$ is added for each spin that is

affected by the pulse. Note that in heteronuclear systems, pulses can be applied independently to nuclei of different kinds

$$H_{\text{pulse},x} = \omega_1 I_{1x} + \omega_1 I_{2x} + \ldots$$

The product functions given above are not eigenfunctions of these Hamiltonians for pulses.

From now it, it will be assumed that all calculations are made in the rotating frame. So, instead of the free precession Hamiltonian being in terms of Larmor frequencies it will be written in terms of offsets. For example, the complete free precession Hamiltonian for two coupled spins is

$$H_{\text{free}} = \Omega_1 I_{1z} + \Omega_2 I_{2z} + 2\pi J_{12} I_{1z} I_{2z}$$

1.5 Time evolution

In general, the wavefunction describing a system varies with time, and this variation can be computed using the time-dependent Schrödinger equation

$$\frac{\mathrm{d}\psi(t)}{\mathrm{d}t} = -iH\psi(t) \qquad [1.13]$$

where $\psi(t)$ indicates that the wavefunction is a function of time. From this equation it is seen that the way in which the wavefunction varies with time depends on the Hamiltonian. In NMR, the Hamiltonian can be manipulated – for example by applying radio-frequency fields – and it is thus possible to manipulate the evolution of the spin system.

As has been seen in section 1.2.5, the size of observable quantities, such as magnetization, can be found by calculating the expectation value of the appropriate operator. For example, the x-magnetization is proportional to the expectation value of the operator I_x

$$M_x = k\langle I_x \rangle = \frac{\langle \psi(t) | I_x | \psi(t) \rangle}{\langle \psi(t) | \psi(t) \rangle}$$

where k is a constant of proportion. As the wavefunction changes with time, so do the expectation values and hence the observable magnetization.

1.6 Superposition states

This section will consider first a single spin and then a collection of a large

number of non-interacting spins, called an *ensemble*. For example, the single spin might be an isolated proton in a single molecule, while the ensemble would be a normal NMR sample made up of a large number of such molecules. In an NMR experiment, the observable magnetization comes from the whole sample; often it is called the *bulk magnetization* to emphasize this point. Each spin in the sample makes a small contribution to the bulk magnetization. The processes of going from a system of one spin to one of many is called *ensemble averaging*.

The wavefunction for one spin can be written

$$\left|\psi(t)\right\rangle = c_\alpha(t)\left|\alpha\right\rangle + c_\beta(t)\left|\beta\right\rangle$$

where $c_\alpha(t)$ and $c_\beta(t)$ are coefficients which depend on time and which in general are complex numbers. Such a wavefunction is called a *superposition state*, the name deriving from the fact that it is a sum of contributions from different wavefunctions.

In elementary quantum mechanics it is all too easy to fall into the erroneous view that "the spin must be either up or down, that is in state α or state β". This simply is not true; quantum mechanics makes no such claim.

1.6.1 Observables

The *x*-, *y*- and *z*-magnetizations are proportional to the expectation values of the operators I_x, I_y and I_z. For brevity, $c_\alpha(t)$ will be written c_α, the time dependence being implied.

$I_z|\alpha\rangle = (1/2)\,|\alpha\rangle$

$I_z|\beta\rangle = -(1/2)\,|\beta\rangle$

$\langle\alpha|\beta\rangle = \langle\beta|\alpha\rangle = 0$

$\langle\alpha|\alpha\rangle = \langle\beta|\beta\rangle = 1$

Consider first the expectation value of I_z (section 1.2.5)

$$\begin{aligned}
\left\langle I_z\right\rangle &= \frac{\left(c_\alpha^*\langle\alpha| + c_\beta^*\langle\beta|\right)I_z\left(c_\alpha|\alpha\rangle + c_\beta|\beta\rangle\right)}{\left(c_\alpha^*\langle\alpha| + c_\beta^*\langle\beta|\right)\left(c_\alpha|\alpha\rangle + c_\beta|\beta\rangle\right)} \\
&= \frac{c_\alpha^* c_\alpha\langle\alpha|I_z|\alpha\rangle + c_\beta^* c_\alpha\langle\beta|I_z|\alpha\rangle + c_a^* c_\beta\langle\alpha|I_z|\beta\rangle + c_\beta^* c_\beta\langle\beta|I_z|\beta\rangle}{c_\alpha^* c_\alpha\langle\alpha|\alpha\rangle + c_\beta^* c_\alpha\langle\beta|\alpha\rangle + c_a^* c_\beta\langle\alpha|\beta\rangle + c_\beta^* c_\beta\langle\beta|\beta\rangle} \\
&= \frac{\frac{1}{2}c_\alpha^* c_\alpha\langle\alpha|\alpha\rangle + \frac{1}{2}c_\beta^* c_\alpha\langle\beta|\alpha\rangle + \left(-\frac{1}{2}\right)c_a^* c_\beta\langle\alpha|\beta\rangle + c_\beta^* c_\beta\left(-\frac{1}{2}\right)\langle\beta|\beta\rangle}{c_\alpha^* c_\alpha\times 1 + c_\beta^* c_\alpha\times 0 + c_a^* c_\beta\times 0 + c_\beta^* c_\beta\times 1} \\
&= \frac{\frac{1}{2}c_\alpha^* c_\alpha\times 1 + \frac{1}{2}c_\beta^* c_\alpha\times 0 + \left(-\frac{1}{2}\right)c_a^* c_\beta\times 0 + c_\beta^* c_\beta\left(-\frac{1}{2}\right)\times 1}{c_\alpha^* c_\alpha + c_\beta^* c_\beta} \\
&= \frac{1}{2}\frac{\left(c_\alpha^* c_\alpha - c_\beta^* c_\beta\right)}{\left(c_\alpha^* c_\alpha + c_\beta^* c_\beta\right)}
\end{aligned}$$

Extensive use has been made of the facts that the two wavefunctions $|\alpha\rangle$ and $|\beta\rangle$ are normalized and orthogonal to one another (section 1.3.2), and that the effect of I_z on these wavefunctions is know (Eqn. [1.10]).

To simplify matters, it will be assumed that the wavefunction $\psi(t)$ is normalized so that $\langle\psi|\psi\rangle = 1$; this implies that $c_\alpha^* c_\alpha + c_\beta^* c_\beta = 1$.

Using this approach, it is also possible to determine the expectation values of I_x and I_y. In summary:

$$\langle I_z \rangle = \tfrac{1}{2}\left(c_\alpha^* c_\alpha - c_\beta^* c_\beta\right) \qquad \langle I_x \rangle = \tfrac{1}{2}\left(c_\beta^* c_\alpha + c_\alpha^* c_\beta\right)$$
$$\langle I_y \rangle = \tfrac{i}{2}\left(c_\beta^* c_\alpha - c_\alpha^* c_\beta\right) \qquad [1.14]$$

It is interesting to note that if the spin were to be purely in state $|\alpha\rangle$, such that $c_\alpha = 1$, $c_\beta = 0$, there would be no *x*- and no *y*-magnetization. The fact that such magnetization is observed in an NMR experiment implies that the spins must be in superposition states.

The coefficients c_α and c_β are in general complex, and it is sometimes useful to rewrite them in the (r/ϕ) format (see section 1.1.2)

$$c_\alpha = r_\alpha \exp(i\phi_\alpha) \qquad c_\beta = r_\alpha \exp(i\phi_\beta)$$
$$c_\alpha^* = r_\alpha \exp(-i\phi_\alpha) \qquad c_\beta^* = r_\beta \exp(-i\phi_\beta)$$

Using these, the expectation values for $I_{x,y,z}$ become:

$$\langle I_z \rangle = \tfrac{1}{2}\left(r_\alpha^2 - r_\beta^2\right) \qquad \langle I_x \rangle = r_\alpha r_\beta \cos(\phi_\alpha - \phi_\beta)$$
$$\langle I_y \rangle = r_\alpha r_\beta \sin(\phi_\alpha - \phi_\beta)$$

The normalization condition, $c_\alpha^* c_\alpha + c_\beta^* c_\beta = 1$, becomes $\left(r_\alpha^2 + r_\beta^2\right) = 1$ in this format. Recall that the *r*'s are always positive and real.

1.6.1.1 Comment on these observables

The expectation value of I_z can take any value between $\frac{1}{2}$ (when $r_\alpha = 1$, $r_\beta = 0$) and $-\frac{1}{2}$ (when $r_\alpha = 0$, $r_\beta = 1$). This is in contrast to the quantum number m_I which is restricted to values $\pm\frac{1}{2}$ ("spin up or spin down"). Likewise, the expectation values of I_x and I_y can take any values between $-\frac{1}{2}$ and $+\frac{1}{2}$, depending on the exact values of the coefficients.

1.6.1.2 Ensemble averages; bulk magnetization

In order to compute, say, the *x*-magnetization from the whole sample, it is necessary to add up the individual contributions from each spin:

$$\overline{\langle I_x \rangle} = \langle I_x \rangle_1 + \langle I_x \rangle_2 + \langle I_x \rangle_3 + \ldots$$

where $\overline{\langle I_x \rangle}$ is the ensemble average, that is the sum over the whole sample. The contribution from the ith spin, $\langle I_x \rangle_i$, can be calculate using Eqn. [1.14].

$$\begin{aligned}
\overline{\langle I_x \rangle} &= \langle I_x \rangle_1 + \langle I_x \rangle_2 + \langle I_x \rangle_3 + \ldots \\
&= \tfrac{1}{2}\left(c_\beta^* c_\alpha + c_\beta^* c_\alpha\right)_1 + \tfrac{1}{2}\left(c_\beta^* c_\alpha + c_\beta^* c_\alpha\right)_2 + \tfrac{1}{2}\left(c_\beta^* c_\alpha + c_\beta^* c_\alpha\right)_3 + \ldots \\
&= \tfrac{1}{2}\left(\overline{c_\beta^* c_\alpha} + \overline{c_\beta^* c_\alpha}\right) \\
&= \overline{r_\alpha r_\beta \cos\left(\phi_\alpha - \phi_\beta\right)}
\end{aligned}$$

On the third line the over-bar is short hand for the average written out explicitly in the previous line. The fourth line is the same as the third, but expressed in the (r,ϕ) format (Eqn. [1.15]).

The contribution from each spin depends on the values of $r_{\alpha,\beta}$ and $\phi_{\alpha,\beta}$ which in general it would be quite impossible to know for each of the enormous number of spins in the sample. However, when the spins are in equilibrium it is reasonable to assume that the phases $\phi_{\alpha,\beta}$ of the individual spins are distributed *randomly*. As $\langle I_x \rangle = r_\alpha r_\beta \cos(\phi_\alpha - \phi_\beta)$ for each spin, the random phases result in the cosine term being randomly distributed in the range –1 to +1, and as a result the sum of all these terms is zero. That is, at equilibrium

$$\overline{\langle I_x \rangle}_{eq} = 0 \qquad \overline{\langle I_y \rangle}_{eq} = 0$$

This is in accord with the observation that at equilibrium there is no transverse magnetization.

The situation for the *z*-magnetization is somewhat different:

$$\begin{aligned}\overline{\langle I_z \rangle} &= \langle I_z \rangle_1 + \langle I_z \rangle_2 + \langle I_z \rangle_3 + \ldots \\ &= \tfrac{1}{2}\left(r_{\alpha,1}^2 - r_{\beta,1}^2\right) + \tfrac{1}{2}\left(r_{\alpha,2}^2 - r_{\beta,2}^2\right) + \tfrac{1}{2}\left(r_{\alpha,3}^2 - r_{\beta,3}^2\right) \\ &= \tfrac{1}{2}\left(r_{\alpha,1}^2 + r_{\alpha,2}^2 + r_{\alpha,3}^2 + \ldots\right) - \tfrac{1}{2}\left(r_{\beta,1}^2 + r_{\beta,2}^2 + r_{\beta,3}^2 + \ldots\right) \\ &= \tfrac{1}{2}\left(\overline{r_\alpha^2} - \overline{r_\beta^2}\right)\end{aligned}$$

Note that the phases ϕ do not enter into this expression, and recall that the *r*'s are positive.

This is interpreted in the following way. In the superposition state $c_\alpha|\alpha\rangle + c_\beta|\beta\rangle$, $c_\alpha c_\alpha^* = r_\alpha^2$ can be interpreted as the *probability* of finding the spin in state $|\alpha\rangle$, and $c_\beta c_\beta^* = r_\beta^2$ as likewise the probability of finding the spin in state $|\beta\rangle$. The idea is that if the state of any one spin is determined by experiment the outcome is always either $|\alpha\rangle$ or $|\beta\rangle$. However, if a large number of spins are taken, initially all in identical superposition states, and the spin states of these determined, a fraction $c_\alpha c_\alpha^*$ would be found to be in state $|\alpha\rangle$, and a fraction $c_\beta c_\beta^*$ in state $|\beta\rangle$.

From this it follows that

$$\overline{\langle I_z \rangle} = \tfrac{1}{2} P_\alpha - \tfrac{1}{2} P_\beta$$

where P_α and P_β are the total probabilities of finding the spins in state $|\alpha\rangle$ or $|\beta\rangle$, respectively. These total probabilities can be identified with the populations of two levels $|\alpha\rangle$ or $|\beta\rangle$. The *z*-magnetization is thus proportional to the population *difference* between the two levels, as expected. At equilibrium, this population difference is predicted by the Boltzmann distribution.

1.6.2 Time dependence

The time dependence of the system is found by solving the time dependent Schrödinger equation, Eqn. [1.13]. From its form, it is clear that the exact nature of the time dependence will depend on the Hamiltonian *i.e.* it will be different for periods of free precession and radiofrequency pulses.

1.6.2.1 Free precession

The Hamiltonian (in a fixed set of axes, not a rotating frame) is $\omega_0 I_z$ and at time = 0 the wavefunction will be assumed to be

$$\left|\psi(0)\right\rangle = c_\alpha(0)|\alpha\rangle + c_\beta(0)\left|\beta\right\rangle$$
$$= r_\alpha(0)\exp\left[i\phi_\alpha(0)\right]|\alpha\rangle + r_\beta(0)\exp\left[i\phi_\beta(0)\right]\left|\beta\right\rangle$$

$I_z|\alpha\rangle = (1/2)\,|\alpha\rangle$

$I_z|\beta\rangle = -(1/2)\,|\beta\rangle$

$\langle\alpha|\beta\rangle = \langle\beta|\alpha\rangle = 0$

$\langle\alpha|\alpha\rangle = \langle\beta|\beta\rangle = 1$

The time dependent Schrödinger equation can therefore be written as

$$\frac{\mathrm{d}\psi(t)}{\mathrm{d}t} = -iH\psi$$
$$\frac{\mathrm{d}\left[c_\alpha(t)|\alpha\rangle + c_\beta(t)\left|\beta\right\rangle\right]}{\mathrm{d}t} = -i\omega_0 I_z\left[c_\alpha(t)|\alpha\rangle + c_\beta(t)\left|\beta\right\rangle\right]$$
$$= -i\omega_0\left[\tfrac{1}{2}c_\alpha(t)|\alpha\rangle - \tfrac{1}{2}c_\beta(t)\left|\beta\right\rangle\right]$$

where use has been made of the properties of I_z when acting on the wavefunctions $|\alpha\rangle$ and $|\beta\rangle$ (section 1.4 Eqn. [1.10]). Both side of this equation are left-multiplied by $\langle\alpha|$, and the use is made of the orthogonality of $|\alpha\rangle$ and $|\beta\rangle$

$$\frac{\mathrm{d}\left[\langle\alpha|c_\alpha(t)|\alpha\rangle + \langle\alpha|c_\beta(t)\left|\beta\right\rangle\right]}{\mathrm{d}t} = -i\omega_0\left[\langle\alpha|\tfrac{1}{2}c_\alpha(t)|\alpha\rangle - \langle\alpha|\tfrac{1}{2}c_\beta(t)\left|\beta\right\rangle\right]$$
$$\frac{\mathrm{d}c_\alpha(t)}{\mathrm{d}t} = -\tfrac{1}{2}i\omega_0\, c_\alpha(t)$$

The corresponding equation for c_β is found by left multiplying by $\langle\beta|$.

$$\frac{\mathrm{d}c_\beta(t)}{\mathrm{d}t} = \tfrac{1}{2}i\omega_0\, c_\beta(t)$$

These are both standard differential equations whose solutions are well know:

$$c_\alpha(t) = c_\alpha(0)\exp\left(-\tfrac{1}{2}i\omega_0\, t\right) \qquad c_\beta(t) = c_\beta(0)\exp\left(\tfrac{1}{2}i\omega_0\, t\right)$$

All that happens is that the coefficients oscillate in phase, at the Larmor frequency.

To find the time dependence of the expectation values of $I_{x,y,z}$, these expressions for $c_{\alpha,\beta}(t)$ are simply substituted into Eqn. [1.14]

$$\begin{aligned}\langle I_z\rangle(t) &= \tfrac{1}{2}\left(c_\alpha^*(t)c_\alpha(t) - c_\beta^*(t)c_\beta(t)\right)\\ &= \tfrac{1}{2}c_\alpha^*(0)c_\alpha(0)\exp\left(\tfrac{1}{2}i\omega_0 t\right)\exp\left(-\tfrac{1}{2}i\omega_0 t\right)\\ &\qquad - \tfrac{1}{2}c_\beta^*(0)c_\beta(0)\exp\left(-\tfrac{1}{2}i\omega_0 t\right)\exp\left(\tfrac{1}{2}i\omega_0 t\right)\\ &= \tfrac{1}{2}c_\alpha^*(0)c_\alpha(0) - \tfrac{1}{2}c_\beta^*(0)c_\beta(0)\end{aligned}$$

As expected, the *z*-component does not vary with time, but remains fixed at its initial value. However, the *x*- and *y*-components vary according to the following which can be found in the same way

$$\langle I_x\rangle(t) = \tfrac{1}{2}r_\alpha(0)r_\beta(0)\cos\left(\omega_0 t - \phi_\beta(0) + \phi_\alpha(0)\right)$$
$$\langle I_y\rangle(t) = \tfrac{1}{2}r_\alpha(0)r_\beta(0)\sin\left(\omega_0 t - \phi_\beta(0) + \phi_\alpha(0)\right)$$

Again, as expected, these components oscillate at the Larmor frequency.

1.6.2.2 Pulses

More interesting is the effect of radiofrequency pulses, for which the Hamiltonian (in the rotating frame) is $\omega_1 I_x$. Solving the Schrödinger equation is a little more difficult than for the case above, and yields the result

$$c_\alpha(t) = c_\alpha(0)\cos\tfrac{1}{2}\omega_1 t - ic_\beta(0)\sin\tfrac{1}{2}\omega_1 t$$
$$c_\beta(t) = c_\beta(0)\cos\tfrac{1}{2}\omega_1 t - ic_\alpha(0)\sin\tfrac{1}{2}\omega_1 t$$

In contrast to free precession, the pulse actually causes that coefficients to change, rather than simply to oscillate in phase. The effect is thus much more significant.

A lengthy, but straightforward, calculation gives the following result for $\langle I_y\rangle$

$$\begin{aligned}\langle I_y\rangle(t) &= \tfrac{i}{2}\left(c_\alpha(0)c_\beta^*(0) - c_\alpha^*(0)c_\beta(0)\right)\cos\omega_1 t\\ &\qquad - \tfrac{1}{2}\left(c_\alpha(0)c_\alpha^*(0) - c_\beta^*(0)c_\beta(0)\right)\sin\omega_1 t\end{aligned} \qquad [1.16]$$

The first term in brackets on the right is simply $\langle I_y\rangle$ at time zero (compare Eqn. [1.14]). The second term is $\langle I_z\rangle$ at time zero (compare Eqn. [1.14]). So, $\langle I_y\rangle(t)$ can be written

$$\langle I_y\rangle(t) = \langle I_y\rangle(0)\cos\omega_1 t - \langle I_z\rangle(0)\sin\omega_1 t$$

This result is hardly surprising. It simply says that if a pulse is applied about the *x*-axis, a component which was initially along *z* $\langle I_z \rangle(0)$ is rotated towards *y*. The rotation from *z* to *y* is complete when $\omega_1 t = \pi/2$, *i.e.* a 90° pulse.

The result of Eqn. [1.16] applies to just one spin. To make it apply to the whole sample, the ensemble average must be taken

$$\overline{\langle I_y \rangle}(t) = \overline{\langle I_y \rangle}(0)\cos\omega_1 t - \overline{\langle I_z \rangle}(0)\sin\omega_1 t \qquad [1.17]$$

Suppose that time zero corresponds to equilibrium. As discussed above, at equilibrium then ensemble average of the *y* components is zero, but the *z* components are not, so

$$\overline{\langle I_y \rangle}(t) = -\langle I_z \rangle_{\text{eq}} \sin\omega_1 t$$

where $\langle I_z \rangle_{\text{eq}}$ is the equilibrium ensemble average of the *z* components. In words, Eqn. [1.17] says that the pulse rotates the equilibrium magnetization from *z* to –*y*, just as expected.

1.6.3 Coherences

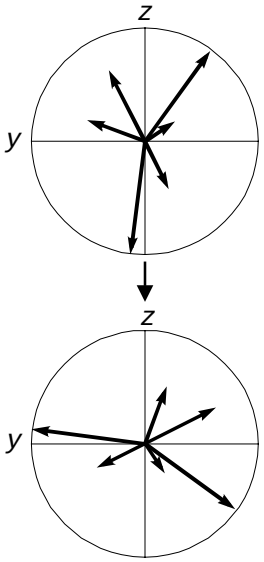

Each spin makes a contribution to the magnetization in each direction (top diagram). A pulse, here 90° about the *x*-axis, rotates all of these contributions in the same sense through the same angle (bottom diagram).

Transverse magnetization is associated in quantum mechanics with what is known as a *coherence*. It was seen above that at equilibrium there is no transverse magnetization, not because each spin does not make a contribution, but because these contributions are random and so add up to zero. However, at equilibrium the *z*-components do not cancel one another, leading to a net magnetization along the *z*-direction.

During the pulse, the *z*-component from each spin is rotated towards *y*, according to Eqn. [1.17]. The key point is that all the contributions from all the spins, although they start in random positions in the *yz*-plane, are rotated through the *same* angle. As a result, what started out as a net alignment in the *z*-direction rotates in the *zy*-plane, becoming a net alignment along –*y* after a 90° pulse.

Another interpretation is to look at the way in which the individual coefficients vary during the pulse

$$c_\alpha(t) = c_\alpha(0)\cos\tfrac{1}{2}\omega_1 t - ic_\beta(0)\sin\tfrac{1}{2}\omega_1 t$$
$$c_\beta(t) = c_\beta(0)\cos\tfrac{1}{2}\omega_1 t - ic_\alpha(0)\sin\tfrac{1}{2}\omega_1 t$$

In words, what happens is that the size of the coefficients at time *t* are related to those at time zero in a way which is the *same* for all spins in the sample. Although the phases are random at time zero, for each spin the phase associated

with c_α at time zero is transferred to c_β, and *vice versa*. It is this correlation of phases between the two coefficients which leads to an overall observable signal from the sample.

1.7 Density matrix

The approach used in the previous section is rather inconvenient for calculating the outcome of NMR experiments. In particular, the need for ensemble averaging after the calculation has been completed is especially difficult. It turns out that there is an alternative way of casting the Schrödinger equation which leads to a much more convenient framework for calculation – this is *density matrix* theory. This theory, can be further modified to give an operator version which is generally the most convenient for calculations in multiple pulse NMR.

First, the idea of *matrix representations* of operators needs to be introduced.

1.7.1 Matrix representations

An operator, Q, can be represented as a matrix in a particular *basis set* of functions. A basis set is a complete set of wavefunctions which are adequate for describing the system, for example in the case of a single spin the two functions $|\alpha\rangle$ and $|\beta\rangle$ form a suitable basis. In larger spin systems, more basis functions are needed, for example the four product functions described in section 1.4.1.2 form such a basis for a two spin system.

The matrix form of Q is defined in this two-dimensional representation is defined as

$$Q = \begin{pmatrix} \langle\alpha|Q|\alpha\rangle & \langle\alpha|Q|\beta\rangle \\ \langle\beta|Q|\alpha\rangle & \langle\beta|Q|\beta\rangle \end{pmatrix}$$

Each of the matrix elements, Q_{ij}, is calculated from an integral of the form $\langle i|Q|j\rangle$, where $|i\rangle$ and $|j\rangle$ are two of the basis functions. The matrix element Q_{ij} appears in the ith row and the jth column.

1.7.1.1 One spin

Particularly important are the matrix representations of the angular momentum operators. For example, I_z:

$I_z|\alpha\rangle = (1/2)\,|\alpha\rangle$

$I_z|\beta\rangle = -(1/2)\,|\beta\rangle$

$\langle\alpha|\beta\rangle = \langle\beta|\alpha\rangle = 0$

$\langle\alpha|\alpha\rangle = \langle\beta|\beta\rangle = 1$

$$I_z = \begin{pmatrix} \langle\alpha|I_z|\alpha\rangle & \langle\alpha|I_z|\beta\rangle \\ \langle\beta|I_z|\alpha\rangle & \langle\beta|I_z|\beta\rangle \end{pmatrix}$$
$$= \begin{pmatrix} \langle\alpha|\tfrac{1}{2}|\alpha\rangle & \langle\alpha|-\tfrac{1}{2}|\beta\rangle \\ \langle\beta|\tfrac{1}{2}|\alpha\rangle & \langle\beta|-\tfrac{1}{2}|\beta\rangle \end{pmatrix}$$
$$= \begin{pmatrix} \tfrac{1}{2} & 0 \\ 0 & -\tfrac{1}{2} \end{pmatrix}$$

As usual, extensive use have been made of the properties of I_z and the orthonormality of the basis functions (see sections 1.3.2).

The representations of I_x and I_y are easily found, by expressing them in terms of the raising and lowering operators (section 1.3.3), to be

$$I_x = \begin{pmatrix} 0 & \tfrac{1}{2} \\ \tfrac{1}{2} & 0 \end{pmatrix} \qquad I_y = \begin{pmatrix} 0 & -\tfrac{i}{2} \\ \tfrac{i}{2} & 0 \end{pmatrix}$$

1.7.1.2 Direct products

The easiest way to find the matrix representations of angular momentum operators in larger basis sets is to use the *direct product*.

When two $n\times n$ matrices are multiplied together the result is another $n\times n$ matrix. The rule is that the ijth element of the product is found by multiplying, element by element, the ith row by the jth column and adding up all the products. For example:

$$\begin{pmatrix} a & b \\ c & d \end{pmatrix}\begin{pmatrix} p & q \\ r & s \end{pmatrix} = \begin{pmatrix} ap+br & aq+bs \\ cp+dr & cq+ds \end{pmatrix}$$

The direct product, symbolized $\otimes$, of two $n\times n$ matrices results in a larger matrix of size $2n\times 2n$. The rule for this multiplication is difficult to express formally but easy enough to describe:

$$\begin{pmatrix} a & b \\ c & d \end{pmatrix}\otimes\begin{pmatrix} p & q \\ r & s \end{pmatrix} = \begin{pmatrix} a\times\begin{pmatrix} p & q \\ r & s \end{pmatrix} & b\times\begin{pmatrix} p & q \\ r & s \end{pmatrix} \\ c\times\begin{pmatrix} p & q \\ r & s \end{pmatrix} & d\times\begin{pmatrix} p & q \\ r & s \end{pmatrix} \end{pmatrix}$$

The right-hand matrix is duplicated four times over, because there are four elements in the left-hand matrix. Each duplication is multiplied by the

corresponding element from the left-hand matrix. The final result is

$$\begin{pmatrix} a & b \\ c & d \end{pmatrix} \otimes \begin{pmatrix} p & q \\ r & s \end{pmatrix} = \left(\begin{array}{cc|cc} ap & aq & bp & bq \\ ar & as & br & bs \\ \hline cp & cq & dp & dq \\ cr & cs & dr & ds \end{array}\right) \equiv \begin{pmatrix} ap & aq & bp & bq \\ ar & as & br & bs \\ cp & cq & dp & dq \\ cr & cs & dr & ds \end{pmatrix}$$

(the lines in the central matrix are just to emphasise the relation to the 2×2 matrices, they have no other significance).

The same rule applies to matrices with just a single row (row vectors)

$$(a,b) \otimes (p,q) = (ap, aq, bp, bq)$$

1.7.1.3 Two spins

The basis set for a single spin can be written $(|\alpha_1\rangle, |\beta_1\rangle)$; the basis set for two spins can be found from the direct product of two such basis sets, one for each spin:

$$\left(|\alpha_1\rangle, |\beta_1\rangle\right) \otimes \left(|\alpha_2\rangle, |\beta_2\rangle\right) = \left(|\alpha_1\rangle|\alpha_2\rangle, |\alpha_1\rangle|\beta_2\rangle, |\beta_1\rangle|\alpha_2\rangle, |\beta_1\rangle|\beta_2\rangle\right)$$

In this basis the matrix representation of I_{1x} can be found by writing the operator as the direct product

$$I_{1x} \otimes E_2 \qquad [1.18]$$

where E is the unit matrix

$$E = \begin{pmatrix} 1 & 0 \\ 0 & 1 \end{pmatrix}$$

The subscript 2 on the E in Eqn. [1.18] is in a sense superfluous as the unit matrix is the same for all spins. However, it is there to signify that in the direct product there must be an operator for each spin. Furthermore, these operators must occur in the correct order, with that for spin 1 leftmost and so on. So, to find the matrix representation of I_{2x} the required direct product is

$$E_1 \otimes I_{2x}$$

In matrix form $E_1 \otimes I_{2x}$ is

$$E_1 \otimes I_{2x} = \begin{pmatrix} 1 & 0 \\ 0 & 1 \end{pmatrix} \otimes \begin{pmatrix} 0 & \frac{1}{2} \\ \frac{1}{2} & 0 \end{pmatrix} = \begin{pmatrix} 0 & \frac{1}{2} & 0 & 0 \\ \frac{1}{2} & 0 & 0 & 0 \\ 0 & 0 & 0 & \frac{1}{2} \\ 0 & 0 & \frac{1}{2} & 0 \end{pmatrix}$$

and $I_{1x} \otimes E_2$ is

$$I_{1x} \otimes E_2 = \begin{pmatrix} 0 & \frac{1}{2} \\ \frac{1}{2} & 0 \end{pmatrix} \otimes \begin{pmatrix} 1 & 0 \\ 0 & 1 \end{pmatrix} = \begin{pmatrix} 0 & 0 & \frac{1}{2} & 0 \\ 0 & 0 & 0 & \frac{1}{2} \\ \frac{1}{2} & 0 & 0 & 0 \\ 0 & \frac{1}{2} & 0 & 0 \end{pmatrix}$$

As a final example $I_{1x} \otimes I_{2y}$ is

$$I_{1x} \otimes I_{2y} = \begin{pmatrix} 0 & \frac{1}{2} \\ \frac{1}{2} & 0 \end{pmatrix} \otimes \begin{pmatrix} 0 & -\frac{i}{2} \\ \frac{i}{2} & 0 \end{pmatrix} = \begin{pmatrix} 0 & 0 & 0 & -\frac{i}{4} \\ 0 & 0 & \frac{i}{4} & 0 \\ 0 & -\frac{i}{4} & 0 & 0 \\ \frac{i}{4} & 0 & 0 & 0 \end{pmatrix}$$

All of these matrices are hermetian, which means that matrix elements related by reflection across the diagonal have the property that $Q_{ji} = Q_{ij}$*.

1.7.2 Density matrix

For a one spin system the density matrix, σ, is defined according to its elements

$$\sigma(t) = \begin{pmatrix} \overline{c_\alpha(t)c_\alpha^*(t)} & \overline{c_\alpha(t)c_\beta^*(t)} \\ \overline{c_\beta(t)c_\alpha^*(t)} & \overline{c_\beta(t)c_\beta^*(t)} \end{pmatrix}$$

where the over-bars indicate ensemble averaging. This matrix contains all the information needed to calculate any observable quantity. Formally, σ is defined in the following way:

$$\sigma(t) = \overline{\left|\psi(t)\right\rangle\left\langle\psi(t)\right|}$$

1.7.2.1 Observables

It can be shown that the expectation value of an operator, *Q*, is given by

$$\overline{\langle Q \rangle} = \mathrm{Tr}\left[\sigma Q\right]$$

where Tr[*A*] means take the *trace*, that is the sum of the diagonal elements, of the matrix *A*.

For example, the expectation value of I_z is

$$\begin{aligned}
\overline{\langle I_z \rangle} &= \mathrm{Tr}\left[\begin{pmatrix} \overline{c_\alpha(t)c_\alpha^*(t)} & \overline{c_\alpha(t)c_\beta^*(t)} \\ \overline{c_\beta(t)c_\alpha^*(t)} & \overline{c_\beta(t)c_\beta^*(t)} \end{pmatrix}\begin{pmatrix} \frac{1}{2} & 0 \\ 0 & -\frac{1}{2} \end{pmatrix}\right] \\
&= \mathrm{Tr}\left[\begin{pmatrix} \frac{1}{2}\overline{c_\alpha(t)c_\alpha^*(t)} & \cdots \\ \cdots & -\frac{1}{2}\overline{c_\beta(t)c_\beta^*(t)} \end{pmatrix}\right] \\
&= \tfrac{1}{2}\left(\overline{c_\alpha(t)c_\alpha^*(t)} - \overline{c_\beta(t)c_\beta^*(t)}\right) \\
&= \tfrac{1}{2}\left(\overline{r_\alpha^2} - \overline{r_\beta^2}\right)
\end{aligned}$$

This is directly comparable to the result obtained in section 1.6.1.2.

The very desirable feature of this definition of the density matrix and the trace property for calculation observables is that the ensemble averaging is done before the observable is computed.

The expectation value of I_x is

$$\begin{aligned}
\overline{\langle I_x \rangle} &= \mathrm{Tr}\left[\begin{pmatrix} \overline{c_\alpha(t)c_\alpha^*(t)} & \overline{c_\alpha(t)c_\beta^*(t)} \\ \overline{c_\beta(t)c_\alpha^*(t)} & \overline{c_\beta(t)c_\beta^*(t)} \end{pmatrix}\begin{pmatrix} 0 & \frac{1}{2} \\ \frac{1}{2} & 0 \end{pmatrix}\right] \\
&= \tfrac{1}{2}\left(\overline{c_\alpha(t)c_\beta^*(t)} + \overline{c_\beta(t)c_\alpha^*(t)}\right)
\end{aligned}$$

Again, this is directly comparable to the result obtained in section 1.6.1.2

The off diagonal elements of the density matrix can contribute to transverse magnetization, whereas the diagonal elements only contribute to longitudinal magnetization. In general, a non-zero off-diagonal element $\overline{c_i(t)c_j^*(t)}$ indicates a *coherence* involving levels *i* and *j*, whereas a diagonal element, $\overline{c_i(t)c_i^*(t)}$, indicates the population of level *i*.

From now on the ensemble averaging and time dependence will be taken as implicit and so the elements of the density matrix will be written simply $c_i c_j^*$ unless there is any ambiguity.

1.7.2.2 Equilibrium

As described in section 1.6.1.2, at equilibrium the phases of the super-position states are random and as a result the ensemble averages $\overline{c_\alpha(t)c_\beta^*(t)}$ and $\overline{c_\beta(t)c_\alpha^*(t)}$ are zero. This is easily seen by writing then in the r/ϕ format

$$\begin{aligned}\overline{c_\alpha c_\beta^*} &= \overline{r_\alpha \exp(i\phi_\alpha) r_\beta \exp(-i\phi_\beta)} \\ &= 0 \text{ at equilibrium}\end{aligned}$$

However, the diagonal elements do not average to zero but rather correspond to the populations, P_i, of the levels, as was described in section 1.6.1.2

$$\begin{aligned}\overline{c_\alpha c_\alpha^*} &= \overline{r_\alpha \exp(i\phi_\alpha) r_\alpha \exp(-i\phi_\alpha)} \\ &= \overline{r_\alpha^2} \\ &= P_\alpha\end{aligned}$$

The equilibrium density matrix for one spin is thus

$$\sigma_{\text{eq}} = \begin{pmatrix} P_\alpha & 0 \\ 0 & P_\beta \end{pmatrix}$$

As the energy levels in NMR are so closely spaced, it turns out that to an excellent approximation the populations can be written in terms of the average population of the two levels, P_{av}, and the difference between the two populations, Δ, where $\Delta = P_\alpha - P_\beta$

$$\sigma_{\text{eq}} = \begin{pmatrix} P_{\text{av}} + \frac{1}{2}\Delta & 0 \\ 0 & P_{\text{av}} - \frac{1}{2}\Delta \end{pmatrix}$$

Comparing this with the matrix representations of I_z and E, σ_{eq}, can be written

$$\begin{aligned} \sigma_{\text{eq}} &= P_{\text{av}} E + \Delta I_z \\ &= P_{\text{av}} \begin{pmatrix} 1 & 0 \\ 0 & 1 \end{pmatrix} + \Delta \begin{pmatrix} \frac{1}{2} & 0 \\ 0 & -\frac{1}{2} \end{pmatrix} \end{aligned}$$

It turns out that the part from the matrix E does not contribute to any observables, so for simplicity it is ignored. The factor Δ depends on details of the spin system and just scales the final result, so often it is simply set to 1. With these simplifications σ_{eq} is simply I_z.

1.7.2.3 Evolution

The density operator evolves in time according to the following equation, which can be derived from the time dependent Schrödinger equation (section 1.5):

$$\frac{\mathrm{d}\sigma(t)}{\mathrm{d}t} = -i\left[H\sigma(t) - \sigma(t)H\right] \qquad [1.19]$$

Note that as H and σ are operators their order is significant. Just as in section 1.5 the evolution depends on the prevailing Hamiltonian.

If H is time independent (something that can usually be arranged by using a rotating frame, see section 1.4.2), the solution to Eqn. [1.19] is straightforward

$$\sigma(t) = \exp(-iHt)\sigma(0)\exp(iHt)$$

where again the ordering of the operators must be preserved. All the terms is this equation can be thought of as either matrices or operators, and it is the second of these options which is discussed in the next section.

1.7.3 Operator form of the density matrix

So far, Hamiltonians have been written in terms of operators, specifically the angular momentum operators $I_{x,y,z}$, and it has also been seen that these operators represent observable quantities, such as magnetizations. In addition, it was shown in section 1.1.2.2 that the equilibrium density matrix has the same form as I_z. These observations naturally lead to the idea that it might be convenient also to write the density matrix in terms of the angular momentum operators.

Specifically, the idea is to expand the density matrix as a combination of the operators:

$$\sigma(t) = a(t)I_z + b(t)I_y + c(t)I_z$$

where *a*, *b* and *c* are coefficients which depend on time.

1.7.3.1 Observables

From this form of the density matrix, the expectation value of, for example, I_x can be computed in the usual way (section 1.7.2.1).

$$\begin{aligned}\langle I_x \rangle &= \mathrm{Tr}\left[\sigma I_x\right] \\ &= \mathrm{Tr}\left[\left(aI_x + bI_y + cI_z\right)I_x\right] \\ &= \mathrm{Tr}\left[aI_xI_x\right] + \mathrm{Tr}\left[bI_yI_x\right] + \mathrm{Tr}\left[cI_zI_x\right]\end{aligned}$$

where to get to the last line the property that the trace of a sum of matrices is equal to the sum of the traces of the matrices has been used.

It turns out that $\mathrm{Tr}[I_pI_q]$ is zero unless $p = q$ when the trace is $= \frac{1}{2}$; for example

$$\begin{aligned}\mathrm{Tr}\left[I_xI_x\right] &= \mathrm{Tr}\left[\begin{pmatrix} 0 & \frac{1}{2} \\ \frac{1}{2} & 0 \end{pmatrix}\begin{pmatrix} 0 & \frac{1}{2} \\ \frac{1}{2} & 0 \end{pmatrix}\right] \\ &= \mathrm{Tr}\left[\begin{pmatrix} \frac{1}{4} & \cdots \\ \cdots & \frac{1}{4} \end{pmatrix}\right] = \frac{1}{2}\end{aligned}$$

$$\begin{aligned}\mathrm{Tr}\left[I_xI_z\right] &= \mathrm{Tr}\left[\begin{pmatrix} 0 & \frac{1}{2} \\ \frac{1}{2} & 0 \end{pmatrix}\begin{pmatrix} \frac{1}{2} & 0 \\ 0 & -\frac{1}{2} \end{pmatrix}\right] \\ &= \mathrm{Tr}\left[\begin{pmatrix} 0 & \cdots \\ \cdots & 0 \end{pmatrix}\right] = 0\end{aligned}$$

In summary it is found that

$$\langle I_x \rangle = \tfrac{1}{2}a \quad \langle I_y \rangle = \tfrac{1}{2}b \quad \langle I_z \rangle = \tfrac{1}{2}c$$

This is a very convenient result. By expressing the density operator in the form $\sigma(t) = a(t)I_z + b(t)I_y + c(t)I_z$ the *x*-, *y*- and *z*-magnetizations can be deduced just by inspection as being proportional to $a(t)$, $b(t)$, and $c(t)$ respectively (the factor of one half is not important). This approach is further developed in the lecture 2 where the *product operator* method is introduced.

1.7.3.2 Evolution

The evolution of the density matrix follows the equation

$$\sigma(t) = \exp(-iHt)\sigma(0)\exp(iHt)$$

Often the Hamiltonian will be a sum of terms, for example, in the case of free precession for two spins $H = \Omega_1 I_{1z} + \Omega_2 I_{2z}$. The exponential of the *sum* of two operators can be expressed as a *product* of two exponentials provided the operators *commute*

$$\exp(A + B) = \exp(A)\exp(B) \quad \text{provided } A \text{ and } B \text{ commute}$$

Commuting operators are ones whose effect is unaltered by changing their order: *i.e.* $AB\psi = BA\psi$; not all operators commute with one another.

Luckily, operators for different spins do commute so, for the free precession Hamiltonian

$$\begin{aligned}\exp(-iHt) &= \exp\left(-i\left[\Omega_1 I_{1z} + \Omega_2 I_{2z}\right]t\right)\\ &= \exp\left(-i\Omega_1 I_{1z}t\right)\exp\left(-i\Omega_2 I_{2z}t\right)\end{aligned}$$

The evolution of the density matrix can then be written

$$\sigma(t) = \exp\left(-i\Omega_1 I_{1z}t\right)\exp\left(-i\Omega_2 I_{2z}t\right)\sigma(0)\exp\left(i\Omega_1 I_{1z}t\right)\exp\left(i\Omega_2 I_{2z}t\right)$$

The operators for the evolution due to offsets and couplings also commute with one another.

For commuting operators the order is immaterial. This applies also to their exponentials, *e.g.* $\exp(A)\,B = B\exp(A)$. This property is used in the following

$$\begin{aligned}\exp\left(-i\Omega_1 I_{1z}t\right)I_{2x}\exp\left(i\Omega_1 I_{1z}t\right) &= \exp\left(-i\Omega_1 I_{1z}t\right)\exp\left(i\Omega_1 I_{1z}t\right)I_{2x}\\ &= \exp\left(-i\Omega_1 I_{1z}t + i\Omega_1 I_{1z}t\right)I_{2x}\\ &= \exp(0)I_{2x} = I_{2x}\end{aligned}$$

In words this says that the offset of spin 1 causes no evolution of transverse magnetization of spin 2.

These various properties will be used extensively in lecture 2.

2 Product Operators

The product operator formalism is a complete and rigorous quantum mechanical description of NMR experiments; the formalism is a version of density matrix theory and is well suited to calculating the outcome of modern multiple-pulse experiments.

One particularly appealing feature is the fact that the operators have a clear physical meaning and that the effects of pulses and delays can be thought of as geometrical rotations. To emphasise this connection the discussion will start with a brief summary of the vector model.

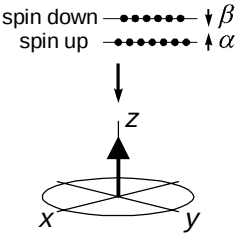

Unequal populations of the two energy levels give rise to a net magnetization, represented as a vector along the *z*-axis.

2.1 Vector model of NMR

The vector model is a complete description of the behaviour of an ensemble (a macroscopic sample) of non-interacting spin-half nuclei. Each spin has two energy levels and at equilibrium the lower of these is more populated. The result is a net magnetization of the sample along the direction of the applied magnetic field (taken to be the *z*-direction). The vector model focuses entirely on the behaviour of this magnetization, which can be represented as a vector.

Radiofrequency pulses are represented as rotations about the *x*- or *y*-axes; if the radiofrequency field strength is ω_1 (rad s^{-1}) then a pulse applied for a time *t* causes a rotation through an angle α, where $\alpha = \omega_1 t$. For example a 90° pulse about the *x*-axis has $\omega_1 t = \pi/2$ and rotates magnetization from the *z*-axis onto the –*y*-axis.

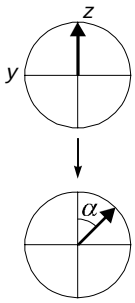

A pulse about the *x*-axis rotates the magnetization through an angle α in the *yz*-plane. The picture shows the view down the *x*-axis.

Free precession is represented as a rotation about the *z*-axis at frequency Ω (rad s^{-1}), where Ω is the offset (that is the difference between the Larmor frequency and the transmitter frequency). Free precession for a time *t* causes a rotation through an angle α, where $\alpha = \Omega t$.

Only *x*- and *y*-magnetization are directly observable in an NMR experiment; it is the precession of the magnetization in the *xy*-plane which gives rise to the free induction signal.

2.1.1 Example – the conventional pulse-acquire experiment

Assume that the system starts at equilibrium; a pulse of flip angle α is applied and then the free induction signal is recorded. Let the equilibrium magnetization (aligned along the *z*-axis) have size M_0. After the pulse the *z*- and *y*-magnetization (M_z and M_y, respectively) are

$$M_z = \cos \alpha M_0 \qquad M_y = -\sin \alpha M_0$$

Free precession, which is a rotation about the *z*-axis, has no effect on the *z*-component. The *y*-component rotates in the *xy*-plane giving the following transverse components after time *t*

$$M_y(t) = -\sin\alpha \cos\Omega t\, M_0 \qquad M_x(t) = \sin\alpha \sin\Omega t\, M_0$$

It is these transverse (that is, *x* and *y*) components of the magnetization that are detected in NMR experiments. It is seen that these are oscillating at frequency Ω, and that their overall size depends on the sine of the flip angle *i.e.* they are a maximum for a 90° pulse.

2.1.2 Example – the spin echo

$$90°(x) \overset{a}{\text{——}} \text{delay}\ \tau \overset{b}{\text{——}} 180°(x) \overset{e}{\text{——}} \text{delay}\ \tau \overset{f}{\text{——}} \text{acquire}$$

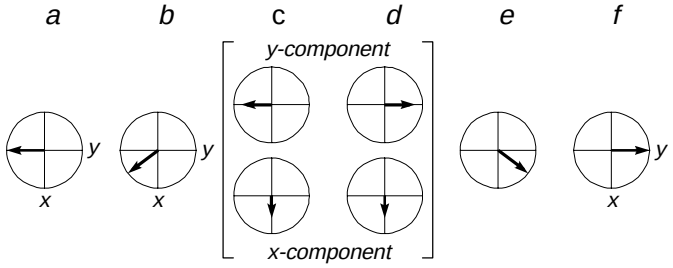

After the delay, point *b*, the vector can be resolved into *y*- and *x*-components as shown in *c*. The 180° pulse about the *x*-axis has no effect on the *x*-component of the magnetization; in contrast the *y*-component is rotated by 180° in the *yz*-plane, ending up along the opposite axis. The individual components after the 180° pulse are shown in *d*, and corresponding vector is shown in *e*. The effect of the 180° pulse about the *x*-axis is to reflect the vector in the *xz*-plane. During the second time τ the vector precesses in the same direction as it did during the first time τ and through the same angle, ending up along the *y*-axis.

At the end of the sequence the vector always ends up along the *y*-axis, regardless of the time τ and the offset; the sequence is said to "refocus the offset (or shift)".

2.2 Operators for one spin

2.2.1 Operators

Operators are mathematical functions which arise in quantum mechanics (see lecture 1); as their name suggest, they operate on functions. In quantum mechanics operators represent observable quantities, such as energy, angular momentum and magnetization.

For a single spin-half, the *x*- *y*- and *z*-components of the magnetization are represented by the spin angular momentum operators I_x, I_y and I_z respectively. Thus at any time the state of the spin system, in quantum mechanics the density operator, σ, can be represented as a sum of different amounts of these three operators

$$\sigma(t) = a(t)I_x + b(t)I_y + c(t)I_z$$

The amounts of the three operators will vary with time during pulses and delays. This expression of the density operator as a combination of the spin angular momentum operators is exactly analogous to specifying the three components of a magnetization vector.

At equilibrium the density operator is proportional to I_z (there is only *z*-magnetization present). The constant of proportionality is usually unimportant, so it is usual to write $\sigma_{eq} = I_z$.

2.2.2 Hamiltonians for pulses and delays

In order to work out how the density operator varies with time we need to know the Hamiltonian (which is also an operator) which is acting during that time.

The free precession Hamiltonian (*i.e.* that for a delay), H_{free}, is

$$H_{free} = \Omega I_z$$

In the vector model free precession involves a rotation at frequency Ω about the *z*-axis; in the quantum mechanical picture the Hamiltonian involves the *z*-angular momentum operator, I_z – there is a direct correspondence.

The Hamiltonian for a pulse about the *x*-axis, H_{pulse}, is

$$H_{pulse,x} = \omega_1 I_x$$

and for a pulse about the *y*-axis it is

$$H_{pulse,y} = \omega_1 I_y$$

Again there is a clear connection to the vector model where pulses result in rotations about the *x*- or *y*-axes.

2.2.3 Equation of motion

The density operator at time *t*, $\sigma(t)$, is computed from that at time 0, $\sigma(0)$, using the following relationship

$$\sigma(t) = \exp(-iHt)\ \sigma(0)\ \exp(iHt)$$

where *H* is the relevant hamiltonian. If *H* and σ are expressed in terms of the angular momentum operators if turns out that this equation can be solved easily with the aid of a few rules.

Suppose that an *x*-pulse, of duration t_p, is applied to equilibrium

magnetization. In this situation $H = \omega_1 I_x$ and $\sigma(0) = I_z$; the equation to be solved is

$$\sigma\left(t_{\mathrm{p}}\right) = \exp\left(-i\omega_1 t_{\mathrm{p}} I_x\right)\, I_z \exp\left(i\omega_1 t_{\mathrm{p}}\, I_x\right)$$

Such equations involving angular momentum operators are common in quantum mechanics and the solution to them are already all know. The identity required here to solve this equation is

$$\exp\left(-i\theta I_x\right)\, I_z \exp\left(i\theta I_x\right) \equiv \cos\theta\, I_z - \sin\theta\, I_y \qquad [2.1]$$

This is interpreted as a *rotation* of I_z by an angle θ about the *x*-axis. By putting $\theta = \omega_1 t_{\mathrm{p}}$ this identity can be used to solve Eqn. [2.1]

$$\sigma\left(t_{\mathrm{p}}\right) = \cos\omega_1 t_{\mathrm{p}}\; I_z - \sin\omega_1 t_{\mathrm{p}}\; I_y$$

The result is exactly as expected from the vector model: a pulse about the *x*-axis rotates *z*-magnetization towards the *–y*-axis, with a sinusoidal dependence on the flip angle, θ.

2.2.4 Standard rotations

Given that there are only three operators, there are a limited number of identities of the type of Eqn. [2.1]. They all have the same form

$$\begin{aligned}&\exp\left(-i\theta I_a\right)\,\{\text{old operator}\}\exp\left(i\theta I_a\right)\\ &\equiv \cos\theta\;\{\text{old operator}\} + \sin\theta\;\{\text{new operator}\}\end{aligned}$$

where {old operator}, {new operator} and I_{a} are determined from the three possible angular momentum operators according to the following diagrams; the label in the centre indicates which axis the rotation is about

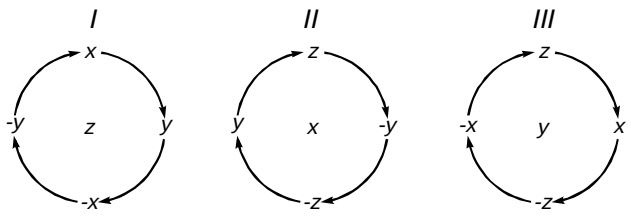

Angle of rotation = Ωt for offsets and $\omega_1 t_{\mathrm{p}}$ for pulses

First example: find the result of rotating the operator I_y by θ about the *x*-axis, that is

$$\exp\left(-i\theta I_x\right)\, I_y \exp\left(i\theta I_x\right)$$

For rotations about *x* the middle diagram *II* is required. The diagram shows that I_y (the "old operator") is rotated to I_z (the "new operator"). The required identity is therefore

$$\exp(-i\theta I_x)\, I_y \exp(i\theta I_x) \equiv \cos\theta\, I_y + \sin\theta\, I_z$$

Second example: find the result of

$$\exp(-i\theta I_y)\, \{-I_z\}\, \exp(i\theta I_y)$$

This is a rotation about *y*, so diagram *III* is required. The diagram shows that $-I_z$ (the "old operator") is rotated to $-I_x$ (the "new operator"). The required identity is therefore

$$\begin{aligned} \exp\left(-i\theta I_y\right)\left\{-I_z\right\}\exp\left(i\theta I_y\right) &\equiv \cos\theta\left\{-I_z\right\} + \sin\theta\left\{-I_x\right\} \\ &\equiv -\cos\theta\ I_z - \sin\theta\ I_x \end{aligned}$$

Finally, note that a rotation of an operator about its own axis has no effect *e.g.* a rotation of I_x about *x* leaves I_x unaltered.

2.2.5 Shorthand notation

To save writing, the arrow notation is often used. In this, the term *Ht* is written over an arrow which connects the old and new density operators. So, for example, the following

$$\sigma\left(t_{\mathrm{p}}\right) = \exp\left(-i\omega_1 t_{\mathrm{p}} I_x\right)\, \sigma(0) \exp\left(i\omega_1 t_{\mathrm{p}} I_x\right)$$

is written

$$\sigma(0) \xrightarrow{\omega_1 t_{\mathrm{p}} I_x} \sigma\left(t_{\mathrm{p}}\right)$$

For the case where $\sigma(0) = I_z$

$$I_z \xrightarrow{\omega_1 t_{\mathrm{p}} I_x} \cos\omega_1 t_{\mathrm{p}}\ I_z - \sin\omega_1 t_{\mathrm{p}}\ I_y$$

2.2.6 Example calculation: spin echo

$$90°(x) \overset{a}{\text{——}} \text{delay } \tau \overset{b}{\text{——}} 180°(x) \overset{e}{\text{——}} \text{delay } \tau \overset{f}{\text{——}} \text{acquire}$$

At a the density operator is $-I_y$. The transformation from *a* to *b* is free precession, for which the Hamiltonian is ΩI_z; the delay τ therefore corresponds to a rotation about the *z*-axis at frequency Ω. In the short-hand notation this is

$$-I_y \xrightarrow{\Omega\tau I_z} \sigma(b)$$

To solve this diagram *I* above is needed with the angle = $\Omega\tau$; the "new operator" is I_x

$$-I_y \xrightarrow{\Omega\tau I_z} -\cos\Omega\tau\, I_y + \sin\Omega\tau\, I_x$$

In words this says that the magnetization precesses from $-y$ towards $+x$.

The pulse about *x* has the Hamiltonian $\omega_1 I_x$; the pulse therefore corresponds to a rotation about *x* for a time t_p such that the angle, $\omega_1 t_p$, is π radians. In the shorthand notation

$$-\cos\Omega\tau\, I_y + \sin\Omega\tau\, I_x \xrightarrow{\omega_1 t_p I_x} \sigma(e) \qquad [2.2]$$

Each term on the left is dealt with separately. The first term is a rotation of *y* about *x*; the relevant diagram is thus *II*

$$-\cos\Omega\tau\, I_y \xrightarrow{\omega_1 t_p I_x} -\cos\Omega\tau\cos\omega_1 t_p\, I_y - \cos\Omega\tau\sin\omega_1 t_p\, I_z$$

However, the flip angle of the pulse, $\omega_1 t_p$, is π so the second term on the right is zero and the first term just changes sign ($\cos\pi = -1$); overall the result is

$$-\cos\Omega\tau\, I_y \xrightarrow{\pi I_x} \cos\Omega\tau\, I_y$$

The second term on the left of Eqn. [2.2] is easy to handle as it is unaffected by a rotation about *x*. Overall, the effect of the 180° pulse is then

$$-\cos\Omega\tau\, I_y + \sin\Omega\tau\, I_x \xrightarrow{\pi I_x} \cos\Omega\tau\, I_y + \sin\Omega\tau\, I_x \qquad [2.3]$$

As was shown using the vector model, the *y*-component just changes sign. The next stage is the evolution of the offset for time τ. Again, each term on the right of Eqn. [2.3] is considered separately

$$\cos\Omega\tau\, I_y \xrightarrow{\Omega\pi I_z} \cos\Omega\tau\cos\Omega\tau\, I_y - \sin\Omega\tau\cos\Omega\tau\, I_x$$
$$\sin\Omega\tau\, I_x \xrightarrow{\Omega\pi I_z} \cos\Omega\tau\sin\Omega\tau\, I_x + \sin\Omega\tau\sin\Omega\tau\, I_y$$

Collecting together the terms in I_x and I_y the final result is

$$\left(\cos\Omega\tau\cos\Omega\tau + \sin\Omega\tau\sin\Omega\tau\right) I_y + \left(\cos\Omega\tau\sin\Omega\tau - \sin\Omega\tau\cos\Omega\tau\right) I_x$$

The bracket multiplying I_x is zero and the bracket multiplying I_y is =1 because of the identity $\cos^2\theta + \sin^2\theta = 1$. Thus the overall result of the spin echo sequence can be summarised

$$I_z \xrightarrow{90°(x)-\tau-180°(x)-\tau-} I_y$$

In words, the outcome is independent of the offset, Ω, and the delay τ, even though there is evolution during the delays. The offset is said to be *refocused* by the spin echo.

In general the sequence

$$-\tau-180°(x)-\tau- \qquad [2.4]$$

refocuses any evolution due to offsets; this is a very useful feature which is much used in multiple-pulse NMR experiments.

One further point is that as far as the offset is concerned the spin echo sequence of Eqn. [2.4] is just equivalent to 180°(*x*).

2.3 Operators for two spins

2.3.1 Product operators for two spins

The product operator approach comes into its own when coupled spin systems are considered; such systems cannot be treated by the vector model. However, product operators provide a clean and simple description of the important phenomena of coherence transfer and multiple quantum coherence.

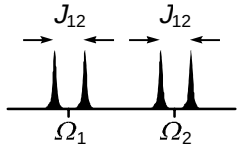

The spectrum from two coupled spins, with offsets Ω_1 and Ω_2 (rad s^{-1}) and mutual coupling J_{12} (Hz).

2.3.2 Product operators for two spins

For a single spin the three operators needed for a complete description are I_x, I_y and I_z. For two spins, three such operators are needed for each spin; an

additional subscript, 1 or 2, indicates which spin they refer to.

spin 1: I_{1x} I_{1y} I_{1z} spin 2: I_{2x} I_{2y} I_{2z}

I_{1z} represents *z*-magnetization of spin 1, and I_{2z} likewise for spin 2. I_{1x} represents *x*-magnetization on spin 1. As spin 1 and 2 are coupled, the spectrum consists of two doublets and the operator I_{1x} can be further identified with the two lines of the spin-1 doublet. In the language of product operators I_{1x} is said to represent *in-phase* magnetization of spin 1; the description in-phase means that the two lines of the spin 1 doublet have the same sign and lineshape.

Following on in the same way I_{2x} represents in-phase magnetization on spin 2. I_{1y} and I_{2y} also represent in-phase magnetization on spins 1 and 2, respectively, but this magnetization is aligned along *y* and so will give rise to a different lineshape. Arbitrarily, an absorption mode lineshape will be assigned to magnetization aligned along *x* and a dispersion mode lineshape to magnetization along *y*.

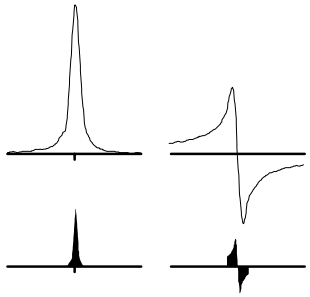

The absorption and dispersion lineshapes. The absorption lineshape is a maximum on resonance, whereas the dispersion goes through zero at this point. The "cartoon" forms of the lineshapes are shown in the lower part of the diagram.

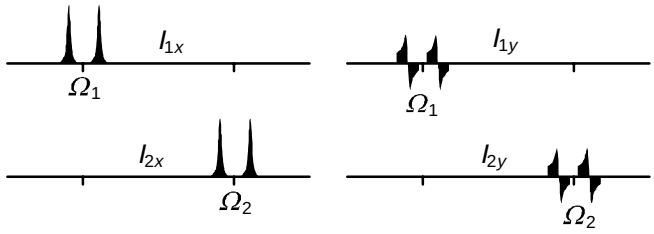

There are four additional operators which represent *anti-phase* magnetization: $2I_{1x}I_{2z}$, $2I_{1y}I_{2z}$, $2I_{1z}I_{2x}$, $2I_{1z}I_{2y}$ (the factors of 2 are needed for normalization purposes). The operator $2I_{1x}I_{2z}$ is described as magnetization on spin 1 which is anti-phase with respect to the coupling to spin 2.

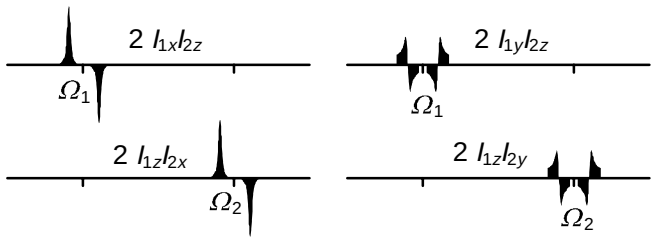

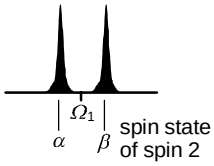

The two lines of the spin-1 doublet can be associated with different spin states of spin 2.

Note that the two lines of the spin-1 multiplet are associated with different spin states of spin-2, and that in an anti-phase multiplet these two lines have different signs. Anti-phase terms are thus sensitive to the spin states of the coupled spins.

There are four remaining product operators which contain two transverse (*i.e.* *x*- or *y*-operators) terms and correspond to multiple-quantum coherences; they are not observable

multiple quantum: $2I_{1x}I_{2y}$ $2I_{1y}I_{2x}$ $2I_{1x}I_{2x}$ $2I_{1y}I_{2y}$

Finally there is the term $2I_{1z}I_{2z}$ which is also not observable and corresponds to a particular kind of non-equilibrium population distribution.

2.3.3 Evolution under offsets and pulses

The operators for two spins evolve under offsets and pulses in the same way as do those for a single spin. The rotations have to be applied separately to each spin and it must be remembered that rotations of spin 1 do not affect spin 2, and *vice versa.*

For example, consider I_{1x} evolving under the offset of spin 1 and spin 2. The relevant Hamiltonian is

$$H_{\text{free}} = \Omega_1 I_{1z} + \Omega_2 I_{2z}$$

where Ω_1 and Ω_2 are the offsets of spin 1 and spin 2 respectively. Evolution under this Hamiltonian can be considered by applying the two terms sequentially (the order is immaterial)

$$\begin{aligned} I_{1x} &\xrightarrow{H_{\text{free}}t} \\ I_{1x} &\xrightarrow{\Omega_1 t I_{1z} + \Omega_2 t I_{2z}} \\ I_{1x} &\xrightarrow{\Omega_1 t I_{1z}} \xrightarrow{\Omega_2 t I_{2z}} \end{aligned}$$

The first "arrow" is a rotation about *z*

$$I_{1x} \xrightarrow{\Omega_1 t I_{1z}} \cos\Omega_1 t\, I_{1x} + \sin\Omega_1 t\, I_{1y} \xrightarrow{\Omega_2 t I_{2z}}$$

The second arrow leaves the intermediate state unaltered as spin-2 operators have not effect on spin-1 operators. Overall, therefore

$$I_{1x} \xrightarrow{\Omega_1 t I_{1z} + \Omega_2 t I_{2z}} \cos\Omega_1 t\, I_{1x} + \sin\Omega_1 t\, I_{1y}$$

A second example is the term $2I_{1x}I_{2z}$ evolving under a 90° pulse about the y-axis applied to both spins. The relevant Hamiltonian is

$$H = \omega_1 I_{1y} + \omega_1 I_{2y}$$

The evolution can be separated into two successive rotations

$$2I_{1x}I_{2z} \xrightarrow{\omega_1 t I_{1y}} \xrightarrow{\omega_1 t I_{2y}}$$

The first arrow affects only the spin-1 operators; a 90° rotation of I_{1x} about *y* gives $-I_{1z}$ (remembering that $\omega_1 t = \pi/2$ for a 90° pulse)

$$2I_{1x}I_{2z} \xrightarrow{\omega_1 tI_{1y}} \cos\omega_1 t\, 2I_{1x}I_{2z} - \sin\omega_1 t\, 2I_{1z}I_{2z} \xrightarrow{\omega_1 tI_{2y}}$$
$$2I_{1x}I_{2z} \xrightarrow{\pi/2\, I_{1y}} -2I_{1z}I_{2z} \xrightarrow{\pi/2\, I_{2y}}$$

The second arrow only affects the spin 2 operators; a 90° rotation of *z* about *y* takes it to *x*

$$2I_{1x}I_{2z} \xrightarrow{\pi/2\, I_{1y}} -2I_{1z}I_{2z} \xrightarrow{\pi/2 I_{2y}} -2I_{1z}I_{2x}$$

The overall result is that anti-phase magnetization of spin 1 has been transferred into anti-phase magnetization of spin 2. Such a process is called *coherence transfer* and is exceptionally important in multiple-pulse NMR.

2.3.4 Evolution under coupling

The new feature which arises when considering two spins is the effect of coupling between them. The Hamiltonian representing this coupling is itself a product of two operators:

$$H_J = 2\pi J_{12}\, I_{1z}I_{2z}$$

where J_{12} is the coupling in Hz.

Evolution under coupling causes the interconversion of in-phase and anti-phase magnetization according to the following diagrams

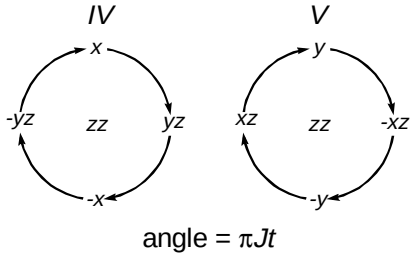

For example, in-phase magnetization along *x* becomes anti-phase along *y* according to the diagram *d*

$$I_{1x} \xrightarrow{2\pi J_{12} t\, I_{1z}I_{2z}} \cos\pi J_{12} t\, I_{1x} + \sin\pi J_{12} t\, 2I_{1y}I_{2z}$$

note that the angle is $\pi J_{12}t$ *i.e.* half the angle for the other rotations, *I–III*.

Anti-phase magnetization along *x* becomes in-phase magnetization along *y*; using diagram *V*:

$$2I_{1x}I_{2z} \xrightarrow{2\pi J_{12} t\, I_{1z}I_{2z}} \cos\pi J_{12} t\, 2I_{1x}I_{2z} + \sin\pi J_{12} t\, I_{1y}$$

The diagrams apply equally well to spin-2; for example

$$-2I_{1z}I_{2y} \xrightarrow{2\pi J_{12}t\, I_{1z}I_{2z}} -\cos\pi J_{12}t\, 2I_{1z}I_{2y} + \sin\pi J_{12}t\, I_{2x}$$

Complete interconversion of in-phase and anti-phase magnetization requires a delay such that $\pi J_{12}t = \pi/2$ *i.e.* a delay of $1/(2J_{12})$. A delay of $1/J_{12}$ causes in-phase magnetization to change its sign:

$$I_{1x} \xrightarrow{2\pi J_{12}t\, I_{1z}I_{2z}\ \ t=1/2J_{12}} 2I_{1y}I_{2z} \qquad I_{2y} \xrightarrow{2\pi J_{12}t\, I_{1z}I_{2z}\ \ t=1/J_{12}} -I_{2y}$$

2.4 Spin echoes

It was shown in section 2.2.6 that the offset is refocused in a spin echo. In this section it will be shown that the evolution of the scalar coupling is not necessarily refocused.

2.4.1 Spin echoes in homonuclear spin system

In this kind of spin echo the 180° pulse affects both spins *i.e.* it is a non-selective pulse:

$$-\tau - 180°(x, \text{ to spin 1 and spin 2}) - \tau -$$

At the start of the sequence it will be assumed that only in-phase *x*-magnetization on spin 1 is present: I_{1x}. In fact the starting state is not important to the overall effect of the spin echo, so this choice is arbitrary.

It was shown in section 2.2.6 that the spin echo applied to one spin refocuses the offset; this conclusion is not altered by the presence of a coupling so the offset will be ignored in the present calculation. This greatly simplifies things.

For the first delay τ only the effect of evolution under coupling need be considered therefore:

$$I_{1x} \xrightarrow{2\pi J_{12}\tau\, I_{1z}I_{2z}} \cos\pi J_{12}\tau\ I_{1x} + \sin\pi J_{12}\tau\ 2I_{1y}I_{2z}$$

The 180° pulse affects both spins, and this can be calculated by applying the 180° rotation to each in succession

$$\cos\pi J_{12}\tau\ I_{1x} + \sin\pi J_{12}\tau\ 2I_{1y}I_{2z} \xrightarrow{\pi I_{1x}} \xrightarrow{\pi I_{2x}}$$

where it has already been written in that $\omega_1 t_p = \pi$, for a 180° pulse. The 180° rotation about *x* for spin 1 has no effect on the operator I_{1x} and I_{2z}, and

it simply reverses the sign of the operator I_{1y}

$$\cos\pi J_{12}\tau I_{1x} + \sin\pi J_{12}\tau\, 2I_{1y}I_{2z} \xrightarrow{\pi I_{1x}} \cos\pi J_{12}\tau I_{1x} - \sin\pi J_{12}\tau\, 2I_{1y}I_{2z} \xrightarrow{\pi I_{2x}}$$

The 180° rotation about *x* for spin 2 has no effect on the operators I_{1x} and I_{1y}, but simply reverses the sign of the operator I_{2z}. The final result is thus

$$\cos\pi J_{12}\tau I_{1x} + \sin\pi J_{12}\tau\, 2I_{1y}I_{2z} \xrightarrow{\pi I_{1x}} \cos\pi J_{12}\tau I_{1x} - \sin\pi J_{12}\tau\, 2I_{1y}I_{2z}$$
$$\xrightarrow{\pi I_{2x}} \cos\pi J_{12}\tau I_{1x} + \sin\pi J_{12}\tau\, 2I_{1y}I_{2z}$$

Nothing has happened; the 180° pulse has left the operators unaffected! So, for the purposes of the calculation it is permissible to ignore the 180° pulse and simply allow the coupling to evolve for 2τ. The final result can therefore just be written down:

$$I_{1x} \xrightarrow{\tau-180°(x)-\tau} \cos 2\pi J_{12}\tau\ I_{1x} + \sin 2\pi J_{12}\tau\ 2I_{1y}I_{2z}$$

From this it is easy to see that complete conversion to anti-phase magnetization requires $2\pi J_{12}\tau = \pi/2$ *i.e.* $\tau = 1/(4\ J_{12})$.

The calculation is not quite as simple if the initial state is chosen as I_{1y} (see exercises), but the final result is just the same – the coupling evolves for 2τ:

$$I_{1y} \xrightarrow{\tau-180°(x)-\tau} -\cos 2\pi J_{12}\tau\, I_{1y} + \sin 2\pi J_{12}\tau\ 2I_{1x}I_{2z}$$

In fact, the general result is that the sequence

$$-\ \tau - 180°(x, \text{ to spin 1 and spin 2}) - \tau -$$

is equivalent to the sequence

$$-\ 2\tau - 180°(x, \text{ to spin 1 and spin 2})$$

in which the offset is ignored and coupling is allowed to act for time 2τ.

2.4.2 Interconverting in-phase and anti-phase states

So far, spin echoes have been demonstrated as being useful for generating anti-phase terms, independent of offsets. For example, the sequence

$$90°(x) - 1/(4J_{12}) - 180°(x) - 1/(4J_{12}) -$$

generates pure anti-phase magnetization.

Equally useful is the sequence

$$- 1/(4J_{12}) - 180°(x) - 1/(4J_{12}) -$$

which will convert pure anti-phase magnetization, such as $2I_{1x}I_{2z}$ into in-phase magnetization, I_{1y}.

2.4.3 Spin echoes in heteronuclear spin systems

If spin 1 and spin 2 are different nuclear species, such as ^{13}C and ^{1}H, it is possible to choose to apply the 180° pulse to either or both spins; the outcome of the sequence depends on the pattern of 180° pulses.

Sequence *a* has already been analysed: the result is that the offset is refocused but that the coupling evolves for time 2τ. Sequence *b* still refocuses the offset of spin 1, but it turns out that the coupling is also refocused. Sequence *c* refocuses the coupling but leaves the evolution of the offset unaffected.

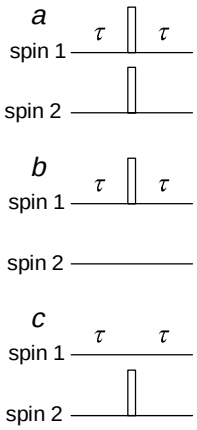

Three different spin echo sequences that can be applied to heteronuclear spin systems. The open rectangles represent 180° pulses.

2.4.3.1 Sequence b

It will be assumed that the offset is refocused, and attention will therefore be restricted to the effect of the coupling

$$I_{1x} \xrightarrow{2\pi J_{12}\tau I_{1z}I_{2z}} \cos\pi J_{12}\tau\ I_{1x} + \sin\pi J_{12}\tau\ 2I_{1y}I_{2z}$$

The 180°(*x*) pulse is only applied to spin 1

$$\cos\pi J_{12}\tau\ I_{1x} + \sin\pi J_{12}\tau\ 2I_{1y}I_{2z} \xrightarrow{\pi I_{1x}} \cos\pi J_{12}\tau\ I_{1x} - \sin\pi J_{12}\tau\ 2I_{1y}I_{2z} \quad [2.5]$$

The two terms on the right each evolve under the coupling during the second delay:

$$\cos\pi J_{12}\tau\ I_{1x} \xrightarrow{2\pi J_{12}\tau I_{1z}I_{2z}}$$
$$\cos\pi J_{12}\tau\cos\pi J_{12}\tau\ I_{1x} + \sin\pi J_{12}\tau\cos\pi J_{12}\tau\ 2I_{1y}I_{2z}$$
$$-\sin\pi J_{12}\tau\ 2I_{1y}I_{2z} \xrightarrow{2\pi J_{12}\tau I_{1z}I_{2z}}$$
$$-\cos\pi J_{12}\tau\sin\pi J_{12}\tau\ 2I_{1y}I_{2z} + \sin\pi J_{12}\tau\ \sin\pi J_{12}\tau\ I_{1x}$$

Collecting the terms together and noting that $\cos^2\theta + \sin^2\theta = 1$ the final result is just I_{1x}. In words, the effect of the coupling has been refocused.

2.4.3.2 Sequence c

As there is no 180° pulse applied to spin 1, the offset of spin 1 is not refocused, but continues to evolve for time 2τ. The evolution of the coupling is easy to calculate:

$$I_{1x} \xrightarrow{2\pi J_{12}\tau I_{1z}I_{2z}} \cos\pi J_{12}\tau\ I_{1x} + \sin\pi J_{12}\tau\ 2I_{1y}I_{2z}$$

This time the 180°(x) pulse is applied to spin 2

$$\cos\pi J_{12}\tau\ I_{1x} + \sin\pi J_{12}\tau\ 2I_{1y}I_{2z} \xrightarrow{\pi I_{2x}} \cos\pi J_{12}\tau\ I_{1x} - \sin\pi J_{12}\tau\ 2I_{1y}I_{2z}$$

The results is exactly as for sequence *b* (Eqn. [2.5]), so the final result is the same *i.e.* the coupling is refocused.

2.4.3.3 Summary

In heteronuclear systems it is possible to choose whether or not to allow the offset and the coupling to evolve; this gives great freedom in generating and manipulating anti-phase states which play a key role in multiple pulse NMR experiments.

2.5 Multiple quantum terms

2.5.1 Coherence order

In NMR the directly observable quantity is the transverse magnetization, which in product operators is represented by terms such as I_{1x} and $2I_{1z}I_{2y}$. Such terms are examples of single quantum coherences, or more generally coherences with order, p, = ±1. Other product operators can also be classified according to coherence order *e.g.* $2I_{1z}I_{2z}$ has $p = 0$ and $2I_{1x}I_{2y}$ has both $p = 0$ (zero-quantum coherence) and ±2 (double quantum coherence). Only single quantum coherences are observable.

In heteronuclear systems it is sometimes useful to classify operators according to their coherence orders with respect to each spin. So, for example, $2I_{1z}I_{2y}$ has $p = 0$ for spin 1 and $p = \pm1$ for spin 2.

2.5.2 Raising and lowering operators

The classification of operators according to coherence order is best carried out be re-expressing the Cartesian operators I_x and I_y in terms of the raising and lowering operators, I_+ and I_-, respectively. These are defined as follows

$$I_+ = I_x + iI_y \qquad I_- = I_x - iI_y \tag{2.6}$$

where i is the square root of –1 (further details of why these operators are called the raising and lowering operators will be given in lecture 1). I_+ has coherence order +1 and I_- has coherence order –1; coherence order is a *signed* quantity.

Using the definitions of Eqn. [2.6] I_x and I_y can be expressed in terms of the raising and lowering operators

$$I_x = \tfrac{1}{2}\left(I_+ + I_-\right) \qquad I_y = \tfrac{1}{2i}\left(I_+ - I_-\right) \tag{2.7}$$

from which it is seen that I_x and I_y are both mixtures of coherences with p = +1 and –1.

The operator product $2I_{1x}I_{2x}$ can be expressed in terms of the raising and lowering operators in the following way (note that separate operators are used for each spin: $I_{1\pm}$ and $I_{2\pm}$)

$$\begin{aligned} 2I_{1x}I_{2x} &= 2\times\tfrac{1}{2}\left(I_{1+} + I_{1-}\right)\times\tfrac{1}{2}\left(I_{2+} + I_{2-}\right) \\ &= \tfrac{1}{2}\left(I_{1+}I_{2+} + I_{1-}I_{2-}\right) + \tfrac{1}{2}\left(I_{1+}I_{2-} + I_{1-}I_{2+}\right) \end{aligned} \tag{2.8}$$

The first term on the right of Eqn. [2.8] has p = (+1+1) = 2 and the second term has p = (–1–1) = –2; both are double quantum coherences. The third and fourth terms both have p = (+1–1) = 0 and are zero quantum coherences. The value of p can be found simply by noting the number of raising and lowering operators in the product.

The pure double quantum part of $2I_{1x}I_{2x}$ is, from Eqn. [2.8],

$$\text{double quantum part}\left[2I_{1x}I_{2x}\right] = \tfrac{1}{2}\left(I_{1+}I_{2+} + I_{1-}I_{2-}\right) \tag{2.9}$$

The raising and lowering operators on the right of Eqn. [2.9] can be re-expressed in terms of the Cartesian operators:

$$\begin{aligned} \tfrac{1}{2}\left(I_{1+}I_{2+} + I_{1-}I_{2-}\right) &= \tfrac{1}{2}\left[\left(I_{1x} + iI_{1y}\right)\left(I_{2x} + iI_{2y}\right) + \left(I_{1x} - iI_{1y}\right)\left(I_{2x} - iI_{2y}\right)\right] \\ &= \tfrac{1}{2}\left[2I_{1x}I_{2x} + 2I_{1y}I_{2y}\right] \end{aligned}$$

So, the pure double quantum part of $2I_{1x}I_{2x}$ is $\frac{1}{2}\left(2I_{1x}I_{2x}+2I_{1y}I_{2y}\right)$; by a similar method the pure zero quantum part can be shown to be $\frac{1}{2}\left(2I_{1x}I_{2x}-2I_{1y}I_{2y}\right)$. Some further useful relationships are given in section 2.9

2.5.3 Definition of coherence order

The formal definition of coherence order depends on the response of a particular operator to a rotation about the *z*-axis. A coherence or operator of order p acquires a phase $p\phi$ when rotated about the *z*-axis through an angle ϕ:

$$\sigma^{(p)} \xrightarrow{\text{rotate by } \phi \text{ about } z} \sigma^{(p)} \exp\left(-ip\phi\right)$$

This property will be used extensively as part of the description of coherence selection by phase cycling or gradient pulses, lecture 4.

2.6 Three spins

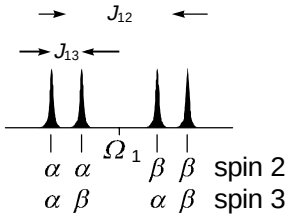

The doublet of doublets from spin 1 coupled to two other spins. The spin states of the coupled spins are also indicated.

The product operator formalism can be extended to three or more spins. No really new features arise, but some of the key ideas will be highlighted in this section. The description will assume that spin 1 is coupled to spins 2 and 3 with coupling constants J_{12} and J_{13}; in the diagrams it will be assumed that $J_{12} > J_{13}$.

2.6.1 Types of operators

I_{1x} represents in-phase magnetization on spin 1; $2I_{1x}I_{2z}$ represents magnetization anti-phase with respect to the coupling to spin 2 and $2I_{1x}I_{3z}$ represents magnetization anti-phase with respect to the coupling to spin 3. $4I_{1x}I_{2z}I_{3z}$ represents magnetization which is doubly anti-phase with respect to the couplings to both spins 2 and 3.

As in the case of two spins, the presence of more than one transverse operator in the product represents multiple quantum coherence. For example, $2I_{1x}I_{2x}$ is a mixture of double- and zero-quantum coherence between spins 1 and 2. The product $4I_{1x}I_{2x}I_{3z}$ is the same mixture, but anti-phase with respect to the coupling to spin 3. Products such as $4I_{1x}I_{2x}I_{3x}$ contain, amongst other things, triple-quantum coherences.

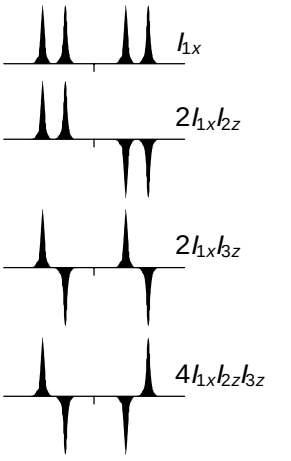

Representations of different types of operators.

2.6.2 Evolution

Evolution under offsets and pulses is simply a matter of applying sequentially the relevant rotations for each spin, remembering that rotations of spin 1 do not affect operators of spins 2 and 3. For example, the term $2I_{1x}I_{2z}$ evolves under the offset in the following way:

$$2I_{1x}I_{2z} \xrightarrow{\Omega_1 t I_{1z}} \xrightarrow{\Omega_2 t I_{2z}} \xrightarrow{\Omega_3 t I_{3z}} \cos\Omega_1 t\ 2I_{1x}I_{2z} + \sin\Omega_1 t\ 2I_{1y}I_{2z}$$

The first arrow, representing evolution under the offset of spin 1, affects only the spin 1 operator I_{1x}. The second arrow has no effect as the spin 2 operator I_{2z} and this is unaffected by a z-rotation. The third arrow also has no effect as there are no spin 3 operators present.

The evolution under coupling follows the same rules as for a two-spin system. For example, evolution of I_{1x} under the influence of the coupling to spin 3 generates $2I_{1y}I_{3z}$

$$I_{1x} \xrightarrow{2\pi J_{13} t I_{1z} I_{3z}} \cos\pi J_{13} t\ I_{1x} + \sin\pi J_{13} t\ 2I_{1y}I_{3z}$$

Further evolution of the term $2I_{1y}\ I_{3z}$ under the influence of the coupling to spin 2 generates a double anti-phase term

$$2I_{1y}I_{3z} \xrightarrow{2\pi J_{12} t I_{1z} I_{2z}} \cos\pi J_{12} t\ 2I_{1y}I_{3z} - \sin\pi J_{13} t\ 4I_{1x}I_{2z}I_{3z}$$

In this evolution the spin 3 operator if unaffected as the coupling does not involve this spin. The connection with the evolution of I_{1y} under a coupling can be made more explicit by writing $2I_{3z}$ as a "constant" γ

$$\gamma I_{1y} \xrightarrow{2\pi J_{12} t I_{1z} I_{2z}} \cos\pi J_{12} t\ \gamma I_{1y} - \sin\pi J_{13} t\ 2\gamma I_{1x}I_{2z}$$

which compares directly to

$$I_{1y} \xrightarrow{2\pi J_{12} t I_{1z} I_{2z}} \cos\pi J_{12} t\ I_{1y} - \sin\pi J_{13} t\ 2I_{1x}I_{2z}$$

2.7 Alternative notation

In this chapter different spins have been designated with a subscript 1, 2, 3 ... Another common notation is to distinguish the spins by using a different letter to represent their operators; commonly *I* and *S* are used for two of the symbols

$$2I_{1x}I_{2z} \equiv 2I_xS_z$$

Note that the order in which the operators are written is not important, although it is often convenient (and tidy) always to write them in the same sequence.

In heteronuclear experiments a notation is sometimes used where the letter represents the nucleus. So, for example, operators referring to protons are given the letter *H*, carbon-13 atoms the letter *C* and nitrogen-15 atoms the letter *N*; carbonyl carbons are sometimes denoted *C'*. For example, $4C_xH_zN_z$ denotes magnetization on carbon-13 which is anti-phase with respect to coupling to both proton and nitrogen-15.

2.8 Conclusion

The product operator method as described here only applies to spin-half nuclei. It can be extended to higher spins, but significant extra complexity is introduced; details can be found in the article by Sørensen *et al.* (*Prog. NMR Spectrosc.* **16**, 163 (1983)).

The main difficulty with the product operator method is that the more pulses and delays that are introduced the greater becomes the number of operators and the more complex the trigonometrical expressions multiplying them. If pulses are either 90° or 180° then there is some simplification as such pulses do not increase the number of terms. As will be seen in lecture 3, it is important to try to simplify the calculation as much as possible, for example by recognizing when offsets or couplings are refocused by spin echoes.

A number of computer programs are available for machine computation using product operators within programs such as *Mathematica* or *Maple*. These can be very labour saving.

2.9 Multiple -quantum coherence

2.9.1 Multiple-quantum terms

In the product operator representation of multiple quantum coherences it is usual to distinguish between *active* and *passive* spins. Active spins contribute transverse operators, such as I_x, I_y and I_+, to the product; passive spins contribute only *z*-operators, I_z. In a sense the spins contributing transverse operators are "involved" in the coherence, while those contributing *z*-operators are simply spectators.

For double- and zero-quantum coherence in which spins *i* and *j* are active it is convenient to define the following set of operators which represent pure multiple quantum states of given order. The operators can be expressed in terms of the Cartesian or raising and lowering operators.

double quantum, $p = \pm 2$

$$\mathrm{DQ}_x^{(ij)} \equiv \tfrac{1}{2}\left(2I_{ix}I_{jx} - 2I_{iy}I_{jy}\right) \equiv \tfrac{1}{2}\left(I_{i+}I_{j+} + I_{i-}I_{j-}\right)$$

$$\mathrm{DQ}_y^{(ij)} \equiv \tfrac{1}{2}\left(2I_{ix}I_{jy} + 2I_{iy}I_{jx}\right) \equiv \tfrac{1}{2i}\left(I_{i+}I_{j+} - I_{i-}I_{j-}\right)$$

zero quantum, $p = 0$

$$\mathrm{ZQ}_x^{(ij)} \equiv \tfrac{1}{2}\left(2I_{ix}I_{jx} + 2I_{iy}I_{jy}\right) \equiv \tfrac{1}{2}\left(I_{i+}I_{j-} + I_{i-}I_{j+}\right)$$

$$\mathrm{ZQ}_y^{(ij)} \equiv \tfrac{1}{2}\left(2I_{iy}I_{jx} - 2I_{ix}I_{jy}\right) \equiv \tfrac{1}{2i}\left(I_{i+}I_{j-} - I_{i-}I_{j+}\right)$$

2.9.2 Evolution of multiple -quantum terms

2.9.2.1 Evolution under offsets

The double- and zero-quantum operators evolve under offsets in a way which is entirely analogous to the evolution of I_x and I_y under free precession except that the frequencies of evolution are ($\Omega_i + \Omega_j$) and ($\Omega_i - \Omega_j$) respectively:

$$\mathrm{DQ}_x^{(ij)} \xrightarrow{\Omega_i t I_{iz} + \Omega_j t I_{jz}} \cos\left(\Omega_i + \Omega_j\right)t\,\mathrm{DQ}_x^{(ij)} + \sin\left(\Omega_i + \Omega_j\right)t\,\mathrm{DQ}_y^{(ij)}$$

$$\mathrm{DQ}_y^{(ij)} \xrightarrow{\Omega_i t I_{iz} + \Omega_j t I_{jz}} \cos\left(\Omega_i + \Omega_j\right)t\,\mathrm{DQ}_y^{(ij)} - \sin\left(\Omega_i + \Omega_j\right)t\,\mathrm{DQ}_x^{(ij)}$$

$$\mathrm{ZQ}_x^{(ij)} \xrightarrow{\Omega_i t I_{iz} + \Omega_j t I_{jz}} \cos\left(\Omega_i - \Omega_j\right)t\,\mathrm{ZQ}_x^{(ij)} + \sin\left(\Omega_i - \Omega_j\right)t\,\mathrm{ZQ}_y^{(ij)}$$

$$\mathrm{ZQ}_y^{(ij)} \xrightarrow{\Omega_i t I_{iz} + \Omega_j t I_{jz}} \cos\left(\Omega_i - \Omega_j\right)t\,\mathrm{ZQ}_y^{(ij)} - \sin\left(\Omega_i - \Omega_j\right)t\,\mathrm{ZQ}_x^{(ij)}$$

2.9.2.2 Evolution under couplings

Multiple quantum coherence between spins *i* and *j* does not evolve under the

influence of the coupling between the two active spins, *i* and *j*.

Double- and zero-quantum operators evolve under passive couplings in a way which is entirely analogous to the evolution of I_x and I_y; the resulting multiple quantum terms can be described as being anti-phase with respect to the effective couplings:

$$\mathrm{DQ}_x^{(ij)} \longrightarrow \cos\pi J_{\mathrm{DQ,eff}} t\ \mathrm{DQ}_x^{(ij)} + \cos\pi J_{\mathrm{DQ,eff}} t\ 2I_{kz}\mathrm{DQ}_y^{(ij)}$$
$$\mathrm{DQ}_y^{(ij)} \longrightarrow \cos\pi J_{\mathrm{DQ,eff}} t\ \mathrm{DQ}_y^{(ij)} - \sin\pi J_{\mathrm{DQ,eff}} t\ 2I_{kz}\mathrm{DQ}_x^{(ij)}$$
$$\mathrm{ZQ}_x^{(ij)} \longrightarrow \cos\pi J_{\mathrm{ZQ,eff}} t\,\mathrm{ZQ}_x^{(ij)} + \sin\pi J_{\mathrm{ZQ,eff}} t\ \ 2I_{kz}\mathrm{ZQ}_y^{(ij)}$$
$$\mathrm{ZQ}_y^{(ij)} \longrightarrow \cos\pi J_{\mathrm{ZQ,eff}} t\,\mathrm{ZQ}_y^{(ij)} - \sin\pi J_{\mathrm{ZQ,eff}} t\ 2I_{kz}\mathrm{ZQ}_x^{(ij)}$$

$J_{\mathrm{DQ,eff}}$ is the sum of the couplings between spin *i* and all other spins *plus* the sum of the couplings between spin *j* and all other spins. $J_{\mathrm{ZQ,eff}}$ is the sum of the couplings between spin *i* and all other spins *minus* the sum of the couplings between spin *j* and all other spins.

For example in a three-spin system the zero-quantum coherence between spins 1 and 2, anti-phase with respect to spin 3, evolves according to

$$2I_{3z}\mathrm{ZQ}_y^{(12)} \longrightarrow \cos\pi J_{\mathrm{ZQ,eff}} t\ 2I_{3z}\mathrm{ZQ}_y^{(12)} - \sin\pi J_{\mathrm{ZQ,eff}} t\ \ \mathrm{ZQ}_x^{(12)}$$
where $J_{\mathrm{ZQ,eff}} = J_{12} - J_{23}$

Further details of multiple-quantum evolution can be found in section 5.3 of Ernst, Bodenhausen and Wokaun *Principles of NMR in One and Two Dimensions* (Oxford University Press, 1987).

3 Basic concepts for two-dimensional NMR

3.1 Introduction

The basic ideas of two-dimensional NMR will be introduced by reference to the appearance of a COSY spectrum; later in this lecture the product operator formalism will be used to predict the form of the spectrum.

Conventional NMR spectra (one-dimensional spectra) are plots of intensity *vs.* frequency; in two-dimensional spectroscopy intensity is plotted as a function of two frequencies, usually called F_1 and F_2. There are various ways of representing such a spectrum on paper, but the one most usually used is to make a contour plot in which the intensity of the peaks is represented by contour lines drawn at suitable intervals, in the same way as a topographical map. The position of each peak is specified by two frequency co-ordinates corresponding to F_1 and F_2. Two-dimensional NMR spectra are always arranged so that the F_2 co-ordinates of the peaks correspond to those found in the normal one-dimensional spectrum, and this relation is often emphasized by plotting the one-dimensional spectrum alongside the F_2 axis.

The figure shows a schematic COSY spectrum of a hypothetical molecule containing just two protons, A and X, which are coupled together. The one-dimensional spectrum is plotted alongside the F_2 axis, and consists of the familiar pair of doublets centred on the chemical shifts of A and X, δ_A and δ_X respectively. In the COSY spectrum, the F_1 co-ordinates of the peaks in the two-dimensional spectrum also correspond to those found in the normal one-dimensional spectrum and to emphasize this point the one-dimensional spectrum has been plotted alongside the F_1 axis. It is immediately clear that this COSY spectrum has some symmetry about the diagonal $F_1 = F_2$ which has been indicated with a dashed line.

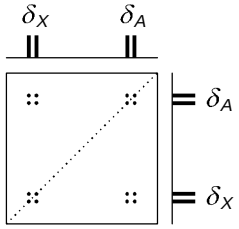

Schematic COSY spectrum for two coupled spins, A and X

In a one-dimensional spectrum scalar couplings give rise to multiplets in the spectrum. In two-dimensional spectra the idea of a multiplet has to be expanded somewhat so that in such spectra a multiplet consists of an array of individual peaks often giving the impression of a square or rectangular outline. Several such arrays of peaks can be seen in the schematic COSY spectrum shown above. These two-dimensional multiplets come in two distinct types: diagonal-peak multiplets which are centred around the same F_1 and F_2 frequency co-ordinates and cross-peak multiplets which are centred around different F_1 and F_2 co-ordinates. Thus in the schematic COSY spectrum there are two diagonal-peak multiplets centred at $F_1 = F_2 = \delta_A$ and $F_1 = F_2 = \delta_X$, one cross-peak multiplet centred at $F_1 = \delta_A$, $F_2 = \delta_X$ and a second cross-peak multiplet centred at $F_1 = \delta_X$, $F_2 = \delta_A$.

The appearance in a COSY spectrum of a cross-peak multiplet $F_1 = \delta_A$, $F_2 = \delta_X$ indicates that the two protons at shifts δ_A and δ_X have a scalar coupling between them. This statement is all that is required for the analysis of a COSY spectrum, and it is this simplicity which is the key to the great utility of such spectra. From a single COSY spectrum it is possible to trace out the whole coupling network in the molecule.

3.1.1 General Scheme for two-Dimensional NMR

In one-dimensional pulsed Fourier transform NMR the signal is recorded as a function of one time variable and then Fourier transformed to give a spectrum which is a function of one frequency variable. In two-dimensional NMR the signal is recorded as a function of two time variables, t_1 and t_2, and the resulting data Fourier transformed twice to yield a spectrum which is a function of two frequency variables. The general scheme for two-dimensional spectroscopy is

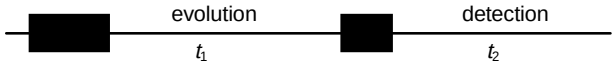

In the first period, called the preparation time, the sample is excited by one or more pulses. The resulting magnetization is allowed to evolve for the first time period, t_1. Then another period follows, called the mixing time, which consists of a further pulse or pulses. After the mixing period the signal is recorded as a function of the second time variable, t_2. This sequence of events is called a pulse sequence and the exact nature of the preparation and mixing periods determines the information found in the spectrum.

It is important to realize that the signal is not recorded during the time t_1, but only during the time t_2 at the end of the sequence. The data is recorded at regularly spaced intervals in both t_1 and t_2.

The two-dimensional signal is recorded in the following way. First, t_1 is set to zero, the pulse sequence is executed and the resulting free induction decay recorded. Then the nuclear spins are allowed to return to equilibrium. t_1 is then set to Δ_1, the sampling interval in t_1, the sequence is repeated and a free induction decay is recorded and stored separately from the first. Again the spins are allowed to equilibrate, t_1 is set to $2\Delta_1$, the pulse sequence repeated and a free induction decay recorded and stored. The whole process is repeated again for $t_1 = 3\Delta_1$, $4\Delta_1$ and so on until sufficient data is recorded, typically 50 to 500 increments of t_1. Thus recording a two-dimensional data set involves repeating a pulse sequence for increasing values of t_1 and recording a free induction decay as a function of t_2 for each value of t_1.

3.1.2 Interpretation of peaks in a two-dimensional spectrum

Within the general framework outlined in the previous section it is now possible to interpret the appearance of a peak in a two-dimensional spectrum at particular frequency co-ordinates.

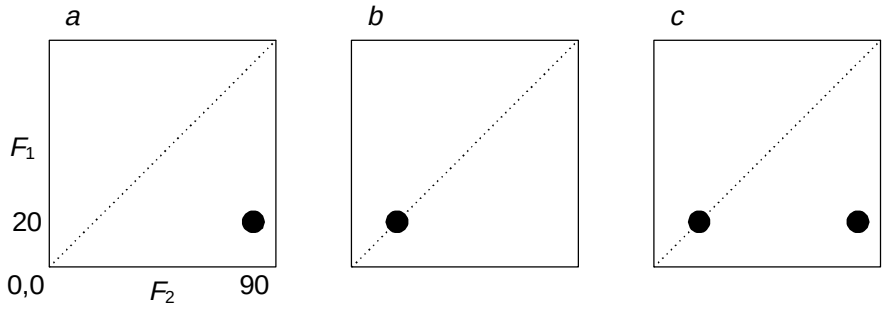

Suppose that in some unspecified two-dimensional spectrum a peak appears at F_1 = 20 Hz, F_2 = 90 Hz (spectrum *a* above) The interpretation of this peak is that a signal was present during t_1 which evolved with a frequency of 20 Hz. During the mixing time this *same* signal was transferred in some way to another signal which evolved at 90 Hz during t_2.

Likewise, if there is a peak at F_1 = 20 Hz, F_2 = 20 Hz (spectrum *b*) the interpretation is that there was a signal evolving at 20 Hz during t_1 which was unaffected by the mixing period and continued to evolve at 20 Hz during t_2. The processes by which these signals are transferred will be discussed in the following sections.

Finally, consider the spectrum shown in *c*. Here there are two peaks, one at F_1 = 20 Hz, F_2 = 90 Hz and one at F_1 = 20 Hz, F_2 = 20 Hz. The interpretation of this is that some signal was present during t_1 which evolved at 20 Hz and that during the mixing period part of it was transferred into another signal which evolved at 90 Hz during t_2. The other part remained unaffected and continued to evolve at 20 Hz. On the basis of the previous discussion of COSY spectra, the part that changes frequency during the mixing time is recognized as leading to a cross-peak and the part that does not change frequency leads to a diagonal-peak. This kind of interpretation is a very useful way of thinking about the origin of peaks in a two-dimensional spectrum.

It is clear from the discussion in this section that the mixing time plays a crucial role in forming the two-dimensional spectrum. In the absence of a mixing time, the frequencies that evolve during t_1 and t_2 would be the same and only diagonal-peaks would appear in the spectrum. To obtain an interesting and useful spectrum it is essential to arrange for some process during the mixing time to transfer signals from one spin to another.

3.2 EXSY and NOESY spectra in detail

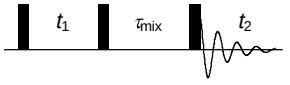

The pulse sequence for EXSY (and NOESY). All pulses have 90° flip angles.

In this section the way in which the EXSY (EXchange SpectroscopY) sequence works will be examined; the pulse sequence is shown opposite. This experiment gives a spectrum in which a cross-peak at frequency co-ordinates $F_1 = \delta_A$, $F_2 = \delta_B$ indicates that the spin resonating at δ_A is chemically exchanging with the spin resonating at δ_B.

The pulse sequence for EXSY is shown opposite. The effect of the sequence will be analysed for the case of two spins, 1 and 2, but without any coupling between them. The initial state, before the first pulse, is equilibrium magnetization, represented as $I_{1z} + I_{2z}$; however, for simplicity only magnetization from the first spin will be considered in the calculation.

The first 90° pulse (of phase *x*) rotates the magnetization onto –*y*

$$I_{1z} \xrightarrow{\pi/2\, I_{1x}} \xrightarrow{\pi/2\, I_{2x}} -I_{1y}$$

(the second arrow has no effect as it involves operators of spin 2). Next follows evolution for time t_1

$$-I_{1y} \xrightarrow{\Omega_1 t_1\, I_{1z}} \xrightarrow{\Omega_2 t_1\, I_{2z}} -\cos\Omega_1 t_1\ I_{1y} + \sin\Omega_1 t_1\ I_{1x}$$

again, the second arrow has no effect. The second 90° pulse turns the first term onto the *z*-axis and leaves the second term unaffected

$$-\cos\Omega_1 t_1\ I_{1y} \xrightarrow{\pi/2\, I_{1x}} \xrightarrow{\pi/2\, I_{2x}} -\cos\Omega_1 t_1\ I_{1z}$$
$$\sin\Omega_1 t_1\ I_{1x} \xrightarrow{\pi/2\, I_{1x}} \xrightarrow{\pi/2\, I_{2x}} \sin\Omega_1 t_1\ I_{1x}$$

Only the I_{1z} term leads to cross-peaks by chemical exchange, so the other term will be ignored (in an experiment this is achieved by appropriate coherence pathway selection – see lecture 4). The effect of the first part of the sequence is to generate, at the start of the mixing time, τ_{mix}, some *z*-magnetization on spin 1 whose size depends, via the cosine term, on t_1 and the frequency, Ω_1, with which the spin 1 evolves during t_1. The magnetization is said to be frequency labelled.

During the mixing time, τ_{mix}, spin 1 may undergo chemical exchange with spin 2. If it does this, it carries with it the frequency label that it acquired during t_1. The extent to which this transfer takes place depends on the details of the chemical kinetics; it will be assumed simply that during τ_{mix} a fraction *f* of the spins of type 1 chemically exchange with spins of type 2. The effect of the mixing process can then be written

$$-\cos\Omega_1 t_1\ I_{1z} \xrightarrow{\text{mixing}} -(1-f)\cos\Omega_1 t_1\ I_{1z} - f\cos\Omega_1 t_1\ I_{2z}$$

The final 90° pulse rotates this *z*-magnetization back onto the *y*-axis

$$-(1-f)\cos\Omega_1 t_1\ I_{1z} \xrightarrow{\pi/2\, I_{1x}} \xrightarrow{\pi/2\, I_{2x}} (1-f)\cos\Omega_1 t_1\ I_{1y}$$
$$-f\cos\Omega_1 t_1\ I_{2z} \xrightarrow{\pi/2\, I_{1x}} \xrightarrow{\pi/2\, I_{2x}} f\cos\Omega_1 t_1\ I_{2y}$$

Although the magnetization started on spin 1, at the end of the sequence there is magnetization present on spin 2 – a process called magnetization transfer. The analysis of the experiment is completed by allowing the I_{1y} and I_{2y} operators to evolve for time t_2.

$$(1-f)\cos\Omega_1 t_1\ I_{1y} \xrightarrow{\Omega_1 t_2\ I_{1z}} \xrightarrow{\Omega_2 t_2\ I_{2z}}$$
$$(1-f)\cos\Omega_1 t_2 \cos\Omega_1 t_1\ I_{1y} - (1-f)\sin\Omega_1 t_2 \cos\Omega_1 t_1\ I_{1x}$$
$$f\cos\Omega_1 t_1\ I_{2y} \xrightarrow{\Omega_1 t_2\ I_{1z}} \xrightarrow{\Omega_2 t_2\ I_{2z}}$$
$$f\cos\Omega_2 t_2 \cos\Omega_1 t_1\ I_{2y} - f\sin\Omega_2 t_2 \cos\Omega_1 t_1\ I_{2x}$$

If it is assumed that the *y*-magnetization is detected during t_2 (this is an arbitrary choice, but a convenient one), the time domain signal has two terms:

$$(1-f)\cos\Omega_1 t_2 \cos\Omega_1 t_1 + f\cos\Omega_2 t_2 \cos\Omega_1 t_1$$

The crucial thing is that the amplitude of the signal recorded during t_2 is modulated by the evolution during t_1. This can be seen more clearly by imagining the Fourier transform, with respect to t_2, of the above function. The $\cos(\Omega_1 t_2)$ and $\cos(\Omega_2 t_2)$ terms transform to give absorption mode signals centred at Ω_1 and Ω_2 respectively in the F_2 dimension; these are denoted $A_1^{(2)}$ and $A_2^{(2)}$ (the subscript indicates which spin, and the superscript which dimension). The time domain function becomes

$$(1-f)A_1^{(2)}\cos\Omega_1 t_1 + fA_2^{(2)}\cos\Omega_1 t_1$$

If a series of spectra recorded as t_1 progressively increases are inspected it would be found that the $\cos(\Omega_1 t_2)$ term causes a change in size of the peaks at Ω_1 and Ω_2 – this is the modulation referred to above.

Fourier transformation with respect to t_1 gives peaks with an absorption lineshape, but this time in the F_1 dimension; an absorption mode signal at Ω_1 in F_1 is denoted $A_1^{(1)}$. The time domain signal becomes, after Fourier transformation in each dimension

$$(1-f)A_2^{(1)}A_1^{(1)} + fA_2^{(2)}A_1^{(1)}$$

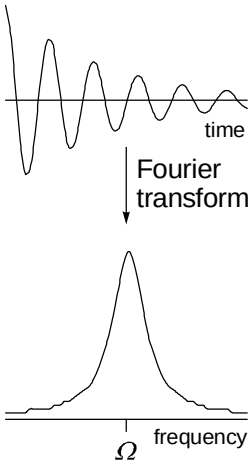

The Fourier transform of a decaying cosine function $\cos\Omega t \exp(-t/T_2)$ is an absorption mode Lorentzian centred at frequency Ω.

Thus, the final two-dimensional spectrum is predicted to have two peaks. One is at $(F_1, F_2) = (\Omega_1, \Omega_1)$ – this is a diagonal peak and arises from those spins of type 1 which did not undergo chemical exchange during τ_{mix}. The second is at $(F_1, F_2) = (\Omega_1, \Omega_2)$ – this is a cross peak which indicates that part of the magnetization from spin 1 was transferred to spin 2 during the mixing time. It is this peak that contains the useful information. If the calculation were repeated starting with magnetization on spin 2 it would be found that there are similar peaks at (Ω_2, Ω_2) and (Ω_2, Ω_1).

The NOESY (Nuclear Overhauser Effect SpectrocopY) spectrum is recorded using the same basic sequence. The only difference is that during the mixing time the cross-relaxation is responsible for the exchange of magnetization between different spins. Thus, a cross-peak indicates that two spins are experiencing mutual cross-relaxation and hence are close in space.

Having completed the analysis it can now be seen how the EXCSY/NOESY sequence is put together. First, the $90° - t_1 - 90°$ sequence is used to generate frequency labelled *z*-magnetization. Then, during τ_{mix}, this magnetization is allowed to migrate to other spins, carrying its label with it. Finally, the last pulse renders the *z*-magnetization observable.

3.3 More about two-dimensional transforms

From the above analysis it was seen that the signal observed during t_2 has an amplitude proportional to $\cos(\Omega_1 t_1)$; the amplitude of the signal observed during t_2 depends on the evolution during t_1. For the first increment of t_1 ($t_1 = 0$), the signal will be a maximum, the second increment will have size proportional to $\cos(\Omega_1 \Delta_1)$, the third proportional to $\cos(\Omega_1 2\Delta_1)$, the fourth to $\cos(\Omega_1 3\Delta_1)$ and so on. This modulation of the amplitude of the observed signal by the t_1 evolution is illustrated in the figure below.

In the figure the first column shows a series of free induction decays that would be recorded for increasing values of t_1 and the second column shows the Fourier transforms of these signals. The final step in constructing the two-dimensional spectrum is to Fourier transform the data along the t_1 dimension. This process is also illustrated in the figure. Each of the spectra shown in the second column are represented as a series of data points, where each point corresponds to a different F_2 frequency. The data point corresponding to a particular F_2 frequency is selected from the spectra for $t_1 = $, $t_1 = \Delta_1$, $t_1 = 2\Delta_1$ and so on for all the t_1 values. Such a process results in a function, called an interferogram, which has t_1 as the running variable.

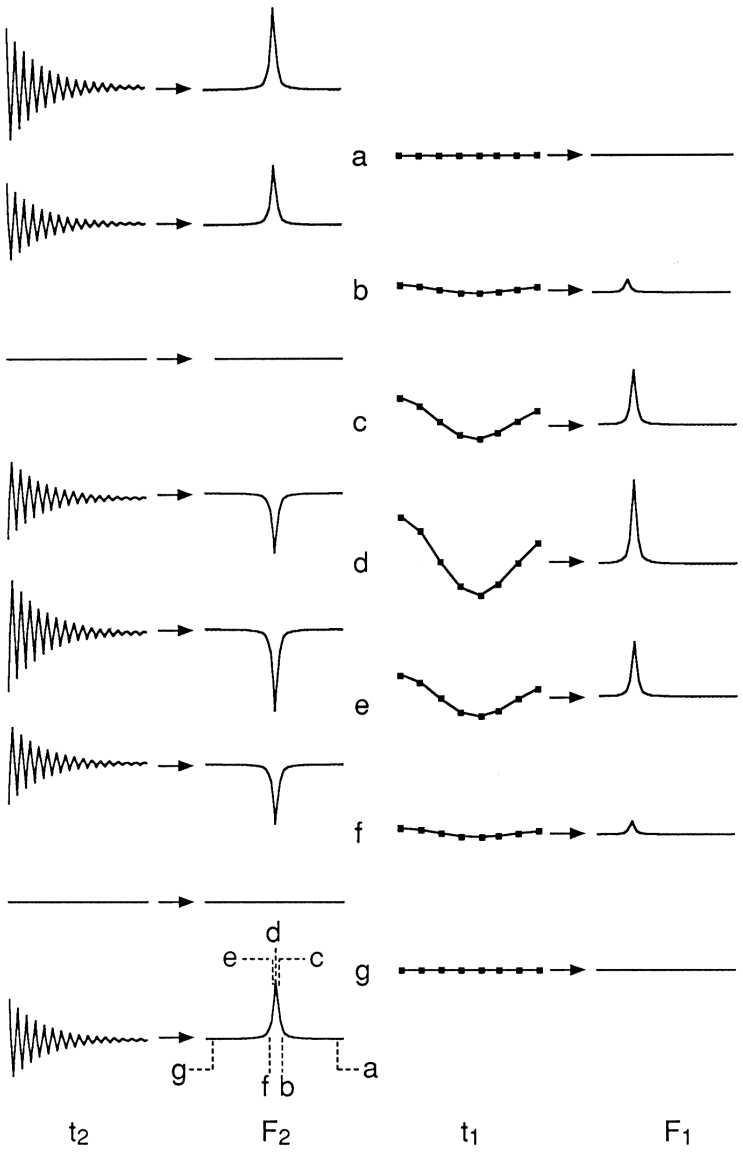

Illustration of how the modulation of a free induction decay by evolution during t_1 gives rise to a peak in the two-dimensional spectrum. In the left most column is shown a series of free induction decays that would be recorded for successive values of t_1; t_1 increases down the page. Note how the amplitude of these free induction decays varies with t_1, something that becomes even plainer when the time domain signals are Fourier transformed, as shown in the second column. In practice, each of these F_2 spectra in column two consist of a series of data points. The data point at the same frequency in each of these spectra is extracted and assembled into an interferogram, in which the horizontal axis is the time t_1. Several such interferograms, labelled *a* to *g*, are shown in the third column. Note that as there were eight F_2 spectra in column two corresponding to different t_1 values there are eight points in each interferogram. The F_2 frequencies at which the interferograms are taken are indicated on the lower spectrum of the second column. Finally, a second Fourier transformation of these interferograms gives a series of F_1 spectra shown in the right hand column. Note that in this column F_2 increases down the page, whereas in the first column t_1 increase down the page. The final result is a two-dimensional spectrum containing a single peak.

Several interferograms, labelled *a* to *g*, computed for different F_2 frequencies are shown in the third column of the figure. The particular F_2 frequency that each interferogram corresponds to is indicated in the bottom spectrum of the second column. The amplitude of the signal in each interferogram is different, but in this case the modulation frequency is the same. The final stage in the processing is to Fourier transform these interferograms to give the series of spectra which are shown in the right most column of the figure. These spectra have F_1 running horizontally and

F_2 running down the page. The modulation of the time domain signal has been transformed into a single two-dimensional peak. Note that the peak appears on several traces corresponding to different F_2 frequencies because of the width of the line in F_2.

The time domain data in the t_1 dimension can be manipulated by multiplying by weighting functions or zero filling, just as with conventional free induction decays.

3.4 Two-dimensional experiments using coherence transfer through *J*-coupling

Perhaps the most important set of two-dimensional experiments are those which transfer magnetization from one spin to another via the scalar coupling between them. As was seen in section 2.3.3, this kind of transfer can be brought about by the action of a pulse on an anti-phase state. In outline the basic process is

$$I_{1x} \xrightarrow{\text{coupling}} 2I_{1y}I_{2z} \xrightarrow{90°(x)\text{ to both spins}} 2I_{1z}I_{2y}$$

spin 1 spin 2

3.4.1 COSY

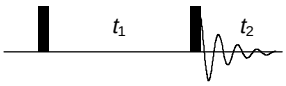

Pulse sequence for the two-dimensional COSY experiment

The pulse sequence for this experiment is shown opposite. It will be assumed in the analysis that all of the pulses are applied about the *x*-axis and for simplicity the calculation will start with equilibrium magnetization only on spin 1. The effect of the first pulse is to generate *y*-magnetization, as has been worked out previously many times

$$I_{1z} \xrightarrow{\pi/2I_{1x}} \xrightarrow{\pi/2I_{2x}} -I_{1y}$$

This state then evolves for time t_1, first under the influence of the offset of spin 1 (that of spin 2 has no effect on spin 1 operators):

$$-I_{1y} \xrightarrow{\Omega_1 t_1 I_{1z}} -\cos\Omega_1 t_1\, I_{1y} + \sin\Omega_1 t_1\, I_{1x}$$

Both terms on the right then evolve under the coupling

$$-\cos\Omega_1 t_1\, I_{1y} \xrightarrow{2\pi J_{12} t_1 I_{1z} I_{2z}} -\cos\pi J_{12} t_1 \cos\Omega_1 t_1\, I_{1y} + \sin\pi J_{12} t_1 \cos\Omega_1 t_1\, 2I_{1x}I_{2z}$$

$$\sin\Omega_1 t_1\, I_{1x} \xrightarrow{2\pi J_{12} t_1 I_{1z} I_{2z}} \cos\pi J_{12} t_1 \sin\Omega_1 t_1\, I_{1x} + \sin\pi J_{12} t_1 \sin\Omega_1 t_1\, 2I_{1y}I_{2z}$$

That completes the evolution under t_1. Now all that remains is to consider the effect of the final pulse, remembering that the effect of the pulse on both spins needs to be computed. Taking the terms one by one:

$$-\cos\pi J_{12}t_1\cos\Omega_1 t_1\ I_{1y} \xrightarrow{\pi/2I_{1x}} \xrightarrow{\pi/2I_{2x}} -\cos\pi J_{12}t_1\cos\Omega_1 t_1\ I_{1z} \quad \{1\}$$

$$\sin\pi J_{12}t_1\cos\Omega_1 t_1\ 2I_{1x}I_{2z} \xrightarrow{\pi/2I_{1x}} \xrightarrow{\pi/2I_{2x}} -\sin\pi J_{12}t_1\cos\Omega_1 t_1\ 2I_{1x}I_{2y} \quad \{2\}$$

$$\cos\pi J_{12}t_1\sin\Omega_1 t_1\ I_{1x} \xrightarrow{\pi/2I_{1x}} \xrightarrow{\pi/2I_{2x}} \cos\pi J_{12}t_1\sin\Omega_1 t_1\ I_{1x} \quad \{3\}$$

$$\sin\pi J_{12}t_1\sin\Omega_1 t_1\ 2I_{1y}I_{2z} \xrightarrow{\pi/2I_{1x}} \xrightarrow{\pi/2I_{2x}} -\sin\pi J_{12}t_1\sin\Omega_1 t_1\ 2I_{1z}I_{2y} \quad \{4\}$$

Terms {1} and {2} are unobservable. Term {3} corresponds to in-phase magnetization of spin 1, aligned along the *x*-axis. The t_1 modulation of this term depends on the offset of spin 1, so a diagonal peak centred at (Ω_1,Ω_1) is predicted. Term {4} is the really interesting one. It shows that anti-phase magnetization on spin 1, $2I_{1y}I_{2z}$, is transferred to anti-phase magnetization on spin 2, $2I_{1z}I_{2y}$; this is an example of coherence transfer. Term {4} appears as observable magnetization on spin 2, but it is modulated in t_1 with the offset of spin 1, thus it gives rise to a cross-peak centred at (Ω_1,Ω_2). It has been shown, therefore, how cross- and diagonal-peaks arise in a COSY spectrum.

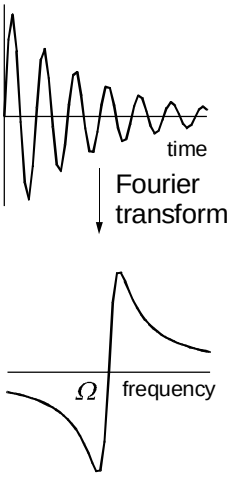

The Fourier transform of a decaying sine function $\sin\Omega t\ \exp(-t/T_2)$ is a dispersion mode Lorentzian centred at frequency Ω.

Some more consideration should be give to the form of the cross- and diagonal peaks. Consider again term {3}: it will give rise to an in-phase multiplet in F_2, and as it is along the *x*-axis, the lineshape will be dispersive. The form of the modulation in t_1 can be expanded, using the formula, $\cos A\sin B = \frac{1}{2}\{\sin(B+A)+\sin(B-A)\}$ to give

$$\cos\pi J_{12}t_1\sin\Omega_1 t_1 = \tfrac{1}{2}\left\{\sin\left(\Omega_1 t_1+\pi J_{12}t_1\right)+\sin\left(\Omega_1 t_1-\pi J_{12}t\right)\right\}$$

Two peaks in F_1 are expected at $\Omega_1 \pm \pi J_{12}$, these are just the two lines of the spin 1 doublet. In addition, since these are sine modulated they will have the dispersion lineshape. Note that both components in the spin 1 multiplet observed in F_2 are modulated in this way, so the appearance of the two-dimensional multiplet can best be found by "multiplying together" the multiplets in the two dimensions, as shown opposite. In addition, all four components of the diagonal-peak multiplet have the same sign, and have the double dispersion lineshape illustrated below

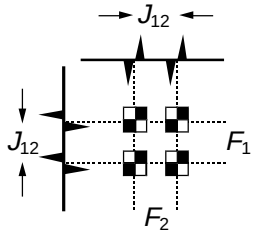

Schematic view of the diagonal peak from a COSY spectrum. The squares are supposed to indicate the two-dimensional double dispersion lineshape illustrated below

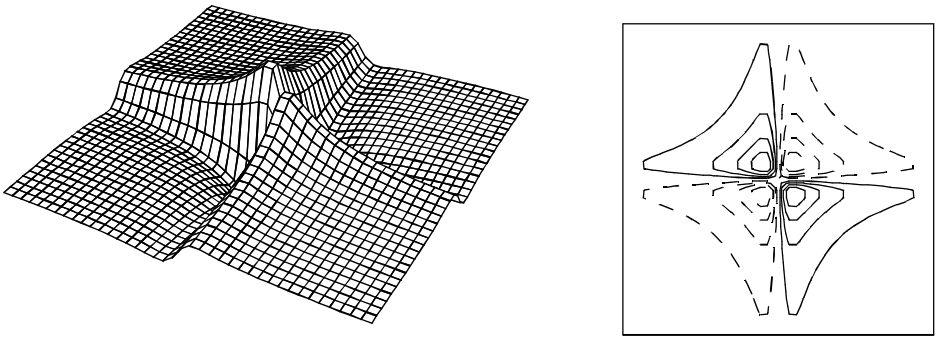

The double dispersion lineshape seen in pseudo 3D and as a contour plot; negative contours are indicated by dashed lines.

Term {4} can be treated in the same way. In F_2 we know that this term

gives rise to an anti-phase absorption multiplet on spin 2. Using the relationship $\sin B \sin A = \frac{1}{2}\{-\cos(B+A) + \cos(B-A)\}$ the modulation in t_1 can be expanded

$$\sin \pi J_{12} t_1 \sin \Omega_1 t = \tfrac{1}{2}\left\{-\cos\left(\Omega_1 t_1 + \pi J_{12} t_1\right) + \cos\left(\Omega_1 t_1 - \pi J_{12} t\right)\right\}$$

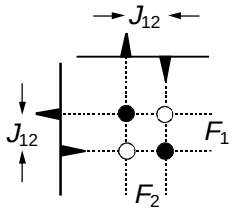

Schematic view of the cross-peak multiplet from a COSY spectrum. The circles are supposed to indicate the two-dimensional double absorption lineshape illustrated below; filled circles represent positive intensity, open represent negative intensity.

Two peaks in F_1, at $\Omega_1 \pm \pi J_{12}$, are expected; these are just the two lines of the spin 1 doublet. Note that the two peaks have opposite signs – that is they are anti-phase in F_1. In addition, since these are cosine modulated we expect the absorption lineshape (see section 3.2). The form of the cross-peak multiplet can be predicted by "multiplying together" the F_1 and F_2 multiplets, just as was done for the diagonal-peak multiplet. The result is shown opposite. This characteristic pattern of positive and negative peaks that constitutes the cross-peak is know as an anti-phase square array.

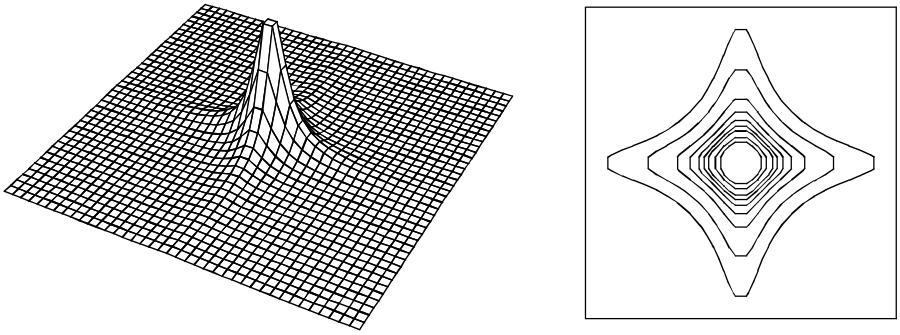

The double absorption lineshape seen in pseudo 3D and as a contour plot.

COSY spectra are sometimes plotted in the absolute value mode, where all the sign information is suppressed deliberately. Although such a display is convenient, especially for routine applications, it is generally much more desirable to retain the sign information. Spectra displayed in this way are said to be phase sensitive; more details of this are given in section 3.6.

As the coupling constant becomes comparable with the linewidth, the positive and negative peaks in the cross-peak multiplet begin to overlap and cancel one another out. This leads to an overall reduction in the intensity of the cross-peak multiplet, and ultimately the cross-peak disappears into the noise in the spectrum. The smallest coupling which gives rise to a cross-peak is thus set by the linewidth and the signal-to-noise ratio of the spectrum.

3.4.2 Double-quantum filtered COSY (DQF COSY)

The conventional COSY experiment suffers from a disadvantage which arises from the different phase properties of the cross- and diagonal-peak multiplets. The components of a diagonal peak multiplet are all in-phase and so tend to reinforce one another. In addition, the dispersive tails of these peaks spread far into the spectrum. The result is a broad intense diagonal which can obscure nearby cross-peaks. This effect is particularly troublesome when the coupling is comparable with the linewidth as in such

cases, as was described above, cancellation of anti-phase components in the cross-peak multiplet reduces the overall intensity of these multiplets.

This difficulty is neatly side-stepped by a modification called double quantum filtered COSY (DQF COSY). The pulse sequence is shown opposite.

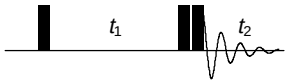

The pulse sequence for DQF COSY; the delay between the last two pulses is usually just a few microseconds.

Up to the second pulse the sequence is the same as COSY. However, it is arranged that only double-quantum coherence present during the (very short) delay between the second and third pulses is ultimately allowed to contribute to the spectrum. Hence the name, "double-quantum filtered", as all the observed signals are filtered through double-quantum coherence. The final pulse is needed to convert the double quantum coherence back into observable magnetization. This double-quantum derived signal is selected by the use of coherence pathway selection using phase cycling or field gradient pulses, further details of which will be given in lecture 4.

In the analysis of the COSY experiment, it is seen that after the second 90° pulse it is term {2} that contains double-quantum coherence; this can be demonstrated explicitly by expanding this term in the raising and lowering operators, as was done in section 2.5

$$\begin{aligned} 2I_{1x}I_{2y} &= 2\times\tfrac{1}{2}\left(I_{1+}+I_{1-}\right)\times\tfrac{1}{2i}\left(I_{2+}-I_{2-}\right) \\ &= \tfrac{1}{2i}\left(I_{1+}I_{2+}-I_{1-}I_{2-}\right)+\tfrac{1}{2i}\left(-I_{1+}I_{2-}+I_{1-}I_{2+}\right) \end{aligned}$$

This term contains both double- and zero-quantum coherence. The pure double-quantum part is the term in the first bracket on the right; this term can be re-expressed in Cartesian operators:

$$\begin{aligned} \tfrac{1}{2i}\left(I_{1+}I_{2+}-I_{1-}I_{2-}\right) &= \tfrac{1}{2i}\left[\left(I_{1x}+iI_{1y}\right)\left(I_{1x}+iI_{1y}\right)+\left(I_{2x}-iI_{2y}\right)\left(I_{2x}-iI_{2y}\right)\right] \\ &= \tfrac{1}{2}\left[2I_{1x}I_{2y}+2I_{1y}I_{2x}\right] \end{aligned}$$

The effect of the last 90°(*x*) pulse on the double quantum part of term {2} is thus

$$-\tfrac{1}{2}\sin\pi J_{12}t_1\cos\Omega_1 t_1\left(2I_{1x}I_{2y}+2I_{1y}I_{2x}\right)\xrightarrow{\pi/2I_{1x}}\xrightarrow{\pi/2I_{2x}} -\tfrac{1}{2}\sin\pi J_{12}t_1\cos\Omega_1 t_1\left(2I_{1x}I_{2z}+2I_{1z}I_{2x}\right)$$

The first term on the right is anti-phase magnetization of spin 1 aligned along the *x*-axis; this gives rise to a diagonal-peak multiplet. The second term is anti-phase magnetization of spin 2, again aligned along *x*; this will give rise to a cross-peak multiplet. Both of these terms have the same modulation in t_1, which can be shown, by a similar analysis to that used above, to lead to an anti-phase multiplet in F_1. As these peaks all have the same lineshape the overall phase of the spectrum can be adjusted so that they are all in absorption; see section 3.6 for further details. In contrast to the case of a simple COSY experiment both the diagonal- and cross-peak multiplets are in anti-phase in both dimensions, thus avoiding the strong in-

phase diagonal peaks found in the simple experiment. The DQF COSY experiment is the method of choice for tracing out coupling networks in a molecule.

3.4.3 Heteronuclear correlation experiments

One particularly useful experiment is to record a two-dimensional spectrum in which the co-ordinate of a peak in one dimension is the chemical shift of one type of nucleus (e.g. proton) and the co-ordinate in the other dimension is the chemical shift of another nucleus (e.g. carbon-13) which is coupled to the first nucleus. Such spectra are often called shift correlation maps or shift correlation spectra.

The one-bond coupling between a carbon-13 and the proton directly attached to it is relatively constant (around 150 Hz), and much larger than any of the long-range carbon-13 proton couplings. By utilizing this large difference experiments can be devised which give maps of carbon-13 shifts *vs* the shifts of directly attached protons. Such spectra are very useful as aids to assignment; for example, if the proton spectrum has already been assigned, simply recording a carbon-13 proton correlation experiment will give the assignment of all the protonated carbons.

Only one kind of nuclear species can be observed at a time, so there is a choice as to whether to observe carbon-13 or proton when recording a shift correlation spectrum. For two reasons, it is very advantageous from the sensitivity point of view to record protons. First, the proton magnetization is larger than that of carbon-13 because there is a larger separation between the spin energy levels giving, by the Boltzmann distribution, a greater population difference. Second, a given magnetization induces a larger voltage in the coil the higher the NMR frequency becomes.

Trying to record a carbon-13 proton shift correlation spectrum by proton observation has one serious difficulty. Carbon-13 has a natural abundance of only 1%, thus 99% of the molecules in the sample do not have any carbon-13 in them and so will not give signals that can be used to correlate carbon-13 and proton. The 1% of molecules with carbon-13 will give a perfectly satisfactory spectrum, but the signals from these resonances will be swamped by the much stronger signals from non-carbon-13 containing molecules. However, these unwanted signals can be suppressed using coherence selection in a way which will be described below and which will be further elaborated in lecture 4.

3.4.3.1 Heteronuclear multiple-quantum correlation (HMQC)

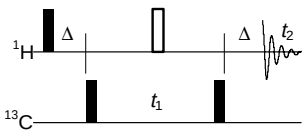

The pulse sequence for HMQC. Filled rectangles represent 90° pulses and open rectangles represent 180° pulses. The delay Δ is set to $1/(2J_{12})$.

The pulse sequence for this popular experiment is given opposite. The sequence will be analysed for a coupled carbon-13 proton pair, where spin 1 will be the carbon-13 and spin 2 the proton.

The analysis will start with equilibrium magnetization on spin 1, I_{1z}. The whole analysis can be greatly simplified by noting that the 180° pulse is exactly midway between the first 90° pulse and the start of data acquisition. As has been shown in section 2.4, such a sequence forms a spin echo and so the evolution of the offset of spin 1 over the entire period (t_1 + 2Δ) is refocused. Thus the evolution of the offset of spin 1 can simply be ignored

for the purposes of the calculation.

At the end of the delay Δ the state of the system is simply due to evolution of the term $-I_{1y}$ under the influence of the scalar coupling:

$$-\cos\pi J_{12}\Delta\ I_{1y} + \sin\pi J_{12}\Delta\ 2I_{1x}I_{2z}$$

It will be assumed that $\Delta = 1/(2J_{12})$, so only the anti-phase term is present.

The second 90° pulse is applied to carbon-13 (spin 2) only

$$2I_{1x}I_{2z} \xrightarrow{\pi/2\,I_{2x}} -2I_{1x}I_{2y}$$

This pulse generates a mixture of heteronuclear double- and zero-quantum coherence, which then evolves during t_1. In principle this term evolves under the influence of the offsets of spins 1 and 2 and the coupling between them. However, it has already been noted that the offset of spin 1 is refocused by the centrally placed 180° pulse, so it is not necessary to consider evolution due to this term. In addition, it can be shown that multiple-quantum coherence involving spins i and j does not evolve under the influence of the coupling, J_{ij}, between these two spins (see appendix x.x). As a result of these two simplifications, the only evolution that needs to be considered is that due to the offset of spin 2 (the carbon-13).

$$-2I_{1x}I_{2y} \xrightarrow{\Omega_2 t_1 I_{2z}} -\cos\Omega_2 t_1\ 2I_{1x}I_{2y} + \sin\Omega_2 t_1\ 2I_{1x}I_{2x}$$

The second 90° pulse to spin 2 (carbon-13) regenerates the first term on the right into spin 1 (proton) observable magnetization; the other remains unobservable

$$-\cos\Omega_2 t_1\ 2I_{1x}I_{2y} \xrightarrow{\pi/2\,I_{2x}} -\cos\Omega_2 t_1\ 2I_{1x}I_{2z}$$

This term then evolves under the coupling, again it is assumed that $\Delta = 1/(2J_{12})$

$$-\cos\Omega_2 t_1\ 2I_{1x}I_{2z} \xrightarrow{2\pi J_{12}\Delta I_{1z}I_{2z},\ \Delta=1/(2J_{12})} -\cos\Omega_2 t_1\ I_{1y}$$

This is a very nice result; in F_2 there will be an in-phase doublet centred at the offset of spin 1 (proton) and these two peaks will have an F_1 co-ordinate simply determined by the offset of spin 2 (carbon-13); the peaks will be in absorption. A schematic spectrum is shown opposite.

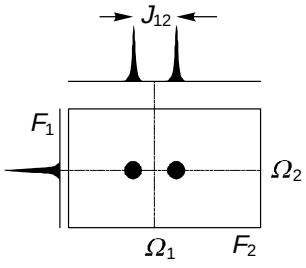

Schematic HMQC spectrum for two coupled spins.

The problem of how to suppress the very strong signals from protons not coupled to any carbon-13 nuclei now has to be addressed. From the point of view of these protons the carbon-13 pulses might as well not even be there, and the pulse sequence looks like a simple spin echo. This insensitivity to the carbon-13 pulses is the key to suppressing the unwanted signals.

Suppose that the phase of the first carbon-13 90° pulse is altered from *x* to –*x*. Working through the above calculation it is found that the wanted signal from the protons coupled to carbon-13 changes sign i.e. the observed spectrum will be inverted. In contrast the signal from a proton not coupled to carbon-13 will be unaffected by this change. Thus, for each t_1 increment the free induction decay is recorded twice: once with the first carbon-13 90° pulse set to phase *x* and once with it set to phase –*x*. The two free induction decays are then subtracted in the computer memory thus cancelling the unwanted signals. This is an example of a very simple phase cycle, more details of which are given in lecture 4.

In the case of carbon-13 and proton the one bond coupling is so much larger than any of the long range couplings that a choice of $\Delta = 1/(2J_{\text{one bond}})$ does not give any correlations other than those through the one-bond coupling. There is simply insufficient time for the long-range couplings to become anti-phase. However, if Δ is set to a much longer value (30 to 60 ms), long-range correlations will be seen. Such spectra are very useful in assigning the resonances due to quaternary carbon-13 atoms. The experiment is often called HMBC (heteronuclear multiple-bond correlation).

Now that the analysis has been completed it can be seen what the function of various elements in the pulse sequence is. The first pulse and delay generate magnetization on proton which is anti-phase with respect to the coupling to carbon-13. The carbon-13 90° pulse turns this into multiple quantum coherence. This forms a filter through which magnetization not bound to carbon-13 cannot pass and it is the basis of discrimination between signals from protons bound and not bound to carbon-13. The second carbon-13 pulse returns the multiple quantum coherence to observable anti-phase magnetization on proton. Finally, the second delay Δ turns the anti-phase state into an in-phase state. The centrally placed proton 180° pulse refocuses the proton shift evolution for both the delays Δ and t_1.

3.4.3.2 Heteronuclear single-quantum correlation (HSQC)

This pulse sequence results in a spectrum identical to that found for HMQC. Despite the pulse sequence being a little more complex than that for HMQC, HSQC has certain advantages for recording the spectra of large molecules, such a proteins. The HSQC pulse sequence is often embedded in much more complex sequences which are used to record two- and three-dimensional spectra of carbon-13 and nitrogen-15 labelled proteins.

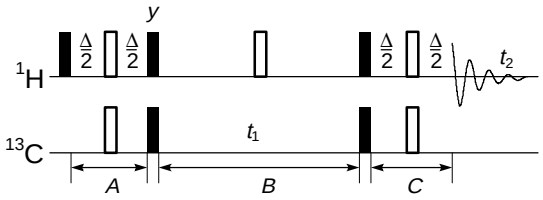

The pulse sequence for HSQC. Filled rectangles represent 90° pulses and open rectangles represent 180° pulses. The delay Δ is set to $1/(2J_{12})$; all pulses have phase x unless otherwise indicated.

If this sequence were to be analysed by considering each delay and pulse in turn the resulting calculation would be far too complex to be useful. A more intelligent approach is needed where simplifications are used, for example

by recognizing the presence of spin echoes who refocus offsets or couplings. Also, it is often the case that attention can be focused a particular terms, as these are the ones which will ultimately lead to observable signals. This kind of "intelligent" analysis will be illustrated here.

Periods *A* and *C* are spin echoes in which 180° pulses are applied to both spins; it therefore follows that the offsets of spins 1 and 2 will be refocused, but the coupling between them will evolve throughout the entire period. As the total delay in the spin echo is $1/(2J_{12})$ the result will be the complete conversion of in-phase into anti-phase magnetization.

Period *B* is a spin echo in which a 180° pulse is applied only to spin 1. Thus, the offset of spin 1 is refocused, as is the coupling between spins 1 and 2; only the offset of spin 2 affects the evolution.

With these simplifications the analysis is easy. The first pulse generates $-I_{1y}$; during period *A* this then becomes $-2I_{1x}I_{2z}$. The 90°(*y*) pulse to spin 1 turns this to $2I_{1z}I_{2z}$ and the 90°(*x*) pulse to spin 2 turns it to $-2I_{1z}I_{2y}$. The evolution during period *B* is simply under the offset of spin 2

$$-2I_{1z}I_{2y} \xrightarrow{\Omega_2 t_1\ I_{2z}} -\cos\Omega_2 t_1\ 2I_{1z}I_{2y} + \sin\Omega_2 t_1\ 2I_{1z}I_{2x}$$

The next two 90° pulses transfer the first term to spin 1; the second term is rotated into multiple quantum and is not observed

$$-\cos\Omega_2 t_1\ 2I_{1z}I_{2y} + \sin\Omega_2 t_1\ 2I_{1z}I_{2x} \xrightarrow{\pi/2(I_{1x}+I_{2x})} -\cos\Omega_2 t_1\ 2I_{1y}I_{2z} - \sin\Omega_2 t_1\ 2I_{1y}I_{2x}$$

The first term on the right evolves during period *C* into in-phase magnetization (the evolution of offsets is refocused). So the final observable term is $\cos\Omega_2 t_1\ I_{1x}$. The resulting spectrum is therefore an in-phase doublet in F_2, centred at the offset of spin 1, and these peaks will both have the same frequency in F_1, namely the offset of spin 2. The spectrum looks just like the HMQC spectrum.

3.5 Multiple-quantum spectroscopy

A key feature of two-dimensional NMR experiments is that no direct observations are made during t_1, it is thus possible to detect, indirectly, the evolution of unobservable coherences. An example of the use of this feature is in the indirect detection of multiple-quantum spectra. A typical pulse sequence for such an experiment is shown opposite

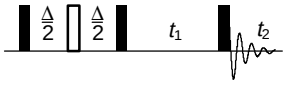

Pulse sequence for multiple-quantum spectroscopy.

For a two-spin system the optimum value for Δ is $1/(2J_{12})$. The sequence can be dissected as follows. The initial 90° – Δ/2 – 180° – Δ/2 – sequence is a spin echo which, at time Δ, refocuses any evolution of offsets but allows the coupling to evolve and generate anti-phase magnetization. This anti-phase magnetization is turned into multiple-quantum coherence by the second 90° pulse. After evolving for time t_1 the multiple quantum is returned into observable (anti-phase) magnetization by the final 90° pulse. Thus the first three pulses form the preparation period and the last pulse is

the mixing period.

3.5.1 Double-quantum spectrum for a three-spin system

The sequence will be analysed for a system of three spins. A complete analysis would be rather lengthy, so attention will be focused on certain terms as above, as many simplifying assumptions as possible will be made about the sequence.

The starting point will be equilibrium magnetization on spin 1, I_{1z}; after the spin echo the magnetization has evolved due to the coupling between spin 1 and spin 2, and the coupling between spin 1 and spin 3 (the 180° pulse causes an overall sign change (see section 2.4.1) but this has no real effect here so it will be ignored)

$$\begin{aligned} -I_{1y} &\xrightarrow{2\pi J_{12}\Delta I_{1z}I_{2z}} -\cos\pi J_{12}\Delta\ I_{1y} + \sin\pi J_{12}\Delta\ 2I_{1x}I_{2z} \\ &\xrightarrow{2\pi J_{13}\Delta I_{1z}I_{3z}} -\cos\pi J_{13}\Delta\ \cos\pi J_{12}\Delta\ I_{1y} + \sin\pi J_{13}\Delta\ \cos\pi J_{12}\Delta\ 2I_{1x}I_{3z} \\ &\qquad + \cos\pi J_{13}\Delta\ \sin\pi J_{12}\Delta\ 2I_{1x}I_{2z} + \sin\pi J_{13}\Delta\ \sin\pi J_{12}\Delta\ 4I_{1y}I_{2z}I_{3z} \end{aligned} \qquad [3.1]$$

Of these four terms, all but the first are turned into multiple-quantum by the second 90° pulse. For example, the second term becomes a mixture of double and zero quantum between spins 1 and 3

$$\sin\pi J_{13}\Delta\ \cos\pi J_{12}\Delta\ 2I_{1x}I_{3z} \xrightarrow{\pi/2\left(I_{1x}+I_{2x}+I_{3x}\right)} -\sin\pi J_{13}\Delta\ \cos\pi J_{12}\Delta\ 2I_{1x}I_{3y}$$

It will be assumed that appropriate coherence pathway selection (see section x.x) has been used so that ultimately only the double-quantum part contributes to the spectrum. This part is

$$\left[-\sin\pi J_{13}\Delta\ \cos\pi J_{12}\Delta\ \right]\left\{\tfrac{1}{2}\left(2I_{1x}I_{3y} + 2I_{1y}I_{3x}\right)\right\} \equiv B_{13}\mathrm{DQ}_y^{(13)}$$

The term in square brackets just gives the overall intensity, but does not affect the frequencies of the peaks in the two-dimensional spectrum as it does not depend on t_1 or t_2; this intensity term is denoted B_{13} for brevity. The operators in the curly brackets represent a pure double quantum state which can be denoted $\mathrm{DQ}_y^{(13)}$; the superscript (13) indicates that the double quantum is between spins 1 and 3 (see section 2.9).

As is shown in section 2.9, such a double-quantum term evolves under the offset according to

$$\begin{aligned} B_{13}\mathrm{DQ}_y^{(13)} &\xrightarrow{\Omega_1 t_1 I_{1z} + \Omega_2 t_1 I_{2z} + \Omega_3 t_1 I_{3z}} \\ &\qquad B_{13}\cos\left(\Omega_1 + \Omega_3\right)t_1\ \mathrm{DQ}_y^{(13)} - B_{13}\sin\left(\Omega_1 + \Omega_3\right)t_1\ \mathrm{DQ}_x^{(13)} \end{aligned}$$

where $\mathrm{DQ}_{\mathrm{x}}^{(13)} \equiv \frac{1}{2}\left(2I_{1x}I_{3x} - 2I_{1y}I_{3y}\right)$. This evolution is analogous to that of a single spin where *y* rotates towards *–x*.

As is also shown in section 2.9, $\mathrm{DQ}_y^{(13)}$ and $\mathrm{DQ}_x^{(13)}$ do not evolve under the coupling between spins 1 and 3, but they do evolve under the sum of the couplings between these two and all other spins; in this case this is simply $(J_{12}+J_{23})$. Taking each term in turn

$$B_{13}\cos\left(\Omega_1+\Omega_3\right)t_1\,\mathrm{DQ}_y^{(13)} \xrightarrow{2\pi J_{12}t_1 I_{1z}I_{2z}+2\pi J_{23}t_1 I_{2z}I_{3z}}$$
$$B_{13}\cos\left(\Omega_1+\Omega_3\right)t_1\cos\pi\left(J_{12}+J_{23}\right)t_1\,\mathrm{DQ}_y^{(13)}$$
$$-B_{13}\cos\left(\Omega_1+\Omega_3\right)t_1\sin\pi\left(J_{12}+J_{23}\right)t_1\,2I_{2z}\mathrm{DQ}_x^{(13)}$$
$$-B_{13}\sin\left(\Omega_1+\Omega_3\right)t_1\,\mathrm{DQ}_x^{(13)} \xrightarrow{2\pi J_{12}t_1 I_{1z}I_{2z}+2\pi J_{23}t_1 I_{2z}I_{3z}}$$
$$-B_{13}\sin\left(\Omega_1+\Omega_3\right)t_1\cos\pi\left(J_{12}+J_{23}\right)t_1\,\mathrm{DQ}_x^{(13)}$$
$$-B_{13}\sin\left(\Omega_1+\Omega_3\right)t_1\sin\pi\left(J_{12}+J_{23}\right)t_1\,2I_{2z}\mathrm{DQ}_y^{(13)}$$

Terms such as $2I_{2z}\mathrm{DQ}_y^{(13)}$ and $2I_{2z}\mathrm{DQ}_x^{(13)}$ can be thought of as double-quantum coherence which has become "anti-phase" with respect to the coupling to spin 2; such terms are directly analogous to single-quantum anti-phase magnetization.

Of all the terms present at the end of t_1, only $\mathrm{DQ}_y^{(13)}$ is rendered observable by the final pulse

$$\cos\left(\Omega_1+\Omega_3\right)t_1\cos\pi\left(J_{12}+J_{23}\right)t_1B_{13}\mathrm{DQ}_y^{(13)} \xrightarrow{\pi/2\left(I_{1x}+I_{2x}+I_{3x}\right)}$$
$$\cos\left(\Omega_1+\Omega_3\right)t_1\cos\pi\left(J_{12}+J_{23}\right)t_1B_{13}\left[2I_{1x}I_{3z}+2I_{1z}I_{3x}\right]$$

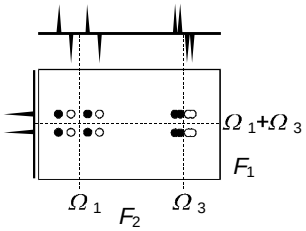

Schematic two-dimensional double quantum spectrum showing the multiplets arising from evolution of double-quantum coherence between spins 1 and 3. If has been assumed that $J_{12} > J_{13} > J_{23}$.

The calculation predicts that two two-dimensional multiplets appear in the spectrum. Both have the same structure in F_1, namely an in–phase doublet, split by $(J_{12} + J_{23})$ and centred at $(\Omega_1 + \Omega_3)$; this is analogous to a normal multiplet. In F_2 one two-dimensional multiplet is centred at the offset of spins 1, Ω_1, and one at the offset of spin 3, Ω_3; both multiplets are anti-phase with respect to the coupling J_{13}. Finally, the overall amplitude, B_{13}, depends on the delay Δ and all the couplings in the system. The schematic spectrum is shown opposite. Similar multiplet structures are seen for the double-quantum between spins 1 & 2 and spins 2 & 3.

3.5.2 Interpretation of double-quantum spectra

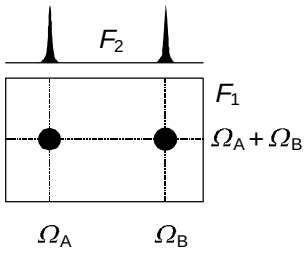

Schematic spectrum showing the relationship between the single- and double-quantum frequencies for coupled spins.

The double-quantum spectrum shows the relationship between the frequencies of the lines in the double quantum spectrum and those in the (conventional) single-quantum spectrum. If two two-dimensional multiplets appear at (F_1, F_2) = (Ω_A + Ω_B, Ω_A) and (Ω_A + Ω_B, Ω_B) the implication is that the two spins A and B are coupled, as it is only if there is a coupling present that double-quantum coherence between the two spins can be generated (e.g. in the previous section, if J_{13} = 0 the term B_{13}, goes to zero). The fact that the two two-dimensional multiplets share a common F_1 frequency and that this frequency is the sum of the two F_2 frequencies constitute a double check as to whether or not the peaks indicate that the spins are coupled.

Double quantum spectra give very similar information to that obtained from COSY i.e. the identification of coupled spins. Each method has particular advantages and disadvantages:

(1) In COSY the cross-peak multiplet is anti-phase in both dimensions, whereas in a double-quantum spectrum the multiplet is only anti-phase in F_2. This may lead to stronger peaks in the double-quantum spectrum due to less cancellation. However, during the two delays Δ magnetization is lost by relaxation, resulting in reduced peak intensities in the double-quantum spectrum.

(2) The value of the delay Δ in the double-quantum experiment affects the amount of multiple-quantum generated and hence the intensity in the spectrum. All of the couplings present in the spin system affect the intensity and as couplings cover a wide range, no single optimum value for Δ can be given. An unfortunate choice for Δ will result in low intensity, and it is then possible that correlations will be missed. No such problems occur with COSY.

(3) There are no diagonal-peak multiplets in a double-quantum spectrum, so that correlations between spins with similar offsets are relatively easy to locate. In contrast, in a COSY the cross-peaks from such a pair of spins could be obscured by the diagonal.

(4) In more complex spin systems the interpretation of a COSY remains unambiguous, but the double-quantum spectrum may show a peak with F_1 co-ordinate (Ω_A + Ω_B) and F_2 co-ordinate Ω_A (or Ω_B) even when spins A and B are not coupled. Such remote peaks, as they are called, appear when spins A and B are both coupled to a third spin. There are various tests that can differentiate these remote from the more useful direct peaks, but these require additional experiments. The form of these remote peaks in considered in the next section.

On the whole, COSY is regarded as a more reliable and simple experiment, although double-quantum spectroscopy is used in some special circumstances.

3.5.3 Remote peaks in double-quantum spectra

The origin of remote peaks can be illustrated by returning to the calculation of section 3.5.1. and focusing on the doubly anti-phase term which is present at the end of the spin echo (the fourth term in Eqn. [3.1])

$$\sin\pi J_{13}\Delta\ \sin\pi J_{12}\Delta\ 4I_{1y}I_{2z}I_{3z}$$

The 90° pulse rotates this into multiple-quantum

$$\sin\pi J_{13}\Delta\ \sin\pi J_{12}\Delta\ 4I_{1y}I_{2z}I_{3z} \xrightarrow{\pi/2\left(I_{1x}+I_{2x}+I_{3x}\right)} \sin\pi J_{13}\Delta\ \sin\pi J_{12}\Delta\ 4I_{1z}I_{2y}I_{3y}$$

The pure double-quantum part of this term is

$$-\tfrac{1}{2}\sin\pi J_{13}\Delta\ \sin\pi J_{12}\Delta\left(4I_{1z}I_{2x}I_{3x}-4I_{1z}I_{2y}I_{3y}\right)\equiv B_{23,1}2I_{1z}DQ_{x}^{(23)}$$

In words, what has been generated in double-quantum between spins 2 and 3, anti-phase with respect to spin 1. The key thing is that no coupling between spins 2 and 3 is required for the generation of this term – the intensity just depends on J_{12} and J_{13}; all that is required is that both spins 2 and 3 have a coupling to the third spin, spin 1.

During t_1 this term evolves under the influence of the offsets and the couplings. Only two terms ultimately lead to observable signals; at the end of t_1 these two terms are

$$B_{23,1}\cos\left(\Omega_2+\Omega_3\right)t_1\cos\pi\left(J_{12}+J_{13}\right)t_1\,2I_{1z}DQ_{x}^{(23)}$$
$$B_{23,1}\cos\left(\Omega_2+\Omega_3\right)t_1\sin\pi\left(J_{12}+J_{13}\right)t_1\,DQ_{y}^{(23)}$$

and after the final 90° pulse the observable parts are

$$B_{23,1}\cos\left(\Omega_2+\Omega_3\right)t_1\cos\pi\left(J_{12}+J_{13}\right)t_1\,4I_{1y}I_{2z}I_{3z}$$
$$B_{23,1}\cos\left(\Omega_2+\Omega_3\right)t_1\sin\pi\left(J_{12}+J_{13}\right)t_1\left(2I_{2x}I_{3z}+2I_{2z}I_{3x}\right)$$

The first term results in a multiplet appearing at Ω_1 in F_2 and at $(\Omega_2+\Omega_3)$ in F_1. The multiplet is doubly anti-phase (with respect to the couplings to spins 2 and 3) in F_2; in F_1 it is in-phase with respect to the sum of the couplings J_{12} and J_{13}. This multiplet is a remote peak, as its frequency coordinates do not conform to the simple pattern described in section 3.5.2. It is distinguished from direct peaks not only by its frequency coordinates, but also by having a different lineshape in F_2 to direct peaks and by being doubly anti-phase in that dimension.

The second and third terms are anti-phase with respect to the coupling between spins 2 and 3, and if this coupling is zero there will be cancellation within the multiplet and no signals will be observed. This is despite the fact that multiple-quantum coherence between these two spins has been generated.

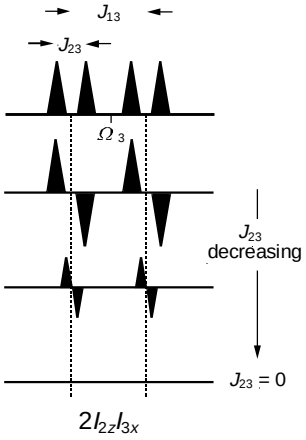

Illustration of how the intensity of an anti-phase multiplet decreases as the coupling which it is in anti-phase with respect to decreases. The in-phase multiplet is shown at the top, and below are three versions of the anti-phase multiplet for successively decreasing values of J_{23}.

3.6 Lineshapes and frequency discrimination

This is a somewhat involved topic which will only be possible to cover in outline in this lecture.

3.6.1 One-dimensional spectra

All modern spectrometers use a method know as quadrature detection, which in effect means that both the *x*- and *y*-components of the magnetization are detected simultaneously.

Suppose that a 90°(*y*) pulse is applied to equilibrium magnetization resulting in the generation of pure *x*-magnetization which then precesses in the transverse plane with frequency Ω. NMR spectrometers are set up to detect the *x*- and *y*-components of this magnetization. If it is assumed (arbitrarily) that these components decay exponentially with time constant T_2 the resulting signals, $S_x(t)$ and $S_y(t)$, from the two channels of the detector can be written

$$S_x(t) = \gamma \cos\Omega t \exp\left(-t/T_2\right) \quad S_y(t) = \gamma \sin\Omega t \exp\left(-t/T_2\right)$$

where γ is a factor which gives the absolute intensity of the signal.

Usually, these two components are combined in the computer to give a complex time-domain signal, $S(t)$

$$\begin{aligned} S(t) &= S_x(t) + iS_y(t) \\ &= \gamma\left(\cos\Omega t + i\sin\Omega t\right)\exp\left(-t/T_2\right) \\ &= \gamma \exp(i\Omega t)\exp\left(-t/T_2\right) \end{aligned} \qquad [3.2]$$

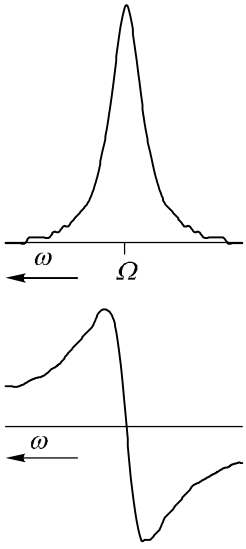

Absorption (above) and dispersion (below) Lorentzian lineshapes, centred at frequency Ω.

The Fourier transform of $S(t)$ is also a complex function, $S(\omega)$:

$$\begin{aligned} S(\omega) &= FT\left[S(t)\right] \\ &= \gamma\left\{A(\omega) + iD(\omega)\right\} \end{aligned}$$

where $A(\omega)$ and $D(\omega)$ are the absorption and dispersion Lorentzian lineshapes:

$$A(\omega) = \frac{1}{(\omega-\Omega)^2 T_2^2 + 1} \qquad D(\omega) = \frac{(\omega-\Omega)T_2}{(\omega-\Omega)^2 T_2^2 + 1}$$

These lineshapes are illustrated opposite. For NMR it is usual to display the spectrum with the absorption mode lineshape and in this case this corresponds to displaying the real part of $S(\omega)$.

3.6.1.1 Phase

Due to instrumental factors it is almost never the case that the real and

imaginary parts of $S(t)$ correspond exactly to the x- and y-components of the magnetization. Mathematically, this is expressed by multiplying the ideal function by an instrumental phase factor, ϕ_{instr}

$$S(t) = \gamma \exp\left(i\phi_{\text{instr}}\right) \exp(i\Omega t) \exp\left(-t/T_2\right)$$

The real and imaginary parts of $S(t)$ are

$$\begin{aligned}
\text{Re}\left[S(t)\right] &= \gamma\left(\cos\phi_{\text{instr}} \cos\Omega t - \sin\phi_{\text{instr}} \sin\Omega t\right) \exp\left(-t/T_2\right) \\
\text{Im}\left[S(t)\right] &= \gamma\left(\cos\phi_{\text{instr}} \sin\Omega t + \sin\phi_{\text{instr}} \cos\Omega t\right) \exp\left(-t/T_2\right)
\end{aligned}$$

Clearly, these do not correspond to the x– and y-components of the ideal time-domain function.

The Fourier transform of $S(t)$ carries forward the phase term

$$S(\omega) = \gamma \exp\left(i\phi_{\text{instr}}\right)\left\{A(\omega) + iD(\omega)\right\}$$

The real and imaginary parts of $S(\omega)$ are no longer the absorption and dispersion signals:

$$\begin{aligned}
\text{Re}\left[S(\omega)\right] &= \gamma\left(\cos\phi_{\text{instr}} A(\omega) - \sin\phi_{\text{instr}} D(\omega)\right) \\
\text{Im}\left[S(\omega)\right] &= \gamma\left(\cos\phi_{\text{instr}} D(\omega) + \sin\phi_{\text{instr}} A(\omega)\right)
\end{aligned}$$

Thus, displaying the real part of $S(\omega)$ will not give the required absorption mode spectrum; rather, the spectrum will show lines which have a mixture of absorption and dispersion lineshapes.

Restoring the pure absorption lineshape is simple. $S(\omega)$ is multiplied, in the computer, by a phase correction factor, ϕ_{corr}:

$$\begin{aligned}
S(\omega)\exp\left(i\phi_{\text{corr}}\right) &= \gamma \exp\left(i\phi_{\text{corr}}\right) \exp\left(i\phi_{\text{instr}}\right)\left\{A(\omega) + iD(\omega)\right\} \\
&= \gamma \exp\left(i\left(\phi_{\text{corr}} + \phi_{\text{instr}}\right)\right)\left\{A(\omega) + iD(\omega)\right\}
\end{aligned}$$

By choosing ϕ_{corr} such that $(\phi_{\text{corr}} + \phi_{\text{inst}}) = 0$ (*i.e.* $\phi_{\text{corr}} = -\phi_{\text{instr}}$) the phase terms disappear and the real part of the spectrum will have the required absorption lineshape. In practice, the value of the phase correction is set "by eye" until the spectrum "looks phased". NMR processing software also allows for an additional phase correction which depends on frequency; such a correction is needed to compensate for, amongst other things, imperfections in radiofrequency pulses.

3.6.1.2 Phase is arbitrary

Suppose that the phase of the 90° pulse is changed from *y* to *x*. The magnetization now starts along –*y* and precesses towards *x*; assuming that the instrumental phase is zero, the output of the two channels of the detector are

$$S_x(t) = \gamma \sin \Omega t \exp\left(-t/T_2\right) \quad S_y(t) = -\gamma \cos \Omega t \exp\left(-t/T_2\right)$$

The complex time-domain signal can then be written

$$\begin{aligned} S(t) &= S_x(t) + iS_y(t) \\ &= \gamma(\sin \Omega t - i \cos \Omega t) \exp\left(-t/T_2\right) \\ &\quad \gamma(-i)(\cos \Omega t + i \sin \Omega t) \exp\left(-t/T_2\right) \\ &= \gamma(-i) \exp(i\Omega t) \exp\left(-t/T_2\right) \\ &= \gamma \exp\left(i\phi_{\text{exp}}\right) \exp(i\Omega t) \exp\left(-t/T_2\right) \end{aligned}$$

Where ϕ_{exp}, the "experimental" phase, is $-\pi/2$ (recall that $\exp(i\phi) = \cos\phi + i \sin\phi$, so that $\exp(-i\,\pi/2) = -i$).

It is clear from the form of $S(t)$ that this phase introduced by altering the experiment (in this case, by altering the phase of the pulse) takes exactly the same form as the instrumental phase error. It can, therefore, be corrected by applying a phase correction so as to return the real part of the spectrum to the absorption mode lineshape. In this case the phase correction would be $\pi/2$.

The Fourier transform of the original signal is

$$\begin{gathered} S(\omega) = \gamma(-i)\{A(\omega) + iD(\omega)\} \\ \text{Re}[S(\omega)] = \gamma D(\omega) \qquad \text{Im}[S(\omega)] = -\gamma A(\omega) \end{gathered}$$

Thus the real part shows the dispersion mode lineshape, and the imaginary part shows the absorption lineshape. The 90° phase shift simply swaps over the real and imaginary parts.

3.6.1.3 Relative phase is important

The conclusion from the previous two sections is that the lineshape seen in the spectrum is under the control of the spectroscopist. It does not matter, for example, whether the pulse sequence results in magnetization appearing along the *x*- or *y*- axis (or anywhere in between, for that matter). It is always possible to phase correct the spectrum afterwards to achieve the desired lineshape.

However, if an experiment leads to magnetization from different processes or spins appearing along different axes, there is no single phase

correction which will put the whole spectrum in the absorption mode. This is the case in the COSY spectrum (section 3.4.1). The terms leading to diagonal-peaks appear along the *x*-axis, whereas those leading to cross-peaks appear along *y*. Either can be phased to absorption, but if one is in absorption, one will be in dispersion; the two signals are fundamentally 90° out of phase with one another.

3.6.1.4 Frequency discrimination

Suppose that a particular spectrometer is only capable of recording one, say the *x*-, component of the precessing magnetization. The time domain signal will then just have a real part (compare Eqn. [3.2] in section 3.6.1)

$$S(t) = \gamma \cos\Omega t \exp\left(-t/T_2\right)$$

Using the identity $\cos\theta = \frac{1}{2}\left(\exp(i\theta) + \exp(-i\theta)\right)$ this can be written

$$\begin{aligned} S(t) &= \tfrac{1}{2}\gamma\left[\exp(i\Omega t) + \exp(-i\Omega t)\right]\exp\left(-t/T_2\right) \\ &= \tfrac{1}{2}\gamma\exp(i\Omega t)\exp\left(-t/T_2\right) + \tfrac{1}{2}\gamma\exp(-i\Omega t)\exp\left(-t/T_2\right) \end{aligned}$$

The Fourier transform of the first term gives, in the real part, an absorption mode peak at $\omega = +\Omega$; the transform of the second term gives the same but at $\omega = -\Omega$.

$$\mathrm{Re}[S(\omega)] = \tfrac{1}{2}\gamma A_+ + \tfrac{1}{2}\gamma A_-$$

where A_+ represents an absorption mode Lorentzian line at $\omega = +\Omega$ and A_- represents the same at $\omega = -\Omega$; likewise, D_+ and D_- represent dispersion mode peaks at $+\Omega$ and $-\Omega$, respectively.

This spectrum is said to lack frequency discrimination, in the sense that it does not matter if the magnetization went round at $+\Omega$ or $-\Omega$, the spectrum still shows peaks at both $+\Omega$ and $-\Omega$. This is in contrast to the case where both the *x*- and *y*-components are measured where one peak appears at either positive or negative ω depending on the sign of Ω.

The lack of frequency discrimination is associated with the signal being modulated by a cosine wave, which has the property that $\cos(\Omega t) = \cos(-\Omega t)$, as opposed to a complex exponential, $\exp(i\Omega t)$ which is sensitive to the sign of Ω. In one-dimensional spectroscopy it is virtually always possible to arrange for the signal to have this desirable complex phase modulation, but in the case of two-dimensional spectra it is almost always the case that the signal modulation in the t_1 dimension is of the form $\cos(\Omega t_1)$ and so such spectra are not naturally frequency discriminated in the F_1 dimension.

Suppose now that only the *y*-component of the precessing magnetization could be detected. The time domain signal will then be (compare Eqn. [3.2] in section 3.6.1)

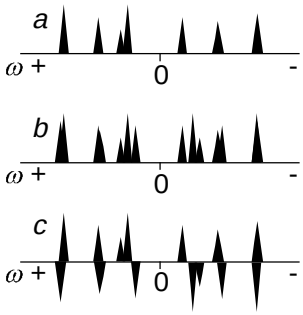

Spectrum *a* has peaks at positive and negative frequencies and is frequency discriminated. Spectrum *b* results from a cosine modulated time-domain data set; each peak appears at both positive and negative frequency, regardless of whether its real offset is positive or negative. Spectrum *c* results from a sine modulated data set; like *b* each peak appears twice, but with the added complication that one peak is inverted. Spectra *b* and *c* lack frequency discrimination and are quite uninterpretable as a result.

$$S(t) = i\gamma \sin \Omega t \exp\left(-t/T_2\right)$$

Using the identity $\sin\theta = \frac{1}{2i}\left(\exp(i\theta) - \exp(-i\theta)\right)$ this can be written

$$\begin{aligned} S(t) &= \tfrac{1}{2}\gamma\left[\exp(i\Omega t) - \exp(-i\Omega t)\right]\exp\left(-t/T_2\right) \\ &= \tfrac{1}{2}\gamma \exp(i\Omega t)\exp\left(-t/T_2\right) - \tfrac{1}{2}\gamma \exp(-i\Omega t)\exp\left(-t/T_2\right) \end{aligned}$$

and so

$$\mathrm{Re}[S(\omega)] = \tfrac{1}{2}\gamma A_+ - \tfrac{1}{2}\gamma A_-$$

This spectrum again shows two peaks, at $\pm\Omega$, but the two peaks have opposite signs; this is associated with the signal being modulated by a sine wave, which has the property that $\sin(-\Omega t) = -\sin(\Omega t)$. If the sign of Ω changes the two peaks swap over, but there are still two peaks. In a sense the spectrum is frequency discriminated, as positive and negative frequencies can be distinguished, but in practice in a spectrum with many lines with a range of positive and negative offsets the resulting set of possibly cancelling peaks would be impossible to sort out satisfactorily.

3.6.2 Two-dimensional spectra

3.6.2.1 Phase and amplitude modulation

There are two basic types of time-domain signal that are found in two-dimensional experiments. The first is phase modulation, in which the evolution in t_1 is encoded as a phase, *i.e.* mathematically as a complex exponential

$$S\left(t_1, t_2\right)_{\text{phase}} = \gamma \exp\left(i\Omega_1 t_1\right)\exp\left(-t_1/T_2^{(1)}\right)\exp\left(i\Omega_2 t_2\right)\exp\left(-t_2/T_2^{(2)}\right)$$

where Ω_1 and Ω_2 are the modulation frequencies in t_1 and t_2 respectively, and $T_2^{(1)}$ and $T_2^{(2)}$ are the decay time constants in t_1 and t_2 respectively.

The second type is amplitude modulation, in which the evolution in t_1 is encoded as an amplitude, *i.e.* mathematically as sine or cosine

$$\begin{aligned} S(t)_c &= \gamma \cos\left(\Omega_1 t_1\right)\exp\left(-t_1/T_2^{(1)}\right)\exp\left(i\Omega_2 t_2\right)\exp\left(-t_2/T_2^{(2)}\right) \\ S(t)_s &= \gamma \sin\left(\Omega_1 t_1\right)\exp\left(-t_1/T_2^{(1)}\right)\exp\left(i\Omega_2 t_2\right)\exp\left(-t_2/T_2^{(2)}\right) \end{aligned}$$

Generally, two-dimensional experiments produce amplitude modulation, indeed all of the experiments analysed in this chapter have produced either sine or cosine modulated data. Therefore most two-dimensional spectra are

fundamentally not frequency discriminated in the F_1 dimension. As explained above for one-dimensional spectra, the resulting confusion in the spectrum is not acceptable and steps have to be taken to introduce frequency discrimination.

It will turn out that the key to obtaining frequency discrimination is the ability to record, in separate experiments, both sine and cosine modulated data sets. This can be achieved by simply altering the phase of the pulses in the sequence.

For example, consider the EXSY sequence analysed in section 3.2 . The observable signal, at time $t_2 = 0$, can be written

$$(1-f)\cos\Omega_1 t_1 \; I_{1y} + f\cos\Omega_1 t_1 \; I_{2y}$$

If, however, the first pulse in the sequence is changed in phase from *x* to *y* the corresponding signal will be

$$-(1-f)\sin\Omega_1 t_1 \; I_{1y} - f\sin\Omega_1 t_1 \; I_{2y}$$

i.e. the modulation has changed from the form of a cosine to sine. In COSY and DQF COSY a similar change can be brought about by altering the phase of the first 90° pulse. In fact there is a general procedure for effecting this change, the details of which are given in lecture 4.

3.6.2.2 Two-dimensional lineshapes

The spectra resulting from two-dimensional Fourier transformation of phase and amplitude modulated data sets can be determined by using the following Fourier pair

$$FT\left[\exp(i\Omega t)\exp\left(-t/T_2\right)\right] = \{A(\omega) + iD(\omega)\}$$

where *A* and *D* are the dispersion Lorentzian lineshapes described in section 3.6.1

Phase modulation

For the phase modulated data set the transform with respect to t_2 gives

$$S(t_1,\omega_2)_{\text{phase}} = \gamma\exp(i\Omega_1 t_1)\exp\left(-t_1/T_2^{(1)}\right)\left[A_+^{(2)} + iD_+^{(2)}\right]$$

where $A_+^{(2)}$ indicates an absorption mode line in the F_2 dimension at $\omega_2 = +\Omega_2$ and with linewidth set by $T_2^{(2)}$; similarly $D_+^{(2)}$ is the corresponding dispersion line.

The second transform with respect to t_1 gives

$$S(\omega_1,\omega_2)_{\text{phase}} = \gamma\left[A_+^{(1)} + iD_+^{(1)}\right]\left[A_+^{(2)} + iD_+^{(2)}\right]$$

where $A_+^{(1)}$ indicates an absorption mode line in the F_1 dimension at $\omega_1 = +\Omega_1$ and with linewidth set by $T_2^{(1)}$; similarly $D_+^{(1)}$ is the corresponding dispersion line.

The real part of the resulting two-dimensional spectrum is

$$\text{Re}\left[S(\omega_1,\omega_2)_{\text{phase}}\right] = \gamma\left(A_+^{(1)}A_+^{(2)} - D_+^{(1)}D_+^{(2)}\right)$$

This is a single line at $(\omega_1,\omega_2) = (+\Omega_1,+\Omega_2)$ with the phase-twist lineshape, illustrated below.

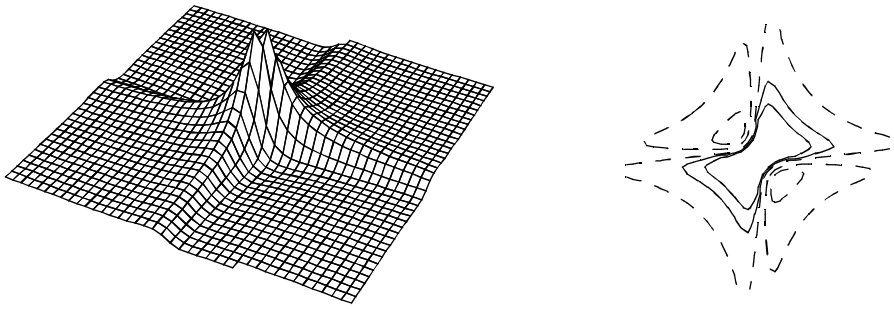

Pseudo 3D view and contour plot of the phase-twist lineshape.

The phase-twist lineshape is an inextricable mixture of absorption and dispersion; it is a superposition of the double absorption and double dispersion lineshape (illustrated in section 3.4.1). No phase correction will restore it to pure absorption mode. Generally the phase twist is not a very desirable lineshape as it has both positive and negative parts, and the dispersion component only dies off slowly.

Cosine amplitude modulation

For the cosine modulated data set the transform with respect to t_2 gives

$$S(t_1,\omega_2)_c = \gamma\cos(\Omega_1 t_1)\exp(-t_1/T_2^{(1)})\left[A_+^{(2)} + iD_+^{(2)}\right]$$

The cosine is then rewritten in terms of complex exponentials to give

$$S(t_1,\omega_2)_c = \tfrac{1}{2}\gamma\left[\exp(i\Omega_1 t_1) + \exp(-i\Omega_1 t_1)\right]\exp(-t_1/T_2^{(1)})\left[A_+^{(2)} + iD_+^{(2)}\right]$$

The second transform with respect to t_1 gives

$$S(\omega_1,\omega_2)_c = \tfrac{1}{2}\gamma\left[\left\{A_+^{(1)} + iD_+^{(1)}\right\} + \left\{A_-^{(1)} + iD_-^{(1)}\right\}\right]\left[A_+^{(2)} + iD_+^{(2)}\right]$$

where $A_-^{(1)}$ indicates an absorption mode line in the F_1 dimension at $\omega_1 = -\Omega_1$ and with linewidth set by $T_2^{(1)}$; similarly $D_-^{(1)}$ is the corresponding dispersion line.

The real part of the resulting two-dimensional spectrum is

$$\mathrm{Re}\left[S(\omega_1,\omega_2)_c\right] = \tfrac{1}{2}\gamma\left(A_+^{(1)}A_+^{(2)} - D_+^{(1)}D_+^{(2)}\right) + \tfrac{1}{2}\gamma\left(A_-^{(1)}A_+^{(2)} - D_-^{(1)}D_+^{(2)}\right)$$

This is a two lines, both with the phase-twist lineshape; one is located at $(+\Omega_1,+\Omega_2)$ and the other is at $(-\Omega_1,+\Omega_2)$. As expected for a data set which is cosine modulated in t_1 the spectrum is symmetrical about $\omega_1 = 0$.

A spectrum with a pure absorption mode lineshape can be obtained by discarding the imaginary part of the time domain data immediately after the transform with respect to t_2; *i.e.* taking the real part of $S(t_1,\omega_2)_c$

$$\begin{aligned} S(t_1,\omega_2)_c^{\mathrm{Re}} &= \mathrm{Re}\left[S(t_1,\omega_2)_c\right] \\ &= \gamma\cos(\Omega_1 t_1)\exp\left(-t_1/T_2^{(1)}\right)A_+^{(2)} \end{aligned}$$

Following through the same procedure as above:

$$S(t_1,\omega_2)_c^{\mathrm{Re}} = \tfrac{1}{2}\gamma\left[\exp(i\Omega_1 t_1) + \exp(-i\Omega_1 t_1)\right]\exp\left(-t_1/T_2^{(1)}\right)A_+^{(2)}$$

$$S(\omega_1,\omega_2)_c^{\mathrm{Re}} = \tfrac{1}{2}\gamma\left[\left\{A_+^{(1)} + iD_+^{(1)}\right\} + \left\{A_-^{(1)} + iD_-^{(1)}\right\}\right]A_+^{(2)}$$

The real part of the resulting two-dimensional spectrum is

$$\mathrm{Re}\left[S(\omega_1,\omega_2)_c^{\mathrm{Re}}\right] = \tfrac{1}{2}\gamma A_+^{(1)}A_+^{(2)} + \tfrac{1}{2}\gamma A_-^{(1)}A_+^{(2)}$$

This is two lines, located at $(+\Omega_1,+\Omega_2)$ and $(-\Omega_1,+\Omega_2)$, but in contrast to the above both have the double absorption lineshape. There is still lack of frequency discrimination, but the undesirable phase-twist lineshape has been avoided.

Sine amplitude modulation

For the sine modulated data set the transform with respect to t_2 gives

$$S(t_1,\omega_2)_s = \gamma \sin(\Omega_1 t_1)\exp(-t_1/T_2^{(1)})\left[A_+^{(2)} + iD_+^{(2)}\right]$$

The cosine is then rewritten in terms of complex exponentials to give

$$S(t_1,\omega_2)_s = \tfrac{1}{2i}\gamma\left[\exp(i\Omega_1 t_1) - \exp(-i\Omega_1 t_1)\right]\exp(-t_1/T_2^{(1)})\left[A_+^{(2)} + iD_+^{(2)}\right]$$

The second transform with respect to t_1 gives

$$S(\omega_1,\omega_2)_s = \tfrac{1}{2i}\gamma\left[\left\{A_+^{(1)} + iD_+^{(1)}\right\} - \left\{A_-^{(1)} + iD_-^{(1)}\right\}\right]\left[A_+^{(2)} + iD_+^{(2)}\right]$$

The imaginary part of the resulting two-dimensional spectrum is

$$\mathrm{Im}\left[S(\omega_1,\omega_2)_s\right] = -\tfrac{1}{2}\gamma\left(A_+^{(1)}A_+^{(2)} - D_+^{(1)}D_+^{(2)}\right) + \tfrac{1}{2}\gamma\left(A_-^{(1)}A_+^{(2)} - D_-^{(1)}D_+^{(2)}\right)$$

This is two lines, both with the phase-twist lineshape but with opposite signs; one is located at $(+\Omega_1,+\Omega_2)$ and the other is at $(-\Omega_1,+\Omega_2)$. As expected for a data set which is sine modulated in t_1 the spectrum is anti-symmetric about $\omega_1 = 0$.

As before, a spectrum with a pure absorption mode lineshape can be obtained by discarding the imaginary part of the time domain data immediately after the transform with respect to t_2; *i.e.* taking the real part of $S(t_1,\omega_2)_s$

$$\begin{aligned} S(t_1,\omega_2)_s^{\mathrm{Re}} &= \mathrm{Re}\left[S(t_1,\omega_2)_s\right] \\ &= \gamma \sin(\Omega_1 t_1)\exp(-t_1/T_2^{(1)})A_+^{(2)} \end{aligned}$$

Following through the same procedure as above:

$$S(t_1,\omega_2)_s^{\mathrm{Re}} = \tfrac{1}{2i}\gamma\left[\exp(i\Omega_1 t_1) - \exp(-i\Omega_1 t_1)\right]\exp(-t_1/T_2^{(1)})A_+^{(2)}$$

$$S(\omega_1,\omega_2)_s^{\mathrm{Re}} = \tfrac{1}{2i}\gamma\left[\left\{A_+^{(1)} + iD_+^{(1)}\right\} - \left\{A_-^{(1)} + iD_-^{(1)}\right\}\right]A_+^{(2)}$$

The imaginary part of the resulting two-dimensional spectrum is

$$\mathrm{Im}\left[S(\omega_1,\omega_2)_s^{\mathrm{Re}}\right] = -\tfrac{1}{2}\gamma A_+^{(1)}A_+^{(2)} + \tfrac{1}{2}\gamma A_-^{(1)}A_+^{(2)}$$

The two lines now have the pure absorption lineshape.

3.6.2.3 Frequency discrimination with retention of absorption lineshapes

It is essential to be able to combine frequency discrimination in the F_1 dimension with retention of pure absorption lineshapes. Three different ways of achieving this are commonly used; each will be analysed here.

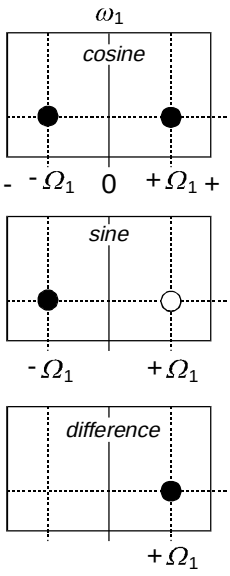

Illustration of the way in which the SHR method achieves frequency discrimination by combining cosine and sine modulated spectra.

States-Haberkorn-Ruben method

The essence of the States-Haberkorn-Ruben (SHR) method is the observation that the cosine modulated data set, processed as described in section 3.6.2.2, gives two positive absorption mode peaks at ($+\Omega_1$,$+\Omega_2$) and ($-\Omega_1$,$+\Omega_2$), whereas the sine modulated data set processed in the same way gives a spectrum in which one peak is negative and one positive. Subtracting these spectra from one another gives the required absorption mode frequency discriminated spectrum (see the diagram below):

$$\begin{aligned}\mathrm{Re}\left[S(\omega_1,\omega_2)_{\mathrm{c}}^{\mathrm{Re}}\right]-\mathrm{Im}\left[S(\omega_1,\omega_2)_{\mathrm{s}}^{\mathrm{Re}}\right]&\\ =\left[\tfrac{1}{2}\gamma A_+^{(1)}A_+^{(2)}+\tfrac{1}{2}\gamma A_-^{(1)}A_+^{(2)}\right]-\left[-\tfrac{1}{2}\gamma A_+^{(1)}A_+^{(2)}+\tfrac{1}{2}\gamma A_-^{(1)}A_+^{(2)}\right]&\\ =\gamma A_+^{(1)}A_+^{(2)}&\end{aligned}$$

In practice it is usually more convenient to achieve this result in the following way, which is mathematically identical.

The cosine and sine data sets are transformed with respect to t_2 and the real parts of each are taken. Then a new complex data set is formed using the cosine data for the real part and the sine data for the imaginary part:

$$\begin{aligned}S(t_1,\omega_2)_{\mathrm{SHR}}&=S(t_1,\omega_2)_{\mathrm{c}}^{\mathrm{Re}}+iS(t_1,\omega_2)_{\mathrm{s}}^{\mathrm{Re}}\\ &=\gamma\cos(\Omega_1 t_1)\exp\left(-t_1/T_2^{(1)}\right)A_+^{(2)}+i\gamma\sin(\Omega_1 t_1)\exp\left(-t_1/T_2^{(1)}\right)A_+^{(2)}\\ &=\gamma\exp(i\Omega_1 t_1)\exp\left(-t_1/T_2^{(1)}\right)A_+^{(2)}\end{aligned}$$

Fourier transformation with respect to t_1 gives a spectrum whose real part contains the required frequency discriminated absorption mode spectrum

$$\begin{aligned}S(\omega_1,\omega_2)_{\mathrm{SHR}}&=\gamma\left[A_+^{(1)}+iD_+^{(1)}\right]A_+^{(2)}\\ &=\gamma A_+^{(1)}A_+^{(2)}+iD_+^{(1)}A_+^{(2)}\end{aligned}$$

Marion-Wüthrich or TPPI method

The idea behind the TPPI (time proportional phase incrementation) or Marion–Wüthrich (MW) method is to arrange things so that all of the peaks have positive offsets. Then, frequency discrimination would not be required as there would be no ambiguity.

One simple way to make all offsets positive is to set the receiver carrier frequency deliberately at the edge of the spectrum. Simple though this is, it is not really a very practical method as the resulting spectrum would be very inefficient in its use of data space and in addition off-resonance effects associated with the pulses in the sequence will be accentuated.

In the TPPI method the carrier can still be set in the middle of the spectrum, but it is made to appear that all the frequencies are positive by phase shifting systematically some of the pulses in the sequence in concert with the incrementation of t_1.

In section 3.2 it was shown that in the EXSY sequence the cosine modulation in t_1, $\cos(\Omega_1 t_1)$, could be turned into sine modulation, $-\sin(\Omega_1 t_1)$, by shifting the phase of the first pulse by 90°. The effect of such a phase shift can be represented mathematically in the following way.

Recall that Ω is in units of radians s^{-1}, and so if t is in seconds Ωt is in radians; Ωt can therefore be described as a phase which depends on time. It is also possible to consider phases which do not depend on time, as was the case for the phase errors considered in section 3.6.1.1

The change from cosine to sine modulation in the EXSY experiment can be though of as a phase shift of the signal in t_1. Mathematically, such a phase shifted cosine wave is written as $\cos(\Omega_1 t_1 + \phi)$, where ϕ is the phase shift in radians. This expression can be expanded using the well known formula $\cos(A+B) = \cos A \cos B - \sin A \sin B$ to give

$$\cos\left(\Omega_1 t_1 + \phi\right) = \cos\Omega_1 t \cos\phi - \sin\Omega_1 t \sin\phi$$

If the phase shift, ϕ, is $\pi/2$ radians the result is

$$\begin{aligned}\cos\left(\Omega_1 t_1 + \pi/2\right) &= \cos\Omega_1 t \cos\pi/2 - \sin\Omega_1 t \sin\pi/2 \\ &= -\sin\Omega_1 t\end{aligned}$$

In words, a cosine wave, phase shifted by $\pi/2$ radians (90°) is the same thing as a sine wave. Thus, in the EXSY experiment the effect of changing the phase of the first pulse by 90° can be described as a phase shift of the signal by 90°.

Suppose that instead of a fixed phase shift, the phase shift is made proportional to t_1; what this means is that each time t_1 is incremented the phase is also incremented in concert. The constant of proportion between the time dependent phase, $\phi(t_1)$, and t_1 will be written $\omega_{\text{additional}}$

$$\phi\left(t_1\right) = \omega_{\text{additional}} t_1$$

Clearly the units of $\omega_{\text{additional}}$ are radians s^{-1}, that is $\omega_{\text{additional}}$ is a frequency. The new time-domain function with the inclusion of this incrementing phase is thus

$$\begin{aligned}\cos\left(\Omega_1 t_1 + \phi(t_1)\right) &= \cos\left(\Omega_1 t_1 + \omega_{\text{additional}} t_1\right) \\ &= \cos\left(\Omega_1 + \omega_{\text{additional}}\right) t_1\end{aligned}$$

In words, the effect of incrementing the phase in concert with t_1 is to add a frequency $\omega_{\text{additional}}$ to all of the offsets in the spectrum. The TPPI method utilizes this option of shifting all the frequencies in the following way.

In one-dimensional pulse-Fourier transform NMR the free induction signal is sampled at regular intervals Δ. After transformation the resulting spectrum displays correctly peaks with offsets in the range –(SW/2) to +(SW/2) where SW is the spectral width which is given by $1/\Delta$ (this comes about from the Nyquist theorem of data sampling). Frequencies outside this range are not represented correctly.

Suppose that the required frequency range in the F_1 dimension is from –(SW_1/2) to +(SW_1/2) (in COSY and EXSY this will be the same as the range in F_2). To make it appear that all the peaks have a positive offset, it will be necessary to add (SW_1/2) to all the frequencies. Then the peaks will be in the range 0 to (SW_1).

As the maximum frequency is now (SW_1) rather than (SW_1/2) the sampling interval, Δ_1, will have to be halved *i.e.* $\Delta_1 = 1/(2SW_1)$ in order that the range of frequencies present are represented properly.

The phase increment is $\omega_{\text{additional}} t_1$, but t_1 can be written as $n\Delta_1$ for the nth increment of t_1. The required value for $\omega_{\text{additional}}$ is $2\pi(SW_1/2)$, where the 2π is to convert from frequency (the units of SW_1) to rad s^{-1}, the units of $\omega_{\text{additional}}$. Putting all of this together $\omega_{\text{additional}} t_1$ can be expressed, for the nth increment as

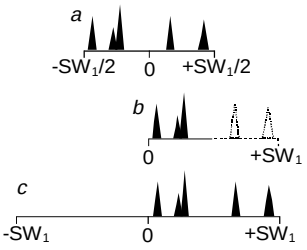

Illustration of the TPPI method. The normal spectrum is shown in *a*, with peaks in the range –SW/2 to +SW/2. Adding a frequency of SW/2 to all the peaks gives them all positive offsets, but some, shown dotted) will then fall outside the spectral window – spectrum *b*. If the spectral width is doubled all peaks are represented correctly – spectrum *c*.

$$\begin{aligned}\omega_{\text{additional}} t_1 &= 2\pi\left(\frac{SW_1}{2}\right)\left(n\Delta_1\right) \\ &= 2\pi\left(\frac{SW_1}{2}\right)\left(n\frac{1}{2SW_1}\right) \\ &= n\frac{\pi}{2}\end{aligned}$$

The way in which the phase incrementation increases the frequency of the cosine wave is shown below:

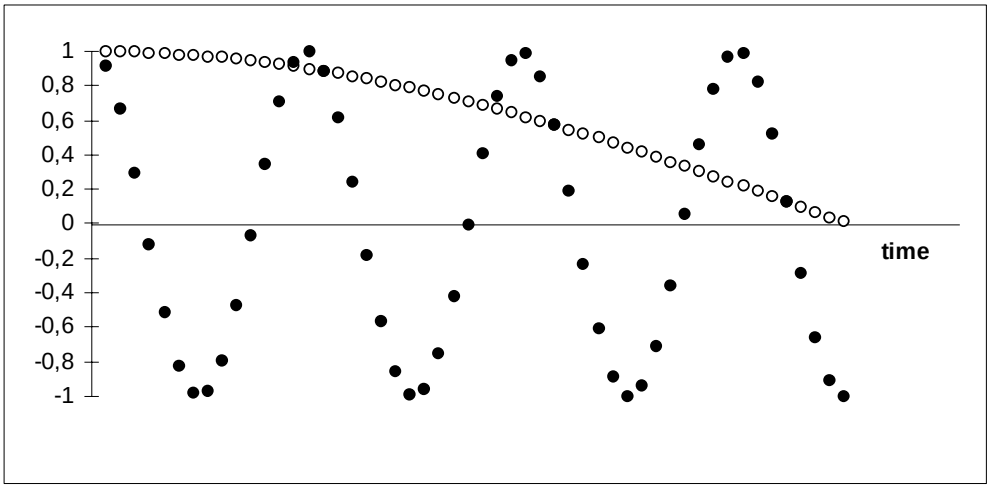

The open circles lie on a cosine wave, $\cos(\Omega \times n\Delta)$, where Δ is the sampling interval and n runs 0, 1, 2 ... The closed circles lie on a cosine wave in which an additional phase is incremented on each point i.e. the function is $\cos(\Omega \times n\Delta + n\phi)$; here $\phi = \pi/8$. The way in which this phase increment increases the frequency of the cosine wave is apparent.

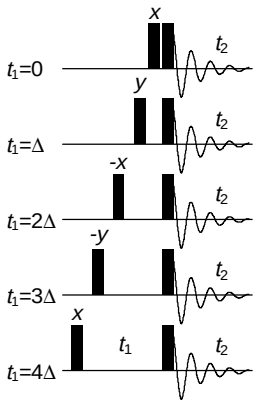

TPPI phase incrementation applied to a COSY sequence. The phase of the first pulse is incremented by 90° each time t_1 is incremented.

In words this means that each time t_1 is incremented, the phase of the signal should also be incremented by 90°, for example by incrementing the phase of one of the pulses. The way in which it can be decided which pulse to increment will be described in lecture 4.

A data set from an experiment to which TPPI has been applied is simply amplitude modulated in t_1 and so can be processed according to the method described for cosine modulated data so as to obtain absorption mode lineshapes. As the spectrum is symmetrical about $F_1 = 0$ it is usual to use a modified Fourier transform routine which saves effort and space by only calculating the positive frequency part of the spectrum.

Echo anti-echo method

Few two-dimensional experiments naturally produce phase modulated data sets, but if gradient pulses are used for coherence pathway selection (see lecture 4) it is then quite often found that the data are phase modulated. In one way this is an advantage, as it means that no special steps are required to obtain frequency discrimination. However, phase modulated data sets give rise to spectra with phase-twist lineshapes, which are very undesirable. So, it is usual to attempt to use some method to eliminate the phase-twist lineshape, while at the same time retaining frequency discrimination.

The key to how this can be done lies in the fact that two kinds of phase modulated data sets can usually be recorded. The first is called the *P*-type or anti-echo spectrum

$$S(t_1,t_2)_{\mathrm{p}} = \gamma \exp(i\Omega_1 t_1)\exp\left(-t_1/T_2^{(1)}\right)\exp(i\Omega_2 t_2)\exp\left(-t_2/T_2^{(2)}\right)$$

the "*P*" indicates positive, meaning here that the sign of the frequencies in F_1 and F_2 are the same.

The second data set is called the echo or *N*-type

$$S(t_1,t_2)_{\mathrm{N}} = \gamma \exp(-i\Omega_1 t_1)\exp\left(-t_1/T_2^{(1)}\right)\exp(i\Omega_2 t_2)\exp\left(-t_2/T_2^{(2)}\right)$$

the "*N*" indicates negative, meaning here that the sign of the frequencies in F_1 and F_2 are opposite. As will be explained in lecture 4 in gradient experiments it is easy to arrange to record either the *P*- or *N*-type spectrum.

The simplest was to proceed is to compute two new data sets which are

$$\begin{aligned}
&\tfrac{1}{2}\left[S(t_1,t_2)_{\mathrm{P}} + S(t_1,t_2)_{\mathrm{N}}\right] = \\
&\quad \tfrac{1}{2}\gamma\left[\exp(i\Omega_1 t_1) + \exp(-i\Omega_1 t_1)\right]\exp\left(-t_1/T_2^{(1)}\right)\exp(i\Omega_2 t_2)\exp\left(-t_2/T_2^{(2)}\right) \\
&\quad = \gamma\cos(\Omega_1 t_1)\exp\left(-t_1/T_2^{(1)}\right)\exp(i\Omega_2 t_2)\exp\left(-t_2/T_2^{(2)}\right)
\end{aligned}$$

$$\begin{aligned}
&\tfrac{1}{2i}\left[S(t_1,t_2)_{\mathrm{P}} - S(t_1,t_2)_{\mathrm{N}}\right] = \\
&\quad \tfrac{1}{2i}\gamma\left[\exp(i\Omega_1 t_1) - \exp(-i\Omega_1 t_1)\right]\exp\left(-t_1/T_2^{(1)}\right)\exp(i\Omega_2 t_2)\exp\left(-t_2/T_2^{(2)}\right) \\
&\quad = \gamma\sin(\Omega_1 t_1)\exp\left(-t_1/T_2^{(1)}\right)\exp(i\Omega_2 t_2)\exp\left(-t_2/T_2^{(2)}\right)
\end{aligned}$$

These two combinations are just the cosine and sine modulated data sets that are the inputs needed for the SHR method. The pure absorption spectrum can therefore be calculated in the same way starting with these combinations.

3.6.2.4 Phase in two-dimensional spectra

In practice there will be instrumental and other phase shifts, possibly in both dimensions, which mean that the time-domain functions are not the idealised ones treated above. For example, the cosine modulated data set might be

$$S(t)_c = \gamma\cos(\Omega_1 t_1 + \phi_1)\exp\left(-t_1/T_2^{(1)}\right)\exp(i\Omega_2 t_2 + i\phi_2)\exp\left(-t_2/T_2^{(2)}\right)$$

where ϕ_1 and ϕ_2 are the phase errors in F_1 and F_1, respectively. Processing this data set in the manner described above will not give a pure absorption spectrum. However, it is possible to recover the pure absorption spectrum by software manipulations of the spectrum, just as was described for the case of one-dimensional spectra. Usually, NMR data processing software provides options for making such phase corrections to two-dimensional data sets.

4 Coherence Selection: Phase Cycling and Gradient Pulses

4.1 Introduction

A multiple-pulse NMR experiment is designed to manipulate the spins in a certain carefully defined way so as to produce a particular spectrum. However, a given pulse sequence usually can affect the spins in several different ways and as a result the final spectrum may contain resonances other than those intended when the experiment was designed. The presence of such resonances may result in extra crowding in the spectrum, they may obscure the wanted peaks and they may also lead to ambiguities of interpretation. It is thus all but essential to ensure that the responses seen in the spectrum are just those we intended to generate when the pulse sequence was designed.

There are two principle ways in which this selection of required signals is achieved in practice. The first is the procedure known as *phase cycling*. In this the multiple-pulse experiment is repeated a number of times and for each repetition the phases of the radiofrequency pulses are varied through a carefully designed sequence. The free induction decays resulting from each repetition are then combined in such a way that the desired signals add up and the undesired signals cancel. The second procedure employs field gradient pulses. Such pulses are short periods during which the magnetic field is made deliberately inhomogeneous. During a gradient pulse, therefore, any coherences present dephase are apparently lost. However, the application of a subsequent pulsed field gradient can undo this dephasing and cause some of the coherences to refocus. By a careful choice of the gradient pulses within a pulse sequence it is possible to ensure that only the coherences giving rise to the wanted signals are refocused.

Historically, in the development of multiple-pulse NMR, phase cycling has been the principle method used for selecting the desired outcome. Pulsed field gradients, although their utility had been known from the earliest days of NMR, have only relatively recently been seen as a practical alternative. Both methods can be described using the key concept of *coherence order* and by utilising the idea of a *coherence transfer pathway*. In this lecture we will start out by describing phase cycling, emphasising first its relation to the idea of difference spectroscopy and then moving on to describe the formal methods for writing and analysing phase cycles. The tools needed to describe selection with gradient pulses are quite similar to those used in phase cycling, and this will enable us to make rapid progress through this topic. There are, however, some key differences between the two methods, especially in regard to the sensitivity and other aspects of multi-dimensional NMR experiments.

4.2 Phase Cycling

4.2.1 Phase

In the simple vector picture of NMR the phase of a radiofrequency pulse determines the axis along which the magnetic field, B_1, caused by the

oscillating radiofrequency current in the coil, appears. Viewed in the usual rotating frame (rotating at the frequency of the transmitter) this magnetic field is static and so it is simple to imagine its phase as the angle, β, between a reference axis and the vector representing B_1. There is nothing to indicate which direction ought to be labelled *x* or *y*; all we know is that these directions are perpendicular to the static field and perpendicular to one another. So, provided we are consistent, we are free to decide arbitrarily where to put this reference axis. In common with most of the NMR community we will decide that the reference axis is along the *x*-axis of the rotating frame and that the phase of the pulse will be measured from *x*; thus a pulse with phase *x* has a phase angle, β, of zero. Similarly a pulse of phase *y* has a phase angle of 90° or $\pi/2$ radians. Modern spectrometers allow the phase of the pulse to be set to any desired value.

The NMR signal, that is the free induction decay (FID), is recorded by measuring the voltage generated in a coil as it is cut by precessing transverse magnetization. Most spectrometers take this high-frequency signal and convert it to the audio-frequency range by subtracting a fixed reference frequency. Almost always this fixed reference frequency is the same as the transmitter frequency and the effect of this choice is to make it appear that the FID has been detected in the rotating frame. Thus the frequencies which appear in the detected FID are the offset or difference frequencies between the Larmor frequency and the rotating frame frequency.

Like the pulse, the NMR receiver also has associated with it a phase. If we imagine at time zero that there is transverse magnetization along the *x*-axis (of the laboratory frame) and that a small coil is wound around the *x*-axis the voltage induced in the coil as the magnetization precesses is proportional to the *x*-component *i.e.* proportional to $\cos(\omega_0 t)$. On the other hand, if the magnetization starts out along the $-y$ axis the induced voltage is proportional to $\sin(\omega_0 t)$, simply as this is the projection onto the *x*-axis as the magnetization vector rotates in the transverse plane. In mathematical terms the detected signal can be always be written $\cos(\omega_0 t + \phi)$, where ϕ is a phase angle. The magnetization starting out along *x* gives a signal with phase angle zero, whereas that starting along $-y$ has a phase angle of $-\pi/2$.

The NMR receiver can differentiate between the cosine and sine modulated parts of the signals by using two detectors fed with reference signals which are shifted in phase by 90° relative to one another. The detection process involves using a device called a mixer which essentially multiplies together (in an analogue circuit) the incoming and reference signals. The inputs to the mixers at the reference frequency, ω_{ref}, take the form of a cosine and a sine for the two detectors, as these signals have the required 90° phase shift between them. If the incoming signal is $\cos(\omega_0 t + \phi)$ the outputs of the two mixers are

$$0°: \quad \cos(\omega_0 + \phi)t \, \cos\omega_{\text{ref}} t = \tfrac{1}{2}\left[\cos(\omega_0 + \phi + \omega_{\text{ref}})t + \cos(\omega_0 + \phi - \omega_{\text{ref}})t\right]$$

$$90°: \quad \cos(\omega_0 + \phi)t \, \sin\omega_{\text{ref}} t = \tfrac{1}{2}\left[\sin(\omega_0 + \phi + \omega_{\text{ref}})t - \sin(\omega_0 + \phi - \omega_{\text{ref}})t\right]$$

These outputs are filtered to remove the high frequency components (the first terms on the right) and the outputs from the 0° and 90° detectors

become the real and imaginary parts of a complex number. If we add a damping term and ignore the numerical factors, the detected (complex) signal is

$$\left[\cos\left(\omega_0 + \phi - \omega_{\text{ref}}\right)t - \text{i}\sin\left(\omega_0 + \phi - \omega_{\text{ref}}\right)t\right]\exp(-Rt)$$
$$\equiv \exp\left(-\text{i}\left(\omega_0 - \omega_{\text{ref}}\right)t\right)\exp(-\text{i}\phi)\exp(-Rt)$$

Fourier transformation of this signal gives a peak at the offset frequency, $\omega_0 - \omega_{\text{ref}}$, and with phase ϕ. If ϕ is zero, then an absorption mode peak is expected, whereas if ϕ is $\pi/2$ a dispersion mode peak is expected; in general a line of mixed phase is seen. The detector system is thus able to determine not only the frequency at which the magnetization is precessing, but also its phase *i.e.* its position at time zero.

In the above example the two reference signals sent to the two detectors were chosen deliberately so that magnetization with phase $\phi = 0$ would result in an absorption mode signal. However, we could alter the phase of these reference signals to produce any phase we liked in the spectrum. If the reference signals were $\cos(\omega_{\text{ref}}t + \beta)$ and $\sin(\omega_{\text{ref}}t + \beta)$ the FID would be of the form

$$\left[\cos\left(\omega_0 + \phi - \omega_{\text{ref}} - \beta\right)t - \text{i}\sin\left(\omega_0 + \phi - \omega_{\text{ref}} - \beta\right)t\right]\exp(-Rt)$$
$$\equiv \exp\left(-\text{i}\left(\omega_0 - \omega_{\text{ref}}\right)t\right)\exp(-\text{i}(\phi - \beta))\exp(-Rt)$$

Now we see that the line has phase $(\phi - \beta)$. The key point to note that as β is under our control we can alter the phase of the lines in the spectrum simply by altering the reference phase to the detector.

In modern NMR spectrometers the phase, β, of this reference is under the control of the pulse programmer. This *receiver phase* and the ability to alter it freely is a key part of phase cycling. The usual language in which the receiver phase is specified is to talk about "the receiver being aligned along *x*", by which it is meant that the receiver phase is set to a value such that if, at the start of the FID, there were solely magnetization along *x* the resulting spectrum would contain an absorption mode signal. Likewise, "aligning the receiver along *–y*" means that an absorption mode spectrum would result if the magnetization were solely along *–y* at the start of the FID. If the magnetization were aligned along *x* instead, such a receiver phase would result in a dispersion mode spectrum ($\beta = \pi/2$).

Of course in practice we can always phase the spectrum to produce whatever lineshape we like, regardless of the setting of the receiver phase. Indeed the process of phasing the spectrum and altering the receiver phase are the same. However, as signals are often combined *before* Fourier transformation and phasing, the relative phase shifts that can be obtained by altering the receiver phase are important.

Figure 1 shows, using the vector model, the relationship between the position of magnetization at the start of the FID, the receiver phase and the phase of the lineshape in the corresponding spectrum. In this diagram the

axis along which the receiver is "aligned" is indicated by a dot, •.

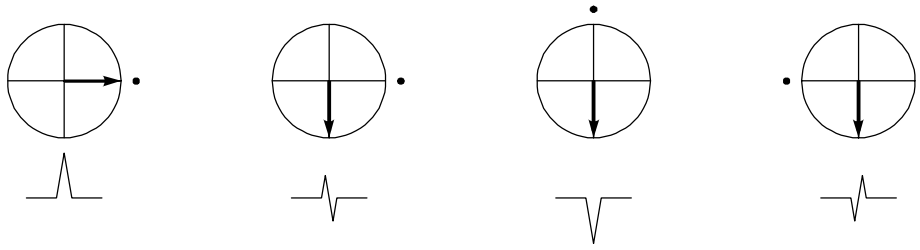

Figure 1. Illustration of the lineshape expected in the spectrum (shown underneath the vector diagrams) for different relative phases of the magnetization (the vector) and the receiver phase, indicated by •.

4.2.2 Two Simple Examples

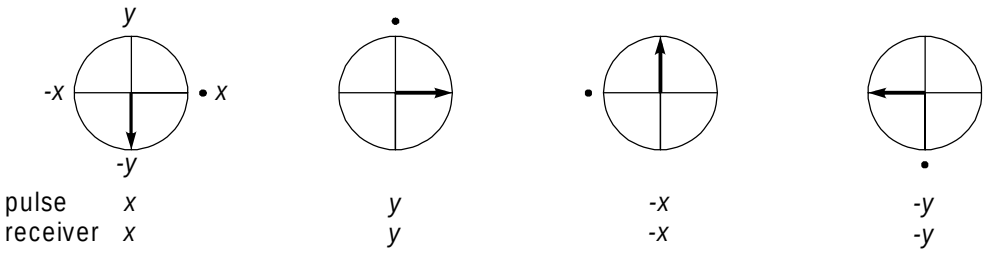

Figure 2 Illustration of how the receiver phase is made to follow the phase of the magnetization.

The CYCLOPS phase cycling scheme is commonly used in even the simplest pulse-acquire experiments. The sequence is designed to cancel some imperfections associated with errors in the two phase detectors mentioned above; a description of how this is achieved is beyond the scope of this discussion. However, the cycle itself illustrates very well the points made in the previous section. There are four steps in the cycle, the pulse phase is advanced by 90° on each step, as is the phase of the receiver. Figure 2 shows simple vector diagrams which illustrate that as the pulse phase causes the magnetization to appear along different axes the receiver phase is advanced in step so as to always be in the same position *relative* to the magnetization. The result is that the lineshape is the same for each repetition of the experiment so that they can all be added together without cancellation. This is exactly what we require as a FID is time-averaged. It is easily seen that the absolute phase of the receiver is unimportant, all that matters is that the receiver phase advances in step with the magnetization (see exercises).

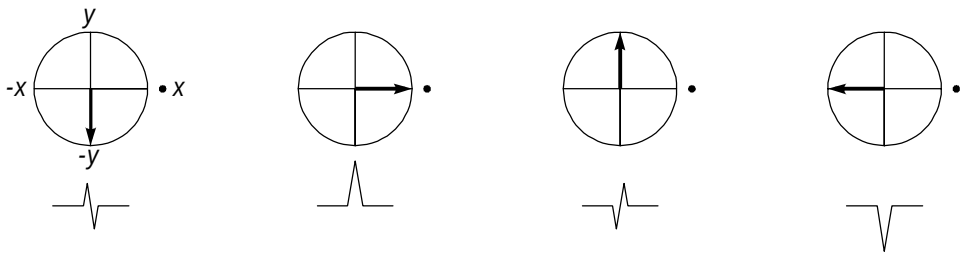

Figure 3. Illustration of how failing to move the receiver phase in concert with the phase of the magnetization leads to signal cancellation; the sum of the spectra shown is zero.

Finally, Fig. 3 shows the result of "forgetting" to move the receiver phase; if the signals from all four steps are added together the signal cancels completely. Similar cancellation arises if the receiver phase is moved backwards *i.e.* *x*, –*y*, –*x*, *y* rather than *x*, *y*, –*x*, –*y* (see exercises).

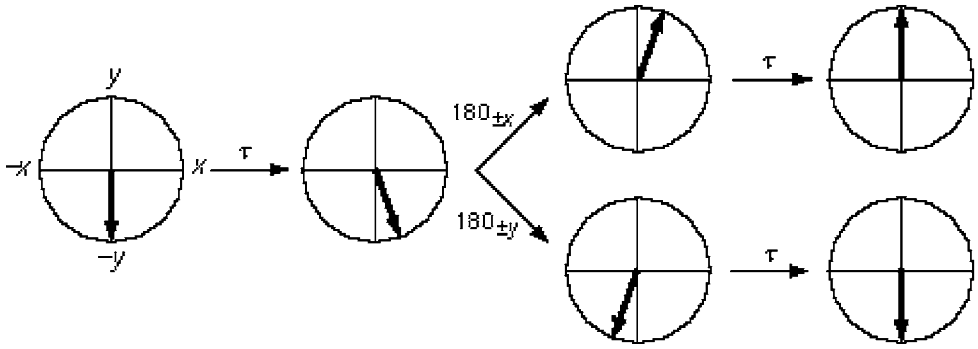

Figure 4. The effect of altering the phase of the 180° pulse in a spin echo.

A second familiar phase cycle is EXORCYLE which is used in conjunction with 180° pulses used in spin echoes. Figure 4 shows a simple vector diagram which illustrates the effect on the final position of the vector when the phase of the 180° pulse is altered through the sequence *x*, *y*, –*x*, –*y*. It is seen that the magnetization refocuses along the *y*, –*y*, *y* and –*y* axes respectively as the 180° pulse goes through its sequence of phases. If the four signals were simply added together in the course of time averaging they would completely cancel one another. However, if the receiver phase is adjusted to follow the position of the refocused magnetization, *i.e.* to take the values *y*, –*y*, *y*, –*y*, each repetition will give the same lineshape and so the signals will add up. This is the EXORCYCLE sequence.

As before, it does not matter if the receiver is actually aligned along the direction in which the magnetization refocuses, all that matters is that when the magnetization shifts by 180° the receiver should also shift by 180°. Thus the receiver phase could just as well have followed the sequence *x*, –*x*, *x*, –*x*.

For brevity, and because of the way in which these phase cycles are encoded on spectrometers, it is usual to refer to the pulse and receiver phases using numbers with **0**, **1**, **2**, **3** representing phases of 0°, 90°, 180° and 270° respectively (that is alignment with the *x*, *y*, –*x* and –*y* axes). So, the phases for EXORCYCLE can be written as **0 1 2 3** for the 180° pulse and **0 2 0 2** for the receiver.

The EXORCYCLE sequence is designed to eliminate those signals which

do not experience a perfect 180° refocusing pulse. We shall see later that the concept of coherence order and coherence transfer pathways allows us to confirm this in a very general way. However, at this point it is possible to deduce using the vector approach that if the 180° pulse is entirely absent the EXORCYLE phase cycle cancels all of the signal (see exercises).

4.2.3 Difference Spectroscopy

So far we have seen that the phase of the detected NMR signal can be influenced by the phase of both the pulses and the receiver. We have also seen that it is perfectly possible to cancel out all of the signal by making inappropriate choices of the pulse and receiver phases. Of course we generally do not want to cancel the desired signal, so these examples were not of practical relevance. However, there are many occasions in which we do want to cancel certain signals and preserve others. Often the required cancellation can be brought about by a simple *difference* experiment in which the signal is recorded twice with such a choice of pulse phases that the required signals change sign between the two experiments experiment and the unwanted signals do not. Subtracting the two signals then cancels the unwanted signals. Such a difference experiment can be considered as a two-step phase cycle.

A good example of the use of this simple difference procedure is in the INEPT experiment, used to transfer magnetization from spin *I* to a coupled spin *S*. The sequence is shown in Fig. 5.

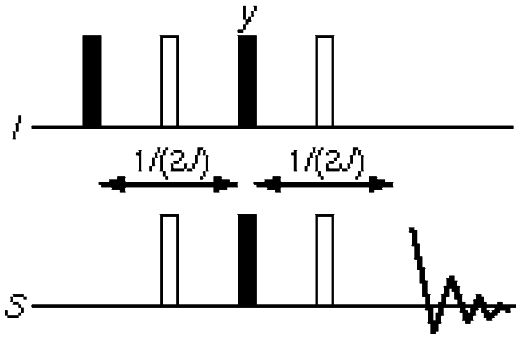

Figure 5 The pulse sequence for INEPT. In this diagram the filled rectangles represent 90° pulses and the open rectangles represent 180° pulses. Unless otherwise stated the pulses have phase *x*.

With the phases and delays shown equilibrium magnetization of spin *I*, I_z, is transferred to spin *S*, appearing as the operator S_x. Equilibrium magnetization of *S*, S_z, appears as $-S_y$. Often this latter signal is an inconvenience and it is desirable to suppress it. The procedure is very simple. If we change the phase of the first *I* pulse from *x* to *–x* the final magnetization arising from transfer of the *I* magnetization to *S* becomes $-S_x$ *i.e.* it changes sign. In contrast, the signal arising from equilibrium *S* magnetization is unaffected simply because the S_z operator is unaffected by the first 90° pulse to spin *I*. By repeating the experiment twice, once with the phase of the first pulse set to *x* and once with it set to *–x*, and then subtracting the two resulting signals, the undesired signal is cancelled and the desired signal adds.

This simple difference experiment can be regarded as a two-step phase

cycle in which the first *I* pulse has phases **0 2** and the receiver follows with phases **0 2**. The difference is achieved in the course of time averaging (*i.e.* as the time domain signals are accumulated from different scans) rather than by recording the signals separately and then subtracting them.

It is easy to confirm that an alternative is to cycle the second *I* spin 90° pulse **0 2** along with a receiver phase of **0 2**. However, cycling the *S* spin 90° pulse is not effective at separating the two sources of signal as they are affected in the same way by changing the phase of this pulse (see exercises).

Difference spectroscopy reveals one of the key features of phase cycling: that is the need to identify a pulse whose phase affects differently the fate of the desired and undesired signals. Cycling the phase of this pulse can then be the basis of discrimination. In many experiments a simple cycle of **0 2** on a suitable pulse and the receiver is all that is required to select the desired signal. This is particularly the case in heteronuclear experiments, of which the INEPT sequence is the prototype. Indeed, even the phase cycling used in the most complex three- and four-dimensional experiments applied to labelled proteins is little more than this simple cycle repeated a number of times for different transfer steps.

4.2.4 Basic Concepts

Although we can make some progress in writing simple phase cycles by considering the vector picture, a more general framework is needed in order to cope with experiments which involve multiple quantum coherence and related phenomena. We also need a theory which enables us to predict the degree to which a phase cycle can discriminate against different classes of unwanted signals. A convenient and powerful way of doing both these things is to use the coherence transfer pathway approach.

4.2.4.1 Coherence Order

Coherences, of which transverse magnetization is one example, can be classified according to a coherence order, *p*, which is an integer taking values 0, ± 1, ± 2 ... Single quantum coherence has $p = \pm 1$, double has $p = \pm 2$ and so on; *z*-magnetization, "*zz*" terms and zero-quantum coherence have $p = 0$. This classification comes about by considering the way in which different coherences respond to a rotation about the *z*-axis. A coherence of order *p*, represented by the density operator $\sigma^{(p)}$, evolves under a *z*-rotation of angle ϕ according to

$$\exp(-\mathrm{i}\phi F_z)\sigma^{(p)}\exp(\mathrm{i}\phi F_z) = \exp(-\mathrm{i}\,p\phi)\sigma^{(p)} \qquad [1]$$

where F_z is the operator for the total *z*-component of the spin angular momentum. In words, a coherence of order *p* experiences a phase shift of $-p\phi$. Equation [1] is the definition of coherence order.

As an example consider the pure double quantum operator for two coupled spins, $2I_{1x}I_{2y} + 2I_{1y}I_{2x}$. This can be rewritten in terms of the raising and lowering operators for spin *i*, I_i^+ and I_i^-, defined as

$$I_i^+ = I_{ix} + \mathrm{i}\, I_{iy} \quad I_i^- = I_{ix} - \mathrm{i}\, I_{iy}$$

to give $\frac{1}{\mathrm{i}}\left(I_1^+ I_2^+ - I_1^- I_2^-\right)$. The effect of a *z*-rotation on the raising and lowering operators is, in the arrow notation,

$$I_i^\pm \xrightarrow{\phi I_{iz}} \exp\left(\mp \mathrm{i}\,\phi\right) I_i^\pm \quad .$$

Using this, the effect of a *z*-rotation on the term $I_1^+ I_2^+$ can be determined as

$$I_1^+ I_2^+ \xrightarrow{\phi I_{1z}} \exp\left(-\mathrm{i}\,\phi\right) I_1^+ I_2^+ \xrightarrow{\phi I_{2z}} \exp\left(-\mathrm{i}\,\phi\right)\exp\left(-\mathrm{i}\,\phi\right) I_1^+ I_2^+$$

Thus, as the coherence experiences a phase shift of -2ϕ the coherence is classified according to Eqn. [1] as having $p = 2$. It is easy to confirm that the term $I_1^- I_2^-$ has $p = -2$. Thus the pure double quantum term, $2I_{1x}I_{2y} + 2I_{1y}I_{2x}$, is an equal mixture of coherence orders +2 and –2.

As this example shows, it is possible to determine the order or orders of any state by writing it in terms of raising and lowering operators and then simply inspecting the number of raising and lowering operators in each term. A raising operator contributes +1 to the coherence order whereas a lowering operator contributes –1. A *z*-operator, I_{iz}, does not contribute to the overall order as it is invariant to *z*-rotations.

Coherences involving heteronuclei can be assigned both an overall order and an order with respect to each nuclear species. For example the term $I_1^+ S_1^-$ has an overall order of 0, is order +1 for the *I* spins and –1 for the *S* spins. The term $I_1^+ I_2^+ S_{1z}$ is overall of order 2, is order 2 for the *I* spins and is order 0 for the *S* spins.

4.2.4.2 Phase Shifted Pulses

A radiofrequency pulse causes coherences to be transferred from one order to one or more different orders; it is this spreading out of the coherence which is responsible both for the richness of multiple-pulse NMR and for the need for phase cycling to select one transfer among many possibilities. An example of this spreading between coherence orders is the effect of a non-selective pulse on antiphase magnetization, such as $2I_{1x}I_{2z}$, which corresponds to coherence orders ±1. Some of the coherence may be transferred into double- and zero-quantum coherence, some may be transferred into two-spin order and some will remain unaffected. The precise outcome depends on the phase and flip angle of the pulse, but in general we can see that there are many possibilities.

If we consider just one coherence, of order *p*, and consider its transfer to a coherence of order *p*' by a radiofrequency pulse we can derive a very general result for the way in which the phase of the pulse affects the phase of the coherence. It is on this relationship that the phase cycling method is based.

We will write the initial state of order p as $\sigma^{(p)}$ and represent the effect of the radiofrequency pulse causing the transfer by the unitary transformation $U(\phi)$where ϕ is the phase of the pulse. The initial and final states are related by the usual transformation

$$U(0)\sigma^{(p)}U(0)^{-1} = \sigma^{(p')} \ + \text{ terms of other orders} \qquad [2]$$

the other terms will be dropped as we are only interested in the transfer from p to p'. The transformation brought about by a radiofrequency pulse phase shifted by ϕ, $U(\phi)$, is related to that with the phase set to zero, $U(0)$, by the rotation

$$U(\phi) = \exp(-\mathrm{i}\phi F_z)U(0)\exp(\mathrm{i}\phi F_z) \qquad [3]$$

Using this the effect of the phase shifted pulse on the initial state $\sigma^{(p)}$ can be written

$$U(\phi)\sigma^{(p)}U(\phi)^{-1} = \exp(-\mathrm{i}\phi F_z)U(0)\exp(\mathrm{i}\phi F_z)\sigma^{(p)}\exp(-\mathrm{i}\phi F_z)U(0)^{-1}\exp(\mathrm{i}\phi F_z) \qquad [4]$$

The central rotation of $\sigma^{(p)}$, $\exp(\mathrm{i}\phi F_z)\sigma^{(p)}\exp(-\mathrm{i}\phi F_z)$, can be replaced, using Eqn. [1], by $\exp(\mathrm{i}\,p\phi)\sigma^{(p)}$ so that the right-hand side of Eqn. [4] simplifies to

$$\exp(\mathrm{i}\,p\phi)\exp(-\mathrm{i}\phi F_z)U(0)\sigma^{(p)}U(0)^{-1}\exp(\mathrm{i}\phi F_z)$$

We now use Eqn. [2] to rewrite $U(0)\sigma^{(p)}U(0)^{-1}$ as $\sigma^{(p')}$ thus giving

$$\exp(\mathrm{i}\,p\phi)\exp(-\mathrm{i}\phi F_z)\sigma^{(p')}\exp(\mathrm{i}\phi F_z)$$

Once again we apply Eqn. [2] to determine the effect of the z-rotations on the state $\sigma^{(p')}$, giving the final result

$$\exp(\mathrm{i}\,p\phi)\exp(-\mathrm{i}\,p'\phi)\sigma^{(p')} = \exp(-\mathrm{i}\,\Delta p\phi)\sigma^{(p')} \qquad [5]$$

where the change is coherence order, Δp, is defined as $(p' - p)$. Returning to Eqn. [] we can now use Eqn. [5] to rewrite the right hand side and hence obtain the simple result

$$U(\phi)\sigma^{(p)}U(\phi)^{-1} = \exp(-i\,\Delta p\,\phi)\sigma^{(p')} \qquad [6]$$

This relationship result tells us that if we consider a pulse which causes a change in coherence order of Δp then altering the phase of that pulse by an angle ϕ will result in the coherence acquiring a phase label $-\Delta p\ \phi$. In other words a particular change in coherence order acquires a phase label when the phase of the pulse causing that change is altered; the size of this label depends on the change in coherence order. It is this property which enables us to separate different changes in coherence order from one another by altering the phase of the pulse.

Before seeing how this key relationship is used in practice there are two remarks to make. The first concerns the transformation $U(\phi)$. We have described this as being due to a radiofrequency pulse, but in fact any sequence of pulses and delays can be represented by such a transformation so our final result is general. Thus we can, for the purposes of analysing the effects of a pulse sequence, group one or more pulses and delays together and simply consider them as a single unit causing a transformation from one coherence order to another. The whole unit can be phase shifted by shifting the phase of all the pulses in the unit. We shall see some practical applications of this later on. The second comment to make concerns the phase which is acquired by the transferred coherence: this phase appears as a phase shift of the final observed signal, *i.e.* the position of the observed magnetization in the *xy*-plane at the start of acquisition. A particular coherence may undergo several transformations before it is observed finally , but at each stage these phase shifts are carried forward and so affect the final signal. Thus, although the coherence of order *p*' resulting from the transformation *U* may not itself be observable, any phase it acquires in the course of the transformation will ultimately be observed as a phase shift in the observed signal derived from this coherence.

4.2.4.3 Selection of a Single Pathway

To focus on the issue at hand let us consider the case of transferring from coherence order +2 to order –1. Such a transfer has $\Delta p = (-1 - (2)) = -3$. Let us imagine that the pulse causing this transformation is cycled around the four cardinal phases (*x*, *y*, *–x*, *–y*, *i.e.* 0°, 90°, 180°, 270°) and draw up a table of the phase shift that will be experienced by the transferred coherence. This is simply computed as $-\Delta p\ \phi$, in this case $= -(-3)\phi$.

step	pulse phase	phase shift experienced by transfer with $\Delta p = -3$	equivalent phase
1	0	0	0
2	90	270	270
3	180	540	180
4	270	810	90

The fourth column, labelled "equivalent phase", is just the phase shift experienced by the coherence, column three, reduced to be in the range 0 to

360° by subtracting multiples of 360° (*e.g.* for step 3 we subtracted 360° and for step 4 we subtracted 720°).

If we wished to select this change in coherence order of –3 we would simply shift the phase of the receiver in order to match the phase that the coherence has acquired, which are the phases shown in the last column. If we did this, then each step of the cycle would give an observed signal of the same phase and so they four contributions would all add up. This is precisely the same thing as we did when considering the CYCLOPS sequence in section 4.2.2; in both cases the receiver phase follows the phase of the desired magnetization or coherence.

We now need to see if this four step phase cycle eliminates the signals from other pathways. Let us consider, as an example, a pathway with $\Delta p = 2$, which might arise from the transfer from coherence order –1 to +1. Again we draw up a table to show the phase experienced by a pathway with $\Delta p = 2$, that is computed as $-(2)\phi$

step	pulse phase	phase shift experienced by transfer with $\Delta p = 2$	equiva-lent phase	rx. phase to select $\Delta p = -3$	difference
1	0	0	0	0	0
2	90	–180	180	270	270 – 180 = 90
3	180	–360	0	180	180 – 0 = 180
4	270	–540	180	90	90 – 180 = –90

As before, the equivalent phase is simply the phase in column 3 reduced to the range 0 to 360°. The fifth column shows the receiver (abbreviated to rx.) phases that would be needed to select the transfer with $\Delta p = -3$, that is the phases determined in the first table. The question we have to ask is whether or not these phase shifts will lead to cancellation of the transfer with $\Delta p = 2$. To do this we compute the difference between the receiver phase, column 5, and the phase shift experienced by the transfer with $\Delta p = 2$, column 4. The results are shown in column 6, labelled "difference", which shows the phase difference between the receiver and the signal arising from the transfer with $\Delta p = 2$. It is quite clear that the receiver is not following the phase shifts of the coherence. Indeed it is quite the opposite. Step 1 will cancel with step 3 as the 180° phase shift between them means that the two signals have opposite sign. Likewise step 2 will cancel with step 4 as there is a 180° phase shift between them. We conclude, therefore, that this four step cycle cancels the signal arising from a pathway with $\Delta p = 2$.

An alternative way of viewing the cancellation is to represent the results of the "difference" column by vectors pointing at the indicated angles. This is shown in Fig. 6 and it is clear that the opposed vectors cancel one another.

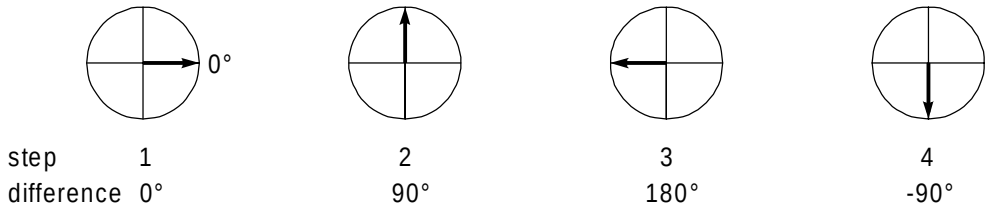

Figure 6. A visualisation of the phases from the "difference" column.

Next we consider the coherence transfer with $\Delta p = +1$. Again, we draw up the table and calculate the phase shifts experience by this transfer from $-(+1)\phi$.

Step	pulse phase	phase shift experienced by transfer with $\Delta p = +1$	equiva-lent phase	rx. phase to select $\Delta p = -3$	difference
1	0	0	0	0	0
2	90	–90	270	270	270 – 270 = 0
3	180	–180	180	180	180 – 180 = 0
4	270	–270	90	90	90 – 90 = 0

Here we see quite different behaviour. The equivalent phases, that is the phase shifts experienced by the transfer with $\Delta p = 1$, match exactly the receiver phase determined for $\Delta p = -3$, thus the phases in the "difference" column are all zero. We conclude that the four step cycle selects transfers both with $\Delta p = -3$ *and* $+1$.

Some more work with tables such as these (see exercises) will reveal that this four step cycle suppresses contributions from changes in coherence order of –2, –1 and 0. It selects $\Delta p = -3$ and 1. It also selects changes in coherence order of 5, 9, 13 and so on. This latter sequence is easy to understand. A pathway with $\Delta p = 1$ experiences a phase shift of –90° when the pulse is shifted in phase by 90°; the equivalent phase is thus 270°. A pathway with $\Delta p = 5$ would experience a phase shift of $-5 \times 90° = -450°$ which corresponds to an equivalent phase of 270°. Thus the phase shifts experienced for $\Delta p = 1$ and 5 are identical and it is clear that a cycle which selects one will select the other. The same goes for the series $\Delta p = 9, 13$ ...

The extension to negative values of Δp is also easy to see. A pathway with $\Delta p = -3$ experiences a phase shift of 270° when the pulse is shifted in phase by 90°. A transfer with $\Delta p = +1$ experiences a phase of –90° which corresponds to an equivalent phase of 270°. Thus both pathways experience the same phase shifts and a cycle which selects one will select the other. The pattern is clear, this four step cycle will select a pathway with $\Delta p = -3$, as it was designed to, and also it will select any pathway with $\Delta p = -3 + 4n$ where $n = \pm 1, \pm 2, \pm 3$ ...

4.2.4.4 General Rules

The discussion in the previous section can be generalised to the following:

Consider a phase cycle in which the phase of a pulse takes N evenly spaced steps covering the range 0 to 2π radians *i.e.* the phases, ϕ_k, are $2\pi k/N$ where $k = 0, 1, 2 \ldots (N - 1)$. To select a change in coherence order, Δp, the receiver phase is set to $-\Delta p \times \phi_k$ for each step and all the resulting signals are summed. This cycle will, in addition to selecting the specified change in coherence order, also select pathways with changes in coherence order $\Delta p \pm nN$ where $n = \pm 1, \pm 2 \ldots$

The way in which phase cycling selects a series of values of Δp which are related by a harmonic condition is closely related to the phenomenon of aliasing in Fourier transformation. Indeed, the whole process of phase cycling can be seen as the computation of a discrete Fourier transformation with respect to the pulse phase. The Fourier co-domains are phase and coherence order.

The fact that a phase cycle inevitably selects more than one change in coherence order is not necessarily a problem. We may actually wish to select more than one pathway, and examples of this will be given below in relation to specific two-dimensional experiments. Even if we only require one value of Δp we may be able to discount the values selected at the same time as being improbable or insignificant. In a system of m coupled spins one-half, the maximum order of coherence that can be generated is m, thus in a two spin system we need not worry about whether or not a phase cycle will discriminate between double quantum and six quantum coherences as the latter simply cannot be present. Even in more extended spin systems the likelihood of generating high-order coherences is rather small and so we may be able to discount them for all practical purposes. If a high level of discrimination between orders is needed, then the solution is simply to use a phase cycle which has more steps *i.e.* in which the phases move in smaller increments. For example a six step cycle will discriminate between $\Delta p = +2$ and +6, whereas a four step cycle will find these to be identical.

4.2.4.5 Coherence Transfer Pathways

In multiple-pulse NMR it is important to specify the coherences which should be present at each stage of the sequence. This is conveniently done using a *coherence transfer pathway* (CTP) diagram. Figure 7 shows such a diagram for the DQF COSY sequence.

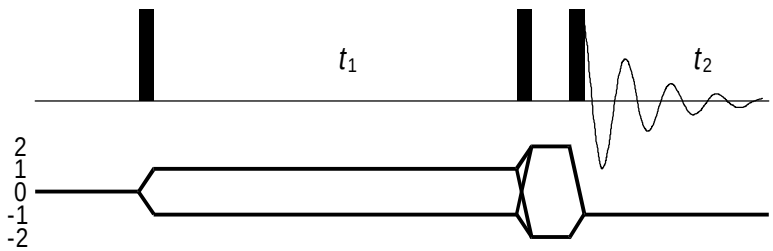

Figure 7. The pulse sequence and coherence transfer pathway for DQF COSY.

The solid lines under the sequence represent the coherence orders required during each part of the sequence; as expected the pulses cause changes in coherence order. In this example we have more that one coherence order present in some of the time periods; this is a common feature. In addition we notice that the second pulse causes a transfer between orders ±1 and ±2, with all connections being present. Again, such a "fanning out" of the coherence transfer pathway is common in many experiments.

There are a number of remarks to be made about the CTP diagram. Firstly, we should remember that this pathway is just the *desired* pathway and that it must be established separately that the pulse sequence and the spin system itself is capable of supporting the specified coherences. Thus the DQF COSY sequence could be applied, along with a suitable phase cycle to select the specified pathway, to uncoupled spins but we would not expect to see any peaks in the spectrum. Likewise, the sequence itself must be designed appropriately, the phase cycle cannot select something that the pulse sequence does not generate.

The second point to note is that the coherence transfer pathway must start with $p = 0$, that is the coherence order which corresponds to equilibrium magnetization. In addition, the pathway has to end with $|p| = 1$ as it is only single quantum coherence that is observable. If one uses quadrature detection, that is the method described in section 4.2.1 in which effectively both the *x* and *y* components of the magnetization are measured, it turns out that one is observing either $p = +1$ or -1. The usual convention, which fits in with the normal convention for the sense of rotation, is to assume that we are detecting $p = -1$; we shall use this throughout.

Finally, we note that only a limited number of possible coherence orders are shown - in this case just those between –2 and +2. As was discussed above we need to remember that the spin system may be capable of supporting higher orders of coherence and take this into account when designing the phase cycle.

4.2.4.6 Refocusing Pulses

180° pulses give rise to a rather special coherence transfer pathway: they simply change the sign of the coherence order. We can see how this arises by considering the effect of a 180° pulse to the operators I_i^+ and I_i^-

$$I_i^{\pm} \xrightarrow{\pi I_{ix}} I_i^{\mp}$$

The operator on the right simply has the opposite sign of coherence order to that on the left. The same will be true of all of the raising or lowering operators of the different spins present and affected by the 180° pulse; the result is also valid, to within a phase factor, for any phase of the pulse (see exercises).

We can now derive the EXORCYLE phase cycle using this property. Consider a spin echo and the coherence transfer diagram shown in Fig. 8.

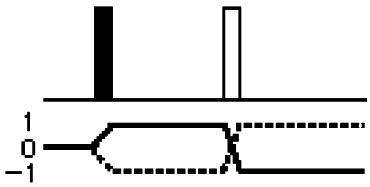

Figure 8. A spin echo and the corresponding CTP.

As discussed above, the CTP starts with coherence order 0 and ends with order –1. Since the 180° pulse simply swaps the sign of the coherence order, the order +1 must be present prior to the 180° pulse. Thus the 180° pulse is causing the transformation from +1 to –1, which is a Δp of –2. A phase cycle of four steps is easy to draw up

step	phase of 180° pulse	phase shift experienced by transfer with $\Delta p = -2$	equivalent phase = rx. phase
1	0	0	0
2	90	180	180
3	180	360	0
4	270	540	180

The phase cycle is thus **0 1 2 3** for the 180° pulse and **0 2 0 2** for the receiver, which is just EXORCYCLE. As the cycle has four steps, the pathway with $\Delta p = +2$ is also selected (shown dotted in Fig. 8). Although this pathway does not lead to an observable signal in this experiment its simultaneous selection in multiple pulse experiments where further pulses follow the spin echo is a useful feature. An eight step cycle can be used to select the refocusing of double quantum in which the transfer is from $p = +2$ to –2 (*i.e.* $\Delta p = -4$) or *vice versa* (see exercises). A two step cycle, **0 2** for the 180° pulse and **0 0** for the receiver, will select all *even* values of Δp (see exercises).

4.2.5 Lineshapes and Frequency Discrimination

The selection of a particular coherence transfer pathway is closely connected to two important aspects of multi-dimensional NMR experiments, that of frequency discrimination and lineshape selection. By frequency discrimination we mean the steps taken to ensure that the signs of the frequencies of the coherences evolving the indirectly detected domains can be determined. Typically this is done by using the States-Haberkorn-Ruben or TPPI methods. Lineshape selection is closely associated with frequency discrimination, and a particular frequency discrimination method results in a particular lineshape in the indirectly detected domains. It is clearly a priority to obtain the best lineshape possible, which generally means an absorption mode line. The issues are the same for two- and higher-dimensional spectra so we will consider just the simplest case.

A typical two-dimensional experiment "works" by transferring a component of magnetization, say of spin *i*, present at the end of the evolution time, $t1$, through some mixing process to another spin, say *j*. The size of the transferred component varies as a function of t_1; it is said to be

modulated in t_1. If the modulation frequency is Ω_i then the final steps of the two-dimensional experiment can be represented as

$$\cos\Omega_i t_1 I_{ix} \xrightarrow{\text{mixing}} \cos\Omega_i t_1 I_{jx} \qquad [7]$$

where we have assumed that the *x*-component is transferred. The signal is detected during t_2 in the usual way, using the detection scheme (called quadrature detection) described in section 4.2.1. This results in a signal which can be considered as a complex quantity and can be written as

$$\cos\Omega_i t_1 \exp\left(\mathrm{i}\,\Omega_j t_2\right)$$

Such a signal is said to be amplitude modulated in t_1. If we return to the mixing step sketched in Eqn. [7] we can reveal the underlying processes by re-writing the operators *Iix* in terms of the raising and lowering operators

$$\tfrac{1}{2}\cos\Omega_i t_1\left[I_i^+ + I_i^-\right] \xrightarrow{\text{mixing}} \tfrac{1}{2}\cos\Omega_i t_1 I_{jx} \qquad [8]$$

The implication of this is that to obtain amplitude modulation coherence orders +1 and –1 must both contribute, and contribute equally, to the transferred signal. This is the condition for obtaining amplitude modulation, and phase cycles for two- and higher-dimensional experiments need to be written in such a way as to retain "symmetrical pathways" in t_1. Once this has been achieved, frequency discrimination can be added by using one of the usual methods.

It is possible to use a phase cycle to achieve frequency discrimination. One simply writes a cycle which selects one coherence order, *i.e.* p = +1, during t_1. In effect what this achieves is the selection of transfer (mixing) from one operator, such as I_i^+, rather than from the combination of I_i^+ and I_i^- given in Eqn. [8]. Since under free evolution the operator I_i^+ simply acquires a phase term, of the form of exp(i $\Omega_i t_1$), the resulting signal is phase modulated in t_1 and thus frequency discrimination is achieved. Such a procedure is called echo-/anti-echo selection, or *P*-/*N*-type selection. It is illustrated in the following section for the simple COSY experiment.

4.2.5.1 P- and N-Type COSY

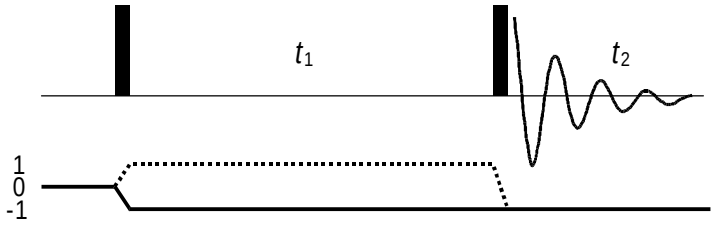

Figure 9. The pulse sequence for COSY with the CTP for the *P*-type spectrum shown as the solid line, and that for the *N*-type spectrum as a dashed line.

Figure 9 shows the simple COSY pulse sequence and two possible (and alternative) coherence transfer pathways. Both pathways start with $p = 0$ and end with $p = -1$, as described above. They differ, however, in the sign of the coherence order present during t_1. In the first case (the solid line) the order present is $p = -1$, the same as present during acquisition. Such a spectrum will be frequency discriminated, as was described above, and a diagonal peak at a positive offset in F_2 will also be at a positive offset in F_1. In contrast, a spectrum recorded such that $p = +1$ is present during t_1 (the dotted line) will have opposite offsets in the two dimensions. This arises because although the operators I_i^+ and I_i^- both acquire a phase dependent on the offset Ω_i, the sign of this phase modulation is opposite. In the usual notation

$$I_i^{\pm} \xrightarrow{\Omega_i t_1 \, I_{iz}} \exp\left(\mp \mathrm{i}\,\Omega_i t_1\right) I_i^{\pm}$$

Selection of one of these pathways gives a signal which is phase modulated in both t_1 and t_2. Subsequent two-dimensional Fourier transformation will give a peak in the spectrum which has the phase-twist lineshape. This is not a suitable lineshape high-resolution work and thus this method of selection is not generally used in demanding applications.

The spectrum in which the sign of the modulating frequencies, and hence the sign of the coherence order, is the same in t_1 and t_2 is called the *P*-type or anti-echo spectrum. Where these signs are opposite, one obtains the *N*-type or echo spectrum. The echo/anti-echo terminology arises because the pathway leading to the echo spectrum has $\Delta p = -2$ for the last pulse, which is analogous to the spin echo and indeed this pulse does result in partial refocusing of inhomogeneous broadening.

The phase cycles are simple to construct. We first note a short-cut in that the first pulse can only generate transverse magnetization from *z*-magnetization. It is quite impossible for it to generate multiple quantum coherence. Thus we can assume that the only $p = \pm 1$ are present during t_1. Our attention is therefore focused on the last pulse. In the case of the *N*-type spectrum we need to select the pathway with $\Delta p = -2$, and we have already devised a cycle to do this in section 4.2.4.6 - it is simply EXORCYCLE in which the last 90° pulse goes **0 1 2 3** and the receiver goes **0 2 0 2**. To select the *P*-type spectrum the required pathway has $\Delta p = 0$, for which the phase cycle is simply **0 1 2 3** on the final 90° pulse and **0 0 0 0** on the receiver, *i.e.* as $\Delta p = 0$ the coherence pathway experiences no phase shifts. Of course the unwanted pathways will experience phase shifts and thus will be cancelled.

If multiple quantum coherence is present during t_1 of a two-dimensional experiment the same principles apply, although smaller steps will be needed in order to select the required pathways (see exercises).

4.2.6 The Tricks of the Trade

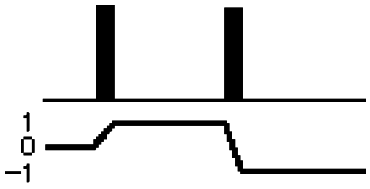

Figure 10 A simple CTP.

Suppose that we wish to select the simple pathway shown in Fig. 10. At the first pulse Δp is 1 and for the second pulse Δp is –2. We can construct a four-step cycle for each pulse, for example, but to select the overall pathway as shown these two cycles have to be completed independently of one another. This means that there will be a total of sixteen steps, and that the phase of the receiver must be set according to the phase acquired by shifting both pulses. The table shows how the appropriate receiver cycling can be determined

step	phase of 1st pulse	phase for $\Delta p = 1$	phase of 2nd pulse	phase for $\Delta p = -2$	total phase	equivalent phase = rx. phase
1	0	0	0	0	0	0
2	90	–90	0	0	–90	270
3	180	–180	0	0	–180	180
4	270	–270	0	0	–270	90
5	0	0	90	180	180	180
6	90	–90	90	180	90	90
7	180	–180	90	180	0	0
8	270	–270	90	180	–90	270
9	0	0	180	360	360	0
10	90	–90	180	360	270	270
11	180	–180	180	360	180	180
12	270	–270	180	360	90	90
13	0	0	270	540	540	180
14	90	–90	270	540	450	90
15	180	–180	270	540	360	0
16	270	–270	270	540	270	270

This is not as complex as it seems. In the first four steps the second pulse has constant phase and the first simply goes through the four cardinal phases, **0 1 2 3**. As we are selecting $\Delta p = 1$, the receiver simply runs backwards (the opposite to CYCLOPS), **0 3 2 1**. Steps 4 to 8 are the same except that the phase of the second pulse has been moved by 90°. This shifts the required pathway with $\Delta p = -2$ by 180° so the receiver phases for these steps are just 180° in advance of the corresponding first four steps, *i.e.* **2 1 0 3**. The next four steps are a repeat of the first four as shifting the

phase of the second pulse by 180° results in a complete rotation of the coherence and so there is no net effect. The final four steps are the same as the second four, except that the second pulse is shifted by 270°.

The key to devising these sequences is to simply work out the two four-step cycles independently and the merge them together rather than trying to work on the whole cycle. One writes down the first four steps, and then duplicates this four times as the second pulse is shifted. You should get the same steps, in a different sequence, if you shift the phase of the *second* pulse in the *first* four steps (see exercises).

We can see that the total size of a phase cycle grows at an alarming rate. With only four phases for each pulse the number of steps grows as 4^l where l is the number of pulses in the sequence. A prospect of a 64 step phase cycle for simple experiments like NOESY and DQF COSY is a daunting one. We may not wish to repeat each t_1 increment 64 times, although of course if the spectrum were weak we may end up doing this anyway simply to improve the signal-to-noise ratio.

The "trick" to learn is that you need not phase cycle each pulse. For various reasons there are shortcuts which can be used to reduce the number of pulses which need to be cycled. To find out what these shortcuts are you need to understand how the pulse sequence works and what all the pulses do. Sometimes, we can make shortcuts by ignoring certain possibilities, on the grounds that there are unlikely and that if they do occur they will sufficiently rare to be tolerable.

We will illustrate all of these points with reference to the DQF COSY pulse sequence, shown in Fig. 7 along with its coherence transfer diagram. We have already noted the need to retain the $p = \pm 1$ pathways during t_1 in order to be able to compute an absorption mode spectrum. Note also that the coherence orders ± 1 in t_1 are each connected to $p = \pm 2$ during the double quantum filter delay and that both of these double quantum levels are connected to $p = -1$ which is observed. A detailed analysis of this sequence will show that in general all of these pathways are present and equally likely.

4.2.6.1 The First Pulse

We have already commented on this in relation to the COSY experiment. Starting from equilibrium magnetization, I_{iz}, a simple pulse can generate only transverse magnetization with coherence orders ± 1. Thus it is not necessary to cycle this first pulse to select the pathway shown in Fig. 7. We note here for completeness that the first pulse, if it is imperfect, may leave some magnetization along the z-axis and thus the fate of this magnetization needs to be considered in relation to the rest of the pulse sequence. This residual z-magnetization is present during t_1 as coherence order zero. We will return to this in section 4.2.6.4.

4.2.6.2 Grouping Pulses Together

In section 4.2.4.2 we noted that the phase shift of a particular pathway by $-\Delta p\ \phi$ applied for the case where the transfer was brought about by a single pulse or by a group of pulses (and delays) whose phases are moved together. Essentially we are regarding the group of pulses as a single entity and may

phase cycle it in such a way as to select a particular value of Δp. It is important to realise, however, that the selection will simply be for a particular change in coherence order brought about by the whole group of pulses. The phase cycle will not select for what coherence transfers take place in the group. The idea of grouping pulses together thus has to be used carefully as it may lead to ambiguities.

In the DQF COSY sequence we have already noted that the pathways $\Delta p = \pm 1$ are inherently selected by the first pulse, so we should create no ambiguity by simply grouping the first two pulses together and cycling them as a unit to select the overall pathway $\Delta p = \pm 2$. Such a move will retain the symmetrical pathways required during t_1 and the complex series of transfers brought about by the second pulse are selected inherently. If we use a four-step cycle to select $\Delta p = +2$, we will also select –2 at the same time, which is just what we require.

The cycle is devised in the usual way

step	phase of first two pulses	phase for $\Delta p = +2$	phase for $\Delta p = -2$	equivalent phase = rx. phase
1	0	0	0	0
2	90	–180	180	180
3	180	–360	360	0
4	270	–540	540	180

The equivalent phase is the same for both pathways, $\Delta p = \pm 2$. The overall phase cycle is thus for the first two pulses to go **0 1 2 3**, the third pulse to remain fixed and the receiver to go **0 2 0 2**. We shall see in the next section that this is sufficient to select the required pathway.

The four-step cycle also selects $\Delta p = \pm 6$, so there is the possibility of signals arising due to filtration through six-quantum coherence. In normal spin systems the amount of such high order coherences that can be generated is usually very small so that in practice we can discount this possibility.

Finally, we need to consider *z*-magnetization which may be left over after an imperfect initial 90° pulse or which arises due to relaxation during t_1. If signals are derived from such magnetization they give rise to peaks at $F_1 = 0$ in the spectrum simply because magnetization does not precess during t_1 and so has no frequency label; such peaks are called *axial peaks*.

z-Magnetization present at the end of t_1 will be turned to the transverse plane by the second 90° pulse, generating coherences ±1 as before. The second pulse is being cycled **0 1 2 3** along with the receiver going **0 2 0 2**; such a cycle suppresses the pathway $\Delta p = \pm 1$ and so axial peaks are suppressed.

4.2.6.3 The Last Pulse

The final pulse in a sequence has some special features which may be exploited when trying to reduce a phase cycle to its minimum. This pulse may cause transfer to many different orders of coherence but only one of these, that with $p = -1$, is observable. Thus, if we have already selected, in

an unambiguous way, a particular set of coherence orders present just before the last pulse, no further cycling of this pulse is needed. The fact that we can only observe $p = -1$ will "naturally" select what we want. The DQF COSY phase cycle proposed in the previous section achieves this result in that it selects $p = \pm 2$ just before the last pulse. No further cycling is required, therefore.

We can view this property of the final pulse in a different way. Looking at the DQF COSY sequence we see that the two required pathways to be brought about by the final pulse have $\Delta p = -3$ and $+1$. As the only detectable signal has $p = -1$, the selection of these two pathways will guarantee that the only contributors to the observed signal will be from coherences with orders $p = \pm 2$ present just before this pulse. Cycling just the last pulse will thus achieve all that we require. In section 4.2.6 we have already devised a phase cycle to select $\Delta p = +1$, the pulse goes **0 1 2 3** and the receiver goes **0 3 2 1**. As this is a four-step cycle we see immediately that $\Delta p = -3$ is also selected, which is what is required. Other, higher order pathways are selected, such as $\Delta p = +5$ or -7; these can most probably be ignored safely.

Finally we ought to consider the fate of any *z*-magnetization present at the end of t_1. This is turned to coherence orders ± 1 by the second pulse and so for it to be observable (*i.e.* $p = -1$) during acquisition it must undergo a transfer by the last pulse of $\Delta p = 0$ or -2. Both of these are blocked by the phase cycle, so axial peaks are suppressed.

We now have two alternative four step cycles for DQF COSY; in section 4.2.6.5, we will show that despite their different origins they are more or less the same.

4.2.6.4 Axial Peak Suppression

Sometimes we want to write a phase cycle in which there is an added explicit step to suppress axial peaks. In principle and strictly according to theory this is not always necessary as the magnetization that leads to axial peaks is often suppressed by the phase cycle used for coherence selection.

A simple two step phase cycle suffices for this suppression. The first pulse is supposed to result in the pathway $\Delta p = \pm 1$ and such a pathway is selected, along with others, using the two step cycle in which the pulse goes **0 2** and the receiver goes **0 2** also. Any magnetization which arrives at the receiver but which has not experienced the phase shift from the first pulse will be cancelled. The cycle thus eliminates all peaks in the spectrum, such as axial peaks, which do not arise from the first pulse. Of course this two-step cycle does not select exclusively $\Delta p = \pm 1$, but most importantly it does reject $\Delta p = 0$ which is one likely source of axial peaks.

4.2.6.5 Shifting the Whole Sequence

If we group *all* of the pulses in the sequence together and regard them as a unit they simply achieve the transformation from equilibrium magnetization, $p = 0$, to observable magnetization, $p = -1$. They could be cycled as a group to select this pathway with $\Delta p = -1$, that is the pulses going **0 1 2 3** and the receiver going **0 1 2 3**. This is of course the

CYCLOPS phase cycle. If time permits we sometimes add CYCLOPS-style cycling of all of the pulses in the sequence so as to suppress some artefacts associated with imperfections in the receiver. Adding such cycling does, of course, extend the phase cycle by a factor of four.

This idea of shifting *all of* the pulses in the sequence has other applications. Consider the DQF COSY phase cycle proposed in section 4.2.6.3:

step	1st pulse	2nd pulse	3rd pulse	receiver
1	0	0	0	0
2	0	0	90	270
3	0	0	180	180
4	0	0	270	90

Suppose we decide, for some reason, that we do not want to shift the receiver phase, but want to keep it fixed at phase zero. If we add 90° to the phase of all the pulses in step 2, then we will need also to add 90° to the receiver as the overall transformation is $\Delta p = -1$; this puts the receiver phase at 0°. In the same way we can add 180° to all the pulses and the receiver for step 3 and 270° for step 4. Once all the phases are reduced to the usual range of 0 to 360° we have

step	1st pulse	2nd pulse	3rd pulse	receiver
1	0	0	0	0
2	90	90	180	0
3	180	180	0	0
4	270	270	180	0

The result looks rather strange, as we seem to be shifting the phase of all of the pulses at the same time. However, we know that, in a formal way, it is exactly the same cycle as was devised in section 4.2.6.3 By writing it in this way, however, the way in which the cycle works is rather obscured.

In the case of DQF COSY there is probably no reason for adopting this procedure. However, a case where it might be useful is when a phase cycle calls for phase shifts of other than multiples of 90° for the receiver. Some spectrometers allow fine resolution phase shifting of the pulse phase, but only allow 90° steps for the receiver. In such cases the required phase shifts of the received can be generated in effect by moving the phase of all the pulses until the receiver phases are at multiples of 90° (see exercises).

We can play one last trick with the phase cycle given in the table. As the third pulse is required to achieve the transformation $\Delta p = -3$ or $+1$ we can alter its phase by 180° and compensate for this by shifting the receiver by 180° also. We apply this trick to the phase of the third pulse for steps 2 and 4 to give the cycle

step	1st pulse	2nd pulse	3rd pulse	receiver
1	0	0	0	0
2	90	90	0	180
3	180	180	0	0
4	270	270	0	180

This is just the cycle proposed in section 4.2.6.2. We have then three different phase cycles, each of which, despite looking rather different achieves the same result.

4.2.7 More Examples

4.2.7.1 Homonuclear Experiments

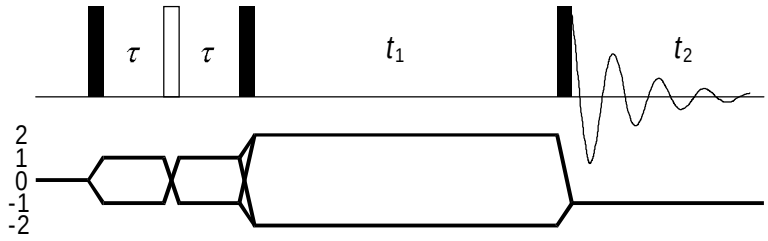

Figure 11 The pulse sequence and CTP for double-quantum spectroscopy.

Double Quantum Spectroscopy: A simple sequence for double quantum spectroscopy is shown in Fig. 11; note the retention of both pathways with $p = \pm 1$ during the initial spin echo and with $p = \pm 2$ during t_1. There are a number of possible phase cycles for this experiment and, not surprisingly, they are essentially the same as those for DQF COSY. If we regard the first three pulses as a unit, then they are required to achieve the overall transformation $\Delta p = \pm 2$, which is the same as that for the first two pulses in the DQF COSY sequence. Thus the same cycle can be used with these three pulses going **0 1 2 3** and the receiver going **0 2 0 2**. Alternatively the final pulse can be cycled **0 1 2 3** with the receiver going **0 3 2 1**, as in section 4.2.6.3.

Both of these phase cycles can be extended by EXORCYCLE phase cycling of the 180° pulse, resulting in a total of 16 steps (see exercises).

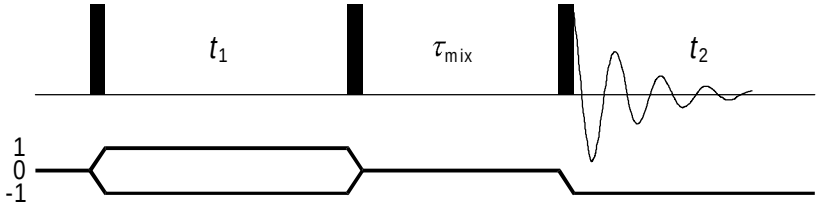

Figure 12. The pulse sequence and CTP for NOESY.

NOESY: The sequence is shown in Fig. 12. Again it can be viewed in two ways. If we group the first two pulses together they are required to achieve

the transformation $\Delta p = 0$ and this leads to a four step cycle in which the pulses go **0 1 2 3** and the receiver remains fixed as **0 0 0 0**. In this experiment axial peaks arise due to *z*-magnetization recovering during the mixing time, and this cycle will *not* suppress these contributions as there is no suppression of the pathway $\Delta p = -1$ caused by the last pulse. Thus we need to add axial peak suppression, which is conveniently done by adding the simple cycle **0 2** on the first pulse and the receiver. The final 8 step cycle is 1st pulse: **0 1 2 3 2 3 0 1**, 2nd pulse: **0 1 2 3 0 1 2 3**, 3rd pulse fixed, receiver: **0 0 0 0 2 2 2 2**.

An alternative is to cycle the last pulse to select the pathway $\Delta p = -1$, giving the cycle **0 1 2 3** for the pulse and **0 1 2 3** for the receiver. Once again, this does not discriminate against *z*-magnetization which recovers during the mixing time, so a two step phase cycle to select axial peaks needs to be added (see exercises).

4.2.7.2 Heteronuclear Experiments

The phase cycling for most heteronuclear experiments tends to be rather trivial in that the usual requirement is simply to select that component which has been transferred from one nucleus to another. We have already seen in section 4.2.3 that this simply boils down to a **0 2** phase cycle on a pulse accompanied by the same on the receiver *i.e.* a difference experiment. The choice of which pulse to cycle depends more on practical problems associated with difference spectroscopy than with any fundamental theoretical considerations.

HMQC: The pulse sequence for HMQC is given in Fig. 13, along with a coherence transfer pathway. We have written a separate pathway for the two nuclear species, thus the heteronuclear multiple quantum coherence which gives the sequence its name appears as a combination of $p_I = \pm 1$ and $p_S = \pm 1$. Again, all symmetrical pathways are retained in order to give optimum sensitivity and pure phase lineshapes.

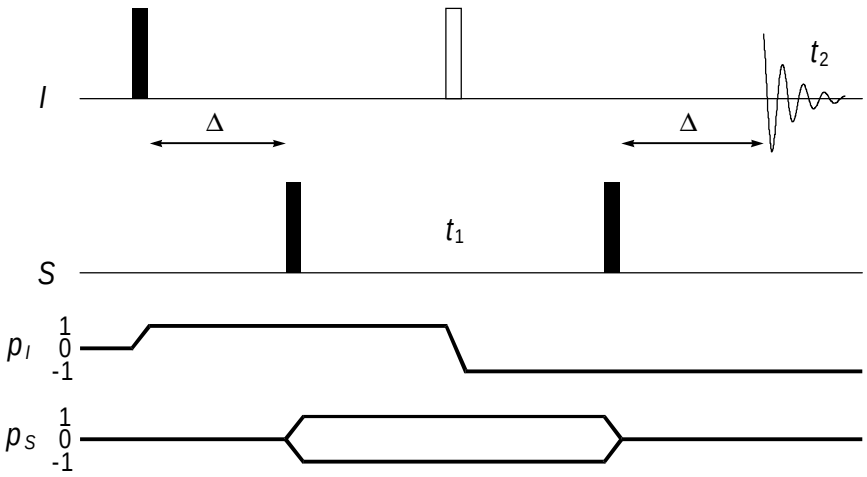

Figure 13. The pulse sequence and CTP for HMQC. Separate pathways are shown for the *I* and *S* spins.

The essential result we need to achieve in this sequence is to suppress the signals arising from *I* spins which are not coupled to *S* spins. This is

achieved by cycling the phase of a pulse which affects the phase of the required coherence and which does not affect that of the unwanted coherence. The obvious targets are the two *S* spin 90° pulses, each of which is required to give the transformation $\Delta p_S = \pm 1$. A two step cycle with either of these pulses going **0 2** and the receiver doing the same will select this pathway and, by difference, suppress any *I* spin magnetization which has not been passed into multiple quantum coherence.

It is also common to add EXORCYCLE phase cycling to the *I* spin 180° pulse, giving a cycle with eight steps overall. Axial peaks should be suppressed by the two step cycle of one of the *S* spin 90° pulses. It is clear that for heteronuclear experiments the coherence transfer pathway approach is not really necessary.

4.2.8 Conclusions

We have seen that phase cycling is a relatively straightforward method of selecting a particular coherence transfer pathway. Even at a theoretical level the method sometimes fails when we are trying to select a complex pathway, particularly one in which we are trying to select may parallel pathways (see exercises); it may not be possible to write a phase cycle which selects the required pathway.

In practice phase cycling suffers from two major problems. The first is that the need to complete the cycle imposes a minimum time on the experiment. In two- and higher-dimensional experiments this minimum time can become excessively long, far longer than would be needed to achieve the desired signal-to-noise ratio. In such cases the only way of reducing the experiment time is to record fewer increments of the indirect times which has the undesirable consequence of reducing the limiting resolution in these dimensions.

The second problem is that phase cycling always relies on recording all possible contributions and then cancelling out the unwanted ones by combining subsequent signals. If the spectrum has high dynamic range, or if spectrometer stability is a problem, this cancellation is less than perfect. The result is unwanted signals appearing in the spectrum and t_1-noise in two-dimensional spectra. These problems become acute when dealing with proton detected heteronuclear experiments on natural abundance samples, or in trying to record spectra with intense solvent resonances.

Both of these problems are alleviated to a large extent by moving to an alternative method of selection, the use of field gradient pulses which are the subject of the next section. However, this alternative method is not without its own difficulties and it is by no means a universal panacea.

Neither phase cycling nor field gradient pulses can discriminate between *z*-magnetization and homonuclear zero-quantum coherence, both of which have coherence order zero. There are methods which can be used to suppress the contribution from zero-quantum coherence; these are all based on the fact that this coherence acquires a phase during a delay or period of spin-locking. There thus exists the possibility of cancellation or dephasing. Further details can be found in section 4.3.7.1.

4.3 Field Gradient Pulses

4.3.1 Introduction

Field gradient pulses can be used to select particular coherence transfer pathways and, as we shall see, selection using gradients offers some advantages when compared to selection using phase cycling. During a pulsed field gradient the applied magnetic field is made deliberately spatially inhomogeneous for a short time. As a result, transverse magnetization and other coherences dephase across the sample and are apparently lost. However, this loss can be reversed by the application of a subsequent gradient which undoes the dephasing process thus restoring the magnetization or coherence. The crucial property of the dephasing process is that it proceeds at a different rate for different coherences. For example, double-quantum coherence dephases twice as fast as single-quantum coherence. Thus, by applying gradient pulses of different strengths or durations it is possible to refocus coherences which have, for example, been changed from single- to double-quantum by a radiofrequency pulse.

Gradient pulses are introduced into the pulse sequence in such a way that only the wanted signals are observed in each experiment. Thus, in contrast to phase cycling, there is no reliance on subtraction of unwanted signals, and it can thus be expected that the level of t_1-noise will be much reduced. Again in contrast to phase cycling, no repetitions of the experiment are needed, enabling the overall duration of the experiment to be set strictly in accord with the required resolution and signal-to-noise ratio.

The properties of gradient pulses and the way in which they can be used to select coherence transfer pathways have been known since the earliest days of multiple-pulse NMR. However, their wide application in the past has been limited by technical problems which made it difficult to use such pulses in high-resolution NMR. The problem is that switching on the gradient pulse induces currents in any nearby conductors, such as the probe can and magnet bore tube. These induced currents, called *eddy currents*, themselves generate magnetic fields which perturb the NMR spectrum. Typically, the eddy currents are large enough to disrupt severely the spectrum and can last many hundreds of milliseconds. It is thus impossible to observe a high-resolution spectrum immediately after the application of a gradient pulse. Similar problems have beset NMR imaging experiments and have led to the development of *shielded gradient coils* which do not produce significant magnetic fields outside the sample volume and thus minimise the generation of eddy currents. The use of this technology in high-resolution NMR probes has made it possible to observe spectra within tens of microseconds of applying a gradient pulse. With such apparatus, the use of field gradient pulses in high resolution NMR is quite straightforward, a fact first realised and demonstrated by Hurd whose work has pioneered this whole area.

4.3.2 Selection with Gradient Pulses

4.3.2.1 Dephasing Caused by Gradients

A field gradient pulse is a period during which the B_0 field is made spatially inhomogeneous; for example an extra coil can be introduced into the sample probe and a current passed through the coil in order to produce a field which varies linearly in the *z*-direction. We can imagine the sample being divided into thin discs which, as a consequence of the gradient, all experience different magnetic fields and thus have different Larmor frequencies. At the beginning of the gradient pulse the vectors representing transverse magnetization in all these discs are aligned, but after some time each vector has precessed through a different angle because of the variation in Larmor frequency. After sufficient time the vectors are disposed in such a way that the net magnetization of the sample (obtained by adding together all the vectors) is zero. The gradient pulse is said to have dephased the magnetization.

It is most convenient to view this dephasing process as being due to the generation by the gradient pulse of a *spatially dependent phase*. Suppose that the magnetic field produced by the gradient pulse, B_g, varies linearly along the *z*-axis according to

$$B_g = Gz \qquad [9]$$

where G is the gradient strength expressed in, for example, $T \cdot m^{-1}$ or $G \cdot cm^{-1}$; the origin of the *z*-axis is taken to be in the centre of the sample. At any particular position in the sample the Larmor frequency, $\omega_L(z)$, depends on the applied magnetic field, B_0, and B_g

$$\omega_L = \gamma\left(B_0 + B_g\right) = \gamma\left(B_0 + Gz\right) \quad , \qquad [10]$$

where γ is the gyromagnetic ratio. After the gradient has been applied for time t, the phase at any position in the sample, $\Phi(z)$, is given by $\Phi(z) = \gamma\left(B_0 + Gz\right)t$. The first part of this phase is just that due to the usual Larmor precession in the absence of a field gradient. Since this is constant across the sample it will be ignored from now on (which is formally the same result as viewing the magnetization in a frame of reference rotating at γB_0). The remaining term γGzt is the *spatially dependent phase* induced by the gradient pulse.

We imagine applying a gradient pulse to pure *x*-magnetization, giving the following evolution at any particular position in the sample

$$I_x \xrightarrow{\gamma G z t I_z} \cos(\gamma G z t) I_x + \sin(\gamma G z t) I_y \quad . \qquad [11]$$

The total *x*-magnetization in the sample, M_x, is found by adding up the magnetization from each of the thin discs, which is equivalent to the integral

$$M_x(t) = \frac{1}{r_{\max}} \int_{-\frac{1}{2}r_{\max}}^{\frac{1}{2}r_{\max}} \cos(\gamma G z t)\,\mathrm{d}z \qquad [12]$$

where it has been assumed that the sample extends over a region $\pm\frac{1}{2}r_{\max}$. Evaluating the integral gives an expression for the decay of *x*-magnetization during a gradient pulse

$$M_x(t) = \frac{2\sin(\frac{1}{2}\gamma G r_{\max} t)}{\gamma G r_{\max} t} \quad . \qquad [13]$$

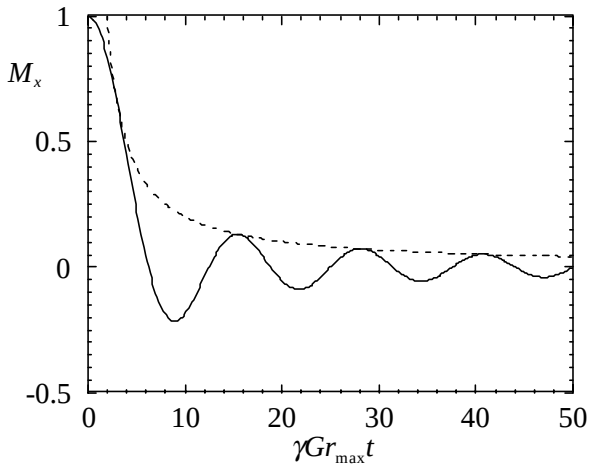

Figure 14. The solid line shows the decay of magnetization due to the action of a gradient pulse. The dashed line is an approximation, valid at long times, for the envelope of the decay.

Figure 14 shows a plot of $M_x(t)$ as a function of time; the oscillations in the decaying magnetization are imposed on an overall decay which for long times is given by $2/(\gamma G t r_{\max})$. Equation [13] embodies the obvious points that the stronger the gradient (the larger *G*) the faster the magnetization decays and that magnetization from nuclei with higher gyromagnetic ratios decays faster. It also allows a quantitative assessment of the gradient strengths required: the magnetization will have decayed to a fraction α of its initial value after a time of the order of $2/(\gamma G \alpha r_{\max})$ (the relation is strictly valid for $\alpha << 1$). For example, if it is assumed that $r_{\max}$ is 1 cm, then a 2 ms gradient pulse of strength 0.37 $T \cdot m^{-1}$ (37 $G \cdot cm^{-1}$) will reduce proton magnetization by a factor of 1000. Gradients of such strength are readily obtainable using modern shielded gradient coils that can be built into high resolution NMR probes

This discussion now needs to be generalised for the case of a field gradient pulse whose amplitude is not constant in time, and for the case of dephasing a general coherence of order *p*. The former modification is of

importance as for instrumental reasons the amplitude envelope of the gradient is often shaped to a smooth function. In general after applying a gradient pulse of duration τ the spatially dependent phase, $\Phi(r,\tau)$ is given by

$$\Phi(r,\tau) = sp\gamma B_g(r)\tau \qquad [14]$$

The proportionality to the coherence order comes about due to the fact that the phase acquired as a result of a *z*-rotation of a coherence of order *p* through an angle ϕ is $p\phi$, (see Eqn. [1] in section 4.2.4.1). In Eqn. [14] *s* is a shape factor: if the envelope of the gradient pulse is defined by the function *A*(*t*), where $|A(t)| \leq 1$, *s* is defined as the area under *A*(*t*)

$$s = \frac{1}{\tau}\int_0^\tau A(t)\,\mathrm{d}t \quad . \qquad [15]$$

The shape factor takes a particular value for a certain shape of gradient, regardless of its duration. A gradient applied in the opposite sense, that is with the magnetic field decreasing as the *z*-coordinate increases rather than *vice versa*, is described by reversing the sign of *s*. The overall amplitude of the gradient is encoded within B_g.

In the case that the coherence involves more than one nuclear species, Eqn. [14] is modified to take account of the different gyromagnetic ratio for each spin, γ_i, and the (possibly) different order of coherence with respect to each nuclear species, p_i:

$$\Phi(r,\tau) = sB_g(r)\tau\sum_i p_i\gamma_i \quad . \qquad [16]$$

From now on we take the dependence of Φ on *r* and *t*, and of B_g on *r* as being implicit, and will not write these explicitly.

4.3.2.2 Selection by Refocusing

The method by which a particular coherence transfer pathway is selected using field gradients is illustrated in Fig.15 (a).

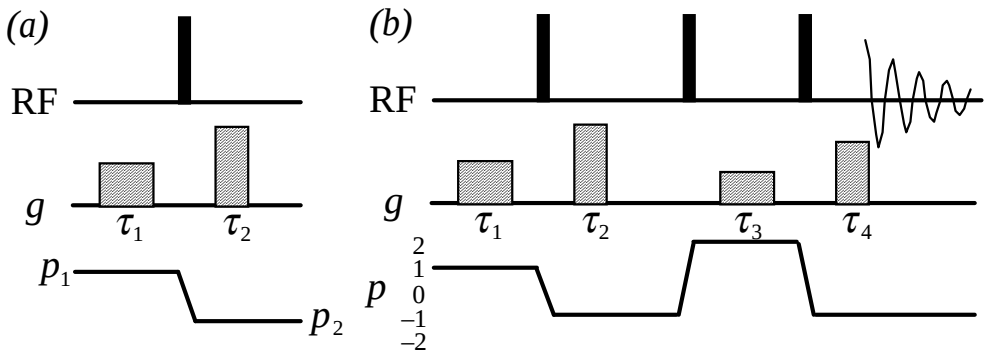

Figure 15 Pulse sequences and associated coherence transfer pathways illustrating coherence selection using gradients. The radiofrequency pulses are given on the line marked RF, solid rectangles indicate 90° pulses and open rectangles indicate 180° pulses; the pulse phase is *x* unless otherwise specified. Gradient pulses are indicated by the rectangles on the line marked *g*.

The first gradient pulse encodes a spatially dependent phase, Φ_1 and the second a phase Φ_2 where

$$\Phi_1 = s_1 p_1 B_{g,1} \tau_1 \quad \text{and} \quad \Phi_2 = s_2 p_2 B_{g,2} \tau_2 \quad . \qquad [17]$$

After the second gradient the net phase is $(\Phi_1 + \Phi_2)$. To select the pathway involving transfer from coherence order p_1 to coherence order p_2, this net phase should be zero; in other words the dephasing induced by the first gradient pulse is undone by the second. The condition $(\Phi_1 + \Phi_2) = 0$ can be rearranged to

$$\frac{s_1 B_{g,1} \tau_1}{s_2 B_{g,2} \tau_2} = \frac{-p_2}{p_1} \quad . \qquad [18]$$

For example, if $p_1 = +2$ and $p_2 = -1$, refocusing can be achieved by making the second gradient either twice as long ($\tau_2 = 2\ \tau_1$), or twice as strong ($B_{g,2} = 2\ B_{g,1}$) as the first; this assumes that the two gradients have identical shape factors. Other pathways remain dephased; for example, assuming that we have chosen to make the second gradient twice as strong and the same duration as the first, a pathway with $p_1 = +3$ to $p_2 = -1$ experiences a net phase

$$\Phi_1 + \Phi_2 = 3sB_{g,1}\tau_1 - sp_2 B_{g,2}\tau_1 = sB_{g,1}\tau_1 \quad . \qquad [19]$$

Provided that this spatially dependent phase is sufficiently large, according the criteria set out in the previous section, the coherence arising from this pathway remains dephased and is not observed. To refocus a pathway in which there is no sign change in the coherence orders, for example, $p_1 = -2$ to $p_2 = -1$, the second gradient needs to be applied in the opposite sense to the first; in terms of Eqn. [18] this is expressed by having $s_2 = -s_1$.

The procedure can easily be extended to select a more complex coherence transfer pathway by applying further gradient pulses as the coherence is transferred by further pulses, as illustrated in Fig. 15 (b). The condition for refocusing is again that the net phase acquired by the required pathway be zero, which can be written formally as

$$\sum_i s_i p_i B_{g,i} \tau_i = 0 \quad . \qquad [20]$$

With more than two gradients there are many ways in which a given pathway can be selected. For example, the second gradient may be used to refocus the first part of the required pathway, leaving the third and fourth to refocus another part. Alternatively, the pathway may be consistently dephased and the magnetization only refocused by the final gradient, just before acquisition.

At this point it is useful to contrast the selection achieved using gradient pulses with that achieved using phase cycling. From Eqn. [18] it is clear that a particular pair of gradient pulses selects a particular *ratio* of coherence orders; in the above example any two coherence orders in the ratio –2 : 1 or 2 : – 1 will be refocused. This selection according to ratio is in contrast to the case of phase cycling in which a phase cycle consisting of N steps of $2\pi/N$ radians selects a particular *change* in coherence order $\Delta p = p_2 - p_1$, and further pathways which have $\Delta p = (p_2 - p_1) \pm mN$, where $m = 0, 1, 2 \ldots$

It is straightforward to devise a series of gradient pulses which will *select* a single coherence transfer pathway. It cannot be assumed, however, that such a sequence of gradient pulses will *reject* all other pathways *i.e.* leave coherence from all other pathways dephased at the end of the sequence. Such assurance can only be given be analysing the fate of *all* other possible coherence transfer pathways under the particular gradient sequence proposed. In complex pulse sequences there may also be several different ways in which gradient pulses can be included in order to achieve selection of the desired pathway. Assessing which of these alternatives is the best, in the light of the requirement of suppression of unwanted pathways and the effects of pulse imperfections may be a complex task.

In this section it has been shown that a *single* coherence transfer pathway can be selected with the aid of gradient pulses. However, it is not unusual to want to select two or more pathways *simultaneously*. A good example of this is the double-quantum filter pulse sequence element shown in Fig. 16 (a).

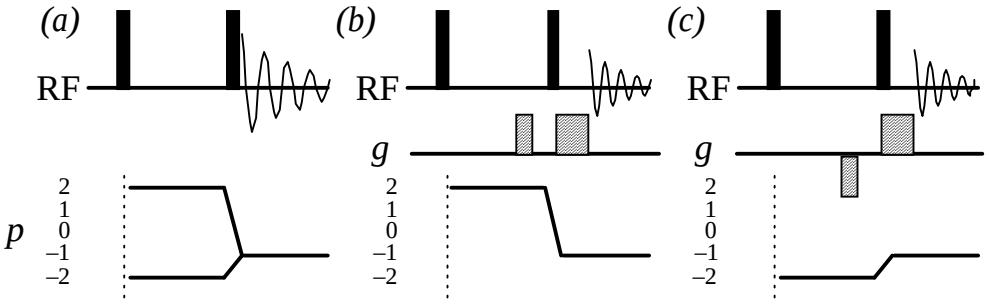

Figure 16 Pulse sequences and pathways for double-quantum filters.

The ideal pathway, shown in (a), preserves coherence orders $p = \pm 2$ during the inter-pulse delay. It can be shown that the first 90° pulse generates equal amounts of coherence orders + 2 and – 2, and these contribute equally to the final observable signal. Gradients can be used to select the pathway – 2 to – 1 or + 2 to – 1, shown in (b) and (c) respectively. However, no combination of gradients can be found which will select simultaneously both of these pathways. In contrast, it is easy to devise a phase cycle which selects both of these pathways (section 4.2.6.2). Thus, selection with gradients will in this case result in a loss of *half* of the available signal when compared to an experiment of equal length which uses selection by phase cycling. Such a loss in signal is, unfortunately, a very common feature when gradients are used for pathway selection.

Coherence order zero, comprising *z*-magnetization, *zz* terms and homonuclear zero-quantum coherence, does not accrue any phase during a gradient pulse. Thus it can be separated from all other orders simply by applying a single gradient. In a sense, however, this is not a gradient selection process; rather it is a simply *suppression* of all other coherences. In contrast to experiments where *selection* is achieved, there is no inherent sensitivity loss.

The simplest experimental arrangement generates a gradient in which the magnetic field varies in the *z* direction, however it is also possible to generate gradients in which the field varies along *x* or *y*. Clearly, the spatially dependent phase generated by a gradient applied in one direction *cannot* be refocused by a gradient applied in a different direction. In sequences where more than one pair of gradients are used, it may be convenient to apply further gradients in different directions to the first pair, so as to avoid the possibility of accidentally refocusing unwanted coherence transfer pathways. Likewise, a gradient which is used to destroy all magnetization and coherences can be applied in a different direction to gradients subsequently used for pathway selection.

4.3.2.3 Spin Echoes

Refocusing pulses play an important role in multiple-pulse NMR experiments and so the interaction between such pulses and field gradient pulses will be explored in some detail. A perfect refocusing pulse achieves two effects. Firstly, it changes the sign of the order of any coherences present, $p \rightarrow -p$. Secondly, *z*-magnetization is inverted $I_z \rightarrow -I_z$. A perfect 180° pulse, applied about any axis, is an example of such a refocusing pulse. An imperfect refocusing pulse will cause transfers to other coherence orders than $-p$, and may generate transverse magnetization from any *z*-magnetization present. We start out the discussion by considering the refocusing of coherences.

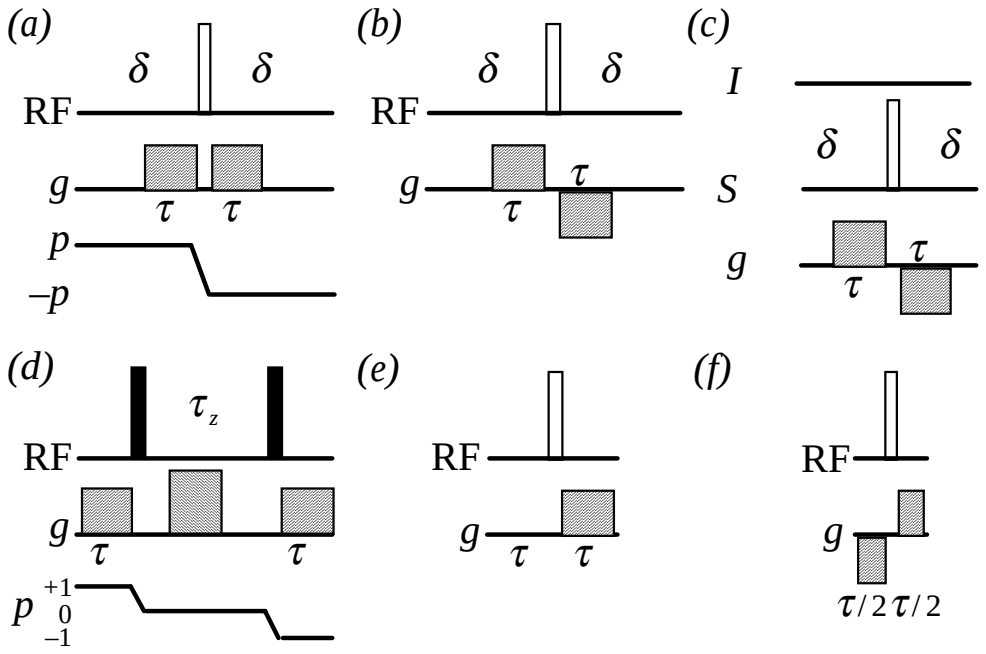

Figure 17 Spin echoes and related sequences. In heteronuclear experiments the radiofrequency pulses applied to the *I* and *S* spins are indicated on the lines so marked

The effect of an imperfect refocusing pulse can be considered by factoring the sample into a part which experiences perfect refocusing and a part which does not. The refocused part can be selected by placing a gradient pulse on either side of the refocusing pulse, as shown in Fig. 17 (a). The net phase at the end of such a sequence is

$$\Phi(2\tau) = \Omega^{(p)}\delta + sp\gamma B_g\tau + \Omega^{(p')}\delta + sp'\gamma B_g\tau \qquad [21]$$

where $\Omega^{(p)}$ is the frequency with which coherence of order p evolves in the absence of a gradient; note that $\Omega(-p) = -\Omega(p)$. This net phase is zero if, and only if, $p' = -p$. With sufficiently strong gradients all other pathways remain dephased and the gradient sequence has thus selected the perfectly refocused component. In addition, any transverse magnetization created by an imperfect refocusing pulse is also dephased. As is expected for a spin echo, the underlying evolution of the coherence (as would occur in the absence of a gradient) for the entire time 2δ is also refocused.

If a refocusing pulse is used in its second context, that of inversion of *z* magnetization, the considerations are somewhat different. Formally, we could regard the problem as selecting the pathway $p = 0 \rightarrow p' = 0$, in which case any combination of gradients would be suitable. However, in practice a gradient combination should be used which gives the maximum dephasing effect to other coherences. Assuming that the refocusing pulse still changes the sign of the larger fraction of the coherences in the sample, the greatest dephasing is obtained when the second gradient is applied in the opposite sense to the first, as is shown in Fig. 17 (b).

In heteronuclear experiments a refocusing pulse is often used to remove the effects of the heteronuclear coupling over a period. The role of such a

pulse when applied to spins *S* is simply to invert the sign of any operator products involving S_z; in other words to act as an inversion pulse for *S*. This function is selected using the gradient sequence shown in Fig. 17 (c), which in analogous to (b). Of course, any coherences on the spins *I* will be dephased by the first gradient, but these coherences will be rephased by the second gradient as it is applied in the opposite sense. The net effect is that the *I* spin shift evolves for 2δ, but the *IS* coupling is refocused.

If a refocusing pulse is perfect, the inclusion of gradient pulses as shown in Fig. 17 (a) - (c) does not reduce the size of the ultimately observed signal. This is in contrast to most other situations in which selection with gradients results in an inherent loss of signal. However, if the refocusing pulse is imperfect there will be a loss of signal reflecting that part of the sample which does not experience a perfect refocusing pulse.

4.3.2.4 Phase Errors

In the selection process the spatially dependent phase created by a gradient pulse is subsequently refocused by a second gradient pulse. However, the underlying evolution due to chemical shifts (offsets) and couplings is not refocused, and phase errors will accumulate due to the evolution of these terms. Since gradient pulses are typically of a few milliseconds duration, these phase errors are far from insignificant.

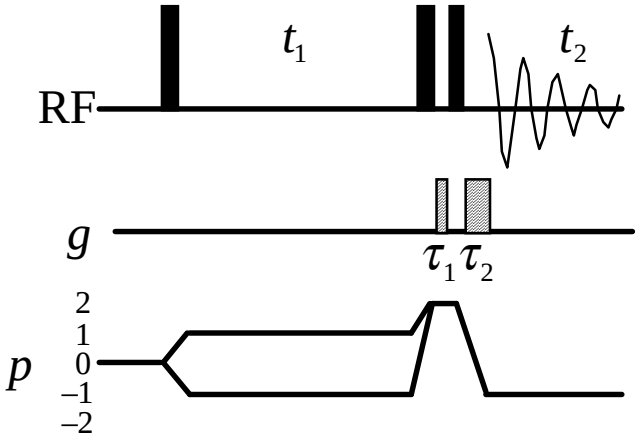

Figure 18. A DQF COSY sequence with gradient selection.

In multi-dimensional NMR the uncompensated evolution of offsets during gradient pulses has disastrous effects on the spectra. This is illustrated here for the double-quantum filtered COSY pulse sequence using the gradient pulses shown in Fig. 18. It will be assumed that only the indicated pathway survives and so the spatially dependent part of the evolution due to the gradients will be ignored. Thus, for a two spin system, coherence order of + 2 present during the filter evolves as follows during the first gradient pulse

$$I_{1+}I_{2+} \xrightarrow{\Omega_1\tau_1 I_{1z}+\Omega_2\tau_1 I_{2z}} I_{1+}I_{2+}\exp\left(-i\left(\Omega_1+\Omega_2\right)\tau_1\right) , \qquad [22]$$

where Ω_1 and Ω_2 are the offsets of spins 1 and 2, respectively. After the

final 90° pulse and the second gradient the observable terms on spin 1 are

$$\tfrac{i}{2}\exp\left(-i\left(\Omega_1+\Omega_2\right)\tau_1\right)\left[\cos\Omega_1\tau_2\ 2I_{1x}I_{2z}+\sin\Omega_1\tau_2\ 2I_{1y}I_{2z}\right] \qquad [23]$$

where it has been assumed that τ_2 is sufficiently short that evolution of the coupling can be ignored. It is clearly seen from Eqn. [23] that, due to the evolution during τ_2, the multiplet observed in the F_2 dimension will be a mixture of dispersion and absorption anti-phase contributions. In addition, the exponential term gives an overall phase shift due to the evolution during τ_1. The phase correction needed to restore this multiplet to absorption depends on both the frequency in F_2 *and* the double-quantum frequency during the first gradient. Thus, no single linear frequency dependent phase correction could phase correct a spectrum containing many multiplets. The need to control these phase errors is plain.

The general way to minimise these problems is to associate each gradient pulse with a refocusing pulse as shown in Fig. 17 (e) and (f). Using the results from the previous section it is easily seen that sequence (e) generates a net phase of $sp\gamma B_g\tau$; (f) gives the same result with a sign change. The desired effect of refocusing the evolution due to the offset and not that due to the gradient has been achieved. In sequence (f) the gradient is split into two halves by the refocusing pulse, and in order to avoid the second gradient refocusing the effect of the first, the two gradients have to be applied in opposite senses. Of these two options (f) is the most time efficient as the gradient is applied for the entire duration, whereas option (e) lengthens the experiment by doubling the time needed for each gradient; if relaxation is rapid, option (f) is the method of choice. As was explained in the previous section, if the refocusing pulse is imperfect coherences undergoing transfers other than the required $p \rightarrow -p$ should be dephased by (f). However, sequence (e) will dephase the results of only some of these unwanted coherence transfers.

In many pulse sequences there are periods during which the evolution of offsets is refocused. The evolution of offsets during a gradient pulse placed within such a period will therefore also be refocused, making it unnecessary to include extra refocusing pulses. Likewise, a gradient may be placed during a "constant time" evolution period of a multi-dimensional pulse sequence without introducing phase errors in the corresponding dimension; the gradient simply becomes part of the constant time period. This approach is especially useful in the constant time three- and four-dimensional experiments used to record spectra of nitrogen-15, carbon-13 labelled proteins.

4.3.3 Lineshapes in Multi-Dimensional Spectra

The use of gradient pulses during the incremented time of a multi-dimensional NMR experiment has profound effects on the lineshapes in the resulting spectrum . To illustrate this we will discuss the simple COSY experiment and restrict ourselves to a single spin with offset Ω. The principles remain the same for more complex experiments.

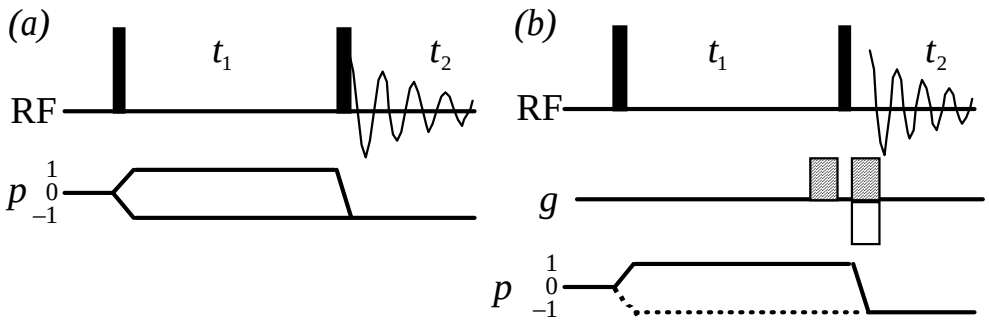

Figure 19. Pulse sequences for COSY, with and without gradient selection.

Figure 19 (a) shows the basic COSY pulse sequence; a simple analysis of this sequence for a one line spectrum gives the observed signal $S_c(t_1,t_2)$ as

$$S_c(t_1,t_2) = \cos\Omega t_1 \exp(-t_1/T_2)\exp(i\Omega t_2)\exp(-t_2/T_2) \qquad [24]$$

where T_2 is the (assumed) transverse relaxation time of the spin and quadrature detection in t_2 is also assumed. The crucial feature of this signal is that it is cosine modulated in t_1 and since $\cos(\Omega t_1) = \cos(-\Omega t_1)$, the modulation of the signal in t_1 is invariant to the sign of the offset, Ω. As a result the spectrum is said to lack *frequency discrimination* in the F_1 dimension. Since the receiver reference is normally placed in the middle of the spectrum, resonances will have both positive and negative offsets, but these are not distinguished in the F_1 dimension leading to a confused and overlapped spectrum.

All methods of achieving frequency discrimination are based on recording a separate signal, S_s, which is sine modulated in t_1. In the COSY experiment this signal is achieved simply by changing the phase of the first pulse by 90°, giving

$$S_s(t_1,t_2) = \sin\Omega t_1 \exp(-t_1/T_2)\exp(i\Omega t_2)\exp(-t_2/T_2) \quad . \qquad [25]$$

The way in which S_c and S_s are used to generate a frequency discriminated spectrum is as follows. The real and imaginary parts of the Fourier transform of this exponentially damped signal are lines with the absorption and dispersion lorentzian lineshapes, denoted $A(\omega)$ and $D(\omega)$ respectively

$$F\left[\exp(\pm i\Omega t_2)\exp(-t_2/T_2)\right] = A_\pm(\omega) + iD_\pm(\omega) \qquad [26]$$

$$\text{where} \quad A_\pm(\omega) = \frac{T_2}{1+(\omega \mp \Omega)^2 T_2^2} \quad , \quad D_\pm(\omega) = \frac{(\omega \mp \Omega)T_2^2}{1+(\omega \mp \Omega)^2 T_2^2} \quad , \qquad [27]$$

and $F[S(t)]$ denotes the Fourier transform of $S(t)$. Thus the transforms with respect to t_2 of S_c and S_s are

$$S_c(t_1,\omega_2) = F_2\left[S_c(t_1,t_2)\right] = \cos\Omega t_1 \exp(-t_1/T_2)\left\{A_+(\omega_2) + iD_+(\omega_2)\right\} \quad [28]$$

$$S_s(t_1,\omega_2) = F_2\left[S_s(t_1,t_2)\right] = \sin\Omega t_1 \exp(-t_1/T_2)\left\{A_+(\omega_2) + iD_+(\omega_2)\right\} \quad .[29]$$

The real part of $S_c(t_1,\omega_2)$ is combined with i times the real part of $S_s(t_1,\omega_2)$ to yield the signal $S(t_1,\omega_2)$ whose transform is the required spectrum

$$\begin{aligned} S(t_1,\omega_2) &= \mathrm{Re}\left[S_c(t_1,\omega_2)\right] + i\,\mathrm{Re}\left[S_s(t_1,\omega_2)\right] \\ &= \exp(i\Omega t_1)\exp(-t_1/T_2)A_+(\omega_2) \end{aligned} \quad [30]$$

$$S(\omega_1,\omega_2) = F_1\left[S(t_1,\omega_2)\right] = \left\{A_+(\omega_1) + iD_+(\omega_1)\right\}A_+(\omega_2) \quad . \quad [31]$$

The real part of $S(\omega_1,\omega_2)$ is a spectrum with the favourable double absorption lineshape, $A_+(\omega_1)A_+(\omega_2)$. In addition, inspection of Eqn. [30] shows that the spectrum is frequency discriminated as the modulation in t_1 is sensitive to the sign of Ω. This process of forming an absorption mode, frequency discriminated spectrum is just that due to States, Haberkorn and Ruben (SHR). A closely related process, knows as the Marion-Wüthrich or TPPI method, achieves the same result by incrementing the phase of the first pulse by 90° each time that t_1 is incremented. It can be shown that provided the increment of t_1 is half that in the SHR method, an identical frequency discriminated double absorption spectrum results.

There are two possible ways, shown in Fig. 19 (b), of using gradients in the COSY sequence. Either coherence level + 1 is selected during t_1, leading to the echo or *N*-type spectrum, or level – 1 is selected leading to the anti-echo or *P*-type spectrum. As has been pointed out, it is not possible to select simultaneously both of these pathways. The time domain signals for the *P*- and *N*-type pathways are

$$S_P(t_1,t_2) = \tfrac{1}{2}\exp(i\Omega t_1)\exp(-t_1/T_2)\exp(i\Omega t_2)\exp(-t_2/T_2) \quad [32]$$

$$S_N(t_1,t_2) = \tfrac{1}{2}\exp(-i\Omega t_1)\exp(-t_1/T_2)\exp(i\Omega t_2)\exp(-t_2/T_2) \quad [33]$$

In each case the resulting spectrum is expected to be frequency discriminated due to the complex exponential modulation in t_1; the factor of

one half arises because the magnetization generated at the start of t_1 is an equal mixture of coherence orders + 1 and – 1, only one of which is refocused by the final field gradient. The use of gradient pulses has resulted in frequency discrimination without any further data processing or without the need to acquire further data sets with phase shifted pulses. This is a consequence of selecting just one coherence level during t_1. Double Fourier transformation of S_P and S_N gives the spectra

$$\begin{aligned} S_P(\omega_1,\omega_2) = \tfrac{1}{2}\left\{A_+(\omega_1)A_+(\omega_2) - D_+(\omega_1)D_+(\omega_2)\right\} \\ + \tfrac{i}{2}\left\{A_+(\omega_1)D_+(\omega_2) + D_+(\omega_1)A_+(\omega_2)\right\} \end{aligned} \quad [34]$$

$$\begin{aligned} S_N(\omega_1,\omega_2) = \tfrac{1}{2}\left\{A_-(\omega_1)A_+(\omega_2) - D_-(\omega_1)D_+(\omega_2)\right\} \\ + \tfrac{i}{2}\left\{A_-(\omega_1)D_+(\omega_2) + D_-(\omega_1)A_+(\omega_2)\right\} \end{aligned} \quad [35]$$

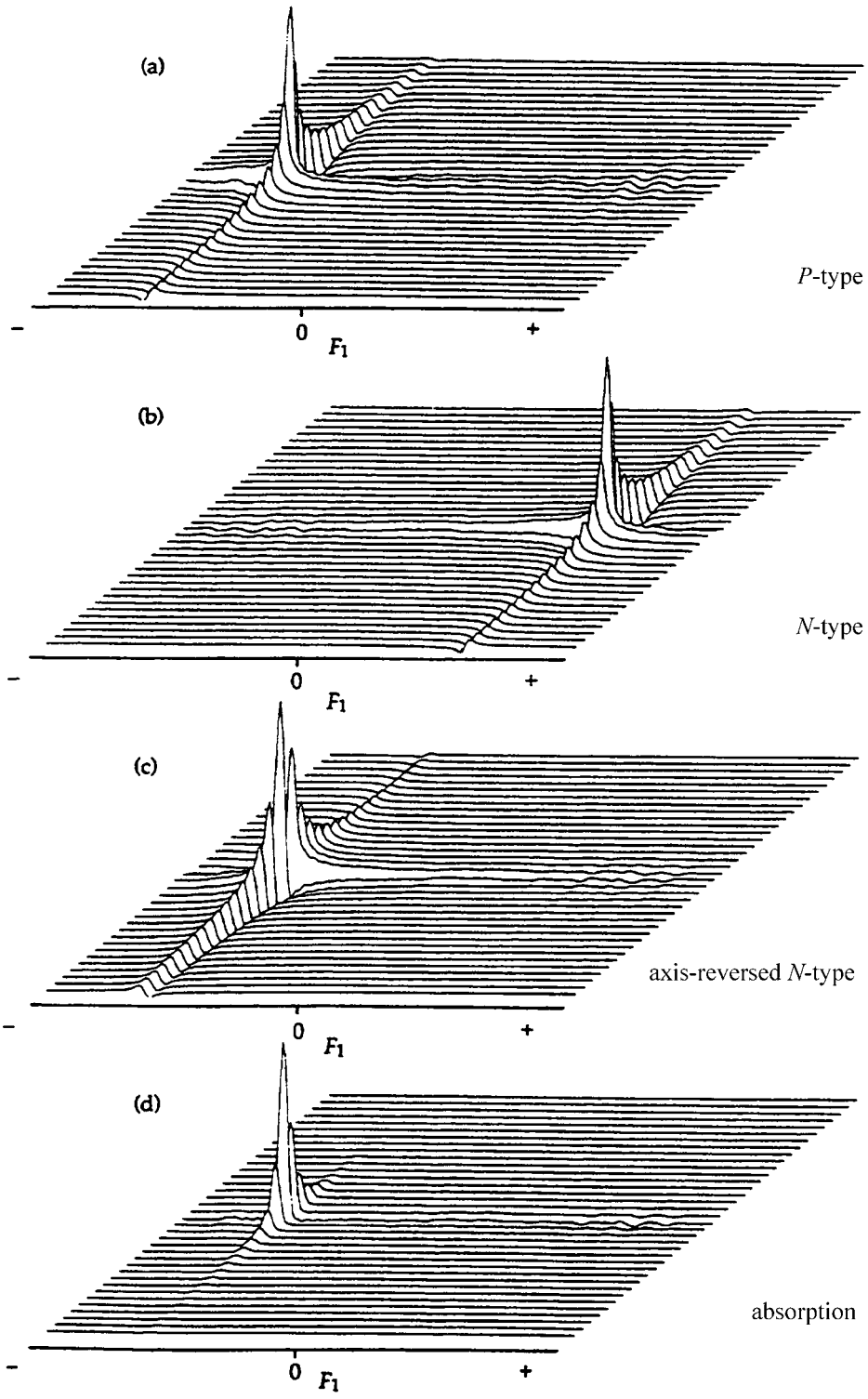

Figure 20 Experimental spectra showing how *P*-type and an axis-reversed *N*-type spectrum, each of which has the phase-twist lineshape, can be added together to give an absorption mode spectrum.

In each case the real part of the spectrum has the phase-twist lineshape, $\left\{A_{\pm}(\omega_1)A_{+}(\omega_2) - D_{\pm}(\omega_1)D_{+}(\omega_2)\right\}$, which is an inextricable mixture of absorption and dispersion. This lineshape is very undesirable in high

resolution NMR both because it is broad and because it has positive and negative parts. Unless further steps are taken, applying a gradient during t_1 will always result in a phase-twist lineshape.

When gradients have been applied during t_1 an absorption mode spectrum can be recovered by repeating the experiment twice, once to give the *P*-type and once to give the *N*-type spectrum. Figure 20 shows typical *P*- and *N*-type spectra recorded using gradient pulse selection. If the F_1 axis of the *N*-type spectrum is reversed the result is identical to the *P*-type spectrum except that the dispersive part of the phase twist is in the opposite sense. Adding the axis-reversed *N*-type and *P*-type spectra together cancels the dispersive parts of the phase twist, leaving a peak with a double absorption lineshape.

This process is conveniently carried out in the following way. The data from the *P*- and *N*-type spectra are transformed with respect to t_2 to give

$$S_P(t_1,\omega_2) = \frac{1}{2}\exp(i\Omega t_1)\exp(-t_1/T_2)\left\{A_+(\omega_2) + iD_+(\omega_2)\right\} \qquad [36]$$

$$S_N(t_1,\omega_2) = \frac{1}{2}\exp(-i\Omega t_1)\exp(-t_1/T_2)\left\{A_+(\omega_2) + iD_+(\omega_2)\right\} \qquad [37]$$

These are combined to give the new signal $S^+(t_1,\omega_2)$ according to

$$\begin{aligned} S^+(t_1,\omega_2) &= S_P(t_1,\omega_2) + S_N(t_1,\omega)^* \\ &= \exp(i\Omega t_1)\exp(-t_1/T_2)A_+(\omega_2) \end{aligned} \qquad [38]$$

Taking the complex conjugate of the time domain signal is equivalent to reversing the corresponding frequency axis in the frequency domain. Finally, Fourier transformation with respect to t_1 yields, in the real part, the required double absorption lineshape

$$S^+(\omega_1,\omega_2) = \left\{A_+(\omega_1) + iD_+(\omega_1)\right\}A_+(\omega_2) \quad . \qquad [39]$$

If the software available is not capable of the manipulations described above, the cosine and sine modulated data sets needed for conventional SHR type processing can be generated by manipulating the *P*- and *N*-type time domain data in the following way. The *P*- and *N*-type data sets are stored separately; adding them together produces a *cosine* modulated data set, whereas subtracting them from one another produces a *sine* modulated data set. These statements can be demonstrated by considering the sum and difference of the functions $S_P(t_1,t_2)$ and $S_N(t_1,t_2)$ (Eqns. [32] and [33] respectively) together with the well known identities $2\cos\theta = \exp(i\theta) + \exp(-i\theta)$ and $2i\sin\theta = \exp(i\theta) - \exp(-i\theta)$.

In the presence of significant inhomogeneous broadening *P*- and *N*-type spectra have different lineshapes. The most convenient way to understand

this is to imagine that the sample is divided into small compartments, in each of which the B_0 field is sufficiently homogeneous that the natural linewidth dominates. Each compartment contributes a phase-twist line to the spectrum, at a frequency determined by the precise value of the B_0 field in that compartment. These phase-twist lines from different compartments will overlap with one another and may cancel or reinforce, depending on how they are distributed. In the *N*-type spectrum the phase-twists lines are so arranged that they reinforce one another, giving, in the limit of a wide distribution of frequencies, a largely positive ridge-like lineshape. In contrast, in the *P*-type spectrum the phase-twists are aligned in such a way that they cancel one another. In the limit of a wide distribution, the cancellation is all but complete.

This strong asymmetry has led some to conclude that frequency discrimination methods based on combining *P*- and *N*-type spectra would be rendered ineffective by the presence of inhomogeneous broadening. However, this view is mistaken as the following argument reveals. Each compartment gives a *P*- and an *N*-type spectra with identical peak heights. Thus, when the spectra are combined, these individual phase-twists add together in precisely the way required, cancelling the dispersion contributions. The observed spectrum is the sum of these individual spectra, thus the dispersive contributions are removed from it as well.

4.3.4 Sensitivity

The use of gradients for coherence selection has consequences for the signal-to-noise ratio of the resulting spectrum when it is compared to a similar spectrum recorded using phase cycling. Most of the differences between the sensitivity of the gradient and phase cycled experiments come about because a gradient is only capable of selecting one coherence order at a particular point in the sequence. In contrast, it is often possible to select more than one coherence order when phase cycling is used (see section 4.3.2.2).

If a gradient is used to *suppress* all coherences other than $p = 0$, *i.e.* it is used simply to remove all coherences, leaving just *z*-magnetization or *zz* terms, there is no inherent loss of sensitivity when compared to a corresponding phase cycled experiment. If, however, the gradient is used to *select* a particular order of coherence the signal which is subsequently refocused will almost always be half the intensity of that which can be observed in a phase cycled experiment. This factor comes about simply because it is likely that the phase cycled experiment will be able to retain two symmetrical pathways, whereas the gradient selection method will only be able to refocuse one of these.

The foregoing discussion applies to the case of a selection gradient placed in a *fixed* delay of a pulse sequence. The matter is quite different if the gradient is placed within the incrementable time of a multi-dimensional experiment, *e.g.* in t_1 of a two-dimensional experiment. To understand the effect that such a gradient has on the sensitivity of the experiment it is necessary to be rather careful in making the comparison between the gradient selected and phase cycled experiments. In the case of the latter experiments we need to include the SHR or TPPI method in order to achieve frequency discrimination with absorption mode lineshapes. If a gradient is

used in t_1 we will need to record separate *P*- and *N*-type spectra so that they can be recombined to give an absorption mode spectrum. We must also ensure that the two spectra we are comparing have the same limiting resolution in the t_1 dimension, that is they achieve the same maximum value of t_1 and, of course, the total experiment time must be the same. The detailed argument which is needed to analyse this problem is beyond the scope of this lecture; it is given in detail in *J. Magn. Reson Ser. A*, **111**, 70-76 (1994) (NB There is an error in this paper: in Fig. 1 (b) the penultimate *S* spin 90° pulse should be phase *y* and the final *S* spin 90° pulse is not required). The conclusion is that the signal-to-noise ratio of an absorption mode spectrum generated by recombining *P*- and *N*-type gradient selected spectra is lower, by $1/\sqrt{2}$, than the corresponding phase cycled spectrum with SHR or TPPI data processing.

The potential reduction in sensitivity which results from selection with gradients may be more than compensated for by an improvement in the *quality* of the spectra obtained in this way. Often, the factor which limits whether or not a cross peak can be seen is not the *thermal* noise level by the presence of other kinds of "noise" associated with imperfect calcellation *etc*.

4.3.5 Diffusion

The process of refocusing a coherence which has been dephased by a gradient pulse is inhibited if the spins move either during or between the defocusing and refocusing gradients. Such movement alters the magnetic field experienced by the spins so that the phase acquired during the refocusing gradient is not exactly opposite to that acquired during the defocusing gradient.

In liquids there is a translational diffusion of both solute and solvent which causes such movement at a rate which is fast enough to cause significant effects on NMR experiments using gradient pulses. As diffusion is a random process we expect to see a smooth attenuation of the intensity of the refocused signal as the diffusion contribution increases. These effects have been known and exploited to measure diffusion constants since the very earliest days of NMR.

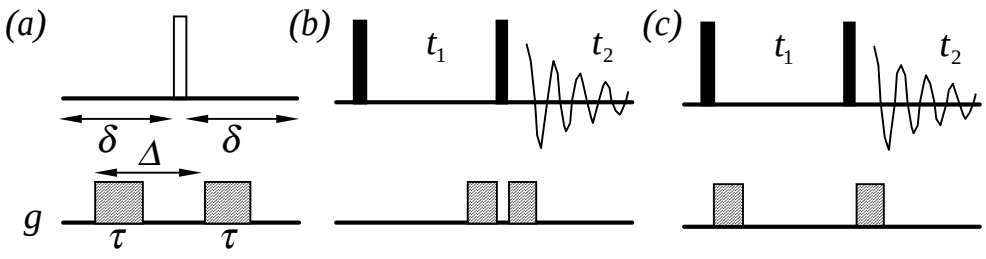

Figure 21. (a) A spin echo sequence used to measure diffusion rates (see text); (b) and (c) are alternative ways of implementing gradients into a COSY spectrum.

An analysis of the simple spin echo sequence, shown in Fig. 21 (a), illustrates very well the way in which diffusion affects refocusing. Note that the two gradient pulses can be placed anywhere in the intervals τ either side of the 180° pulse. For a single uncoupled resonance, the intensity of the

observed signal, S, expressed as a fraction of the signal intensity in the absence of a gradient, S_0 is given by

$$\frac{S}{S_0} = \exp\left(-\gamma^2 G^2 \tau^2 \left(\Delta - \frac{\tau}{3} \right) D \right) \qquad [40]$$

where D is the diffusion constant, Δ is the time between the start of the two gradient pulses and τ is the duration of the gradient pulses; relaxation has been ignored. For a given pair of gradient pulses it is diffusion during the interval between the two pulses, Δ, which determines the attenuation of the echo. The gradients are used to label the magnetization with a spatially dependent phase, and then to refocus it. The stronger the gradient the more rapidly the phase varies across the sample and thus the more rapidly the echo will be attenuated. This is the physical interpretation of the term $\gamma^2 G^2 \tau^2$ in Eqn. [40].

Diffusion constants generally decrease as the molecular mass increases. A small molecule, such as water, will diffuse up to twenty times faster than a protein with molecular weight 20,000. Table 1 shows the loss in intensity due to diffusion for typical gradient pulse pair of 2 ms duration and of strength 10 G·cm^{-1} for a small, medium and large sized molecule; data is given for Δ = 2 ms and Δ = 100 ms. It is seen that even for the most rapidly diffusing molecules the loss of intensity is rather small for Δ = 2 ms, but becomes significant for longer delays. For large molecules, the effect is small in all cases.

Table I : Fraction of Transverse Magnetization Refocused After a Spin Echo with Gradient Refocusing[a]

Δ/ms[b]	small molecule[c]	medium sized molecule[d]	macro molecule[e]
2	0.99	1.00	1.00
100	0.55	0.88	0.97

[a] Calculated for the pulse sequence of Fig. 21 (a) for two gradients of strength

10 G·cm^{-1} and duration, τ, 2 ms; relaxation is ignored.

[b] As defined in Fig. 21 (a).

[c] Diffusion constant, D, taken as that for water, which is 2.1×10^{-9} m^2 s^{-1} at ambient temperatures.

[d] Diffusion constant taken as 0.46×10^{-9} m^2 s^{-1}.

[e] Diffusion constant taken as 0.12×10^{-9} m^2 s^{-1}.

4.3.5.1 Minimisation of Diffusion Losses

The foregoing discussion makes it clear that in order to minimise intensity losses due to diffusion the product of the strength and durations of the gradient pulses, $G^2\tau^2$, should be kept as small as is consistent with achieving the required level of suppression. In addition, a gradient pulse pair should be separated by the shortest time within the limits imposed by the pulse sequence. This condition applies to gradient pairs the first of which is responsible for dephasing, and the second for rephasing. Once the coherence is rephased the time that elapses before further gradient pairs is irrelevant from the point of view of diffusion losses.

In two-dimensional NMR diffusion can lead to line broadening in the F_1 dimension if t_1 intervenes between a gradient pair. Consider the two alternative pulse sequences for recording a simple *N*-type COSY spectrum shown in Fig. 21 (b) and (c). In (b) the gradient pair are separated by the very short time of the final pulse, thus keeping the diffusion induced losses to an absolute minimum. In (c) the two gradients are separated by the incrementable time t_1; as this increases the losses due to diffusion will also increase resulting in an extra decay of the signal in t_1. The extra line broadening due to this decay can be estimated from Eqn. [40], with $\Delta = t_1$, as $\gamma^2G^2\tau^2D/\pi$ Hz. For a pair of 2 ms gradients of strength 10 G·cm^{-1} this amounts ≈ 2 Hz in the case of a small molecule.

This effect by which diffusion causes an extra line broadening in the F_1 dimension is usually described as *diffusion weighting*. Generally it is possible to avoid this effect by careful placing of the gradients. For example, the sequences in Fig. 21 (b) and (c) are in every other respect equivalent, thus there is no reason *not* to chose (b). It should be emphasised that diffusion weighting occurs only when t_1 intervenes between the dephasing and refocusing gradients.

4.3.6 Some Examples of Experiments Using Gradients

4.3.6.1 General Remarks

Reference has already been made to the two general advantages of using gradient pulses for coherence selection, namely the possibility of a general improvement in the quality of spectra and the removal of the requirement of completing a phase cycle for each increment of a multi-dimensional experiment. In the case of recording spectra of proteins and similar molecules a number of particular advantages can be expected. The first of these relates to heteronuclear correlation experiments which form the heart of many two- and higher-dimensional experiments. In such experiments there is a need to suppress both the water resonance and the signals due to protons not coupled to a heteronucleus (nitrogen-15 or carbon-13, typically); selection with gradients will give improve greatly the suppression of both these types of signals. Finally, we note that the dynamic range of the free induction decay recorded after gradient selection will be much lower than in an equivalent phase cycled experiment, allowing best use to be made of the resolution of the digitiser.

As has been discussed above, special care needs to be taken in

experiments which use gradient selection if absorption mode spectra are to be obtained. For demanding applications where spectral resolution and sensitivity is at a premium, it is vital to record absorption mode spectra. This is especially the case in the indirectly detected domains of two- and higher-dimensional spectra.

In the following sections the use of gradient selection in several different experiments will be described. The gradient pulses used in these sequences will be denoted G_1, G_2 *etc.* where G_i implies a gradient of duration τ_i, strength $B_{g,i}$ and shape factor s_i. There is always the choice of altering the duration, strength or, conceivably, shape factor in order to establish refocusing. Thus, for brevity we shall from now on write the spatially dependent phase produced by gradient G_i acting on coherence of order p as pG_i in the homonuclear or $\sum_j \gamma_j p_j G_i$ in the heteronuclear case.

4.3.6.2 Double Quantum Filtered COSY

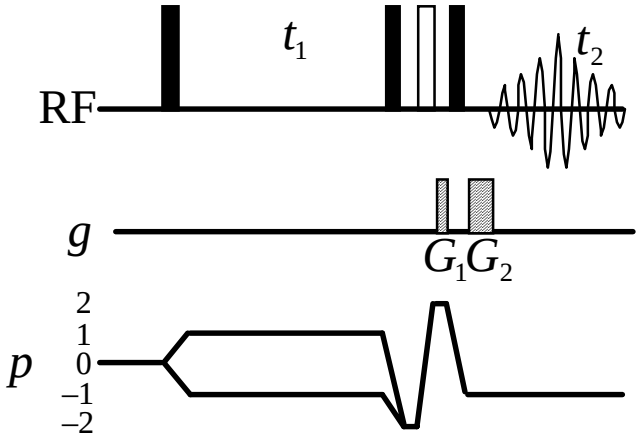

Figure 22. Pulse sequence for recording absorption mode DQF COSY spectra.

The sequence of Fig. 22 is suitable for recording absorption mode DQF COSY spectrum. Here, no gradient is applied during t_1, thus retaining symmetrical pathways and the phase errors which accumulate during the double quantum period are refocused by an extra 180° pulse; the refocusing condition is $G_2 = 2\ G_1$. Frequency discrimination in the F_1 dimension is achieved by the SHR or TPPI procedures. Multiple quantum filters through higher orders can be implemented in the same manner.

In this experiment data acquisition is started *immediately* after the final radiofrequency pulse so as to avoid phase errors which would accumulate during the second gradient pulse. Of course, the signal only rephases towards the end of the final gradient, so there is little signal to be observed. However, the crucial point is that, as the magnetization is all in antiphase at the start of t_2, the signal grows from zero at a rate determined by the size the couplings on the spectrum. Provided that the gradient pulse is much shorter that $1/J$, where J is a typical proton-proton coupling constant, the part of the signal missed during the gradient pulse is not significant and the spectrum is not perturbed. Acquiring the data in this way avoids the need for an extra

180° pulse to refocus the phase errors that would accumulate during the second gradient. If it is more convenient, an alternative procedure is to start to acquire the data *after* the final gradient, and then to right shift the free induction decay, bringing in zeroes from the left, by a time equal to the duration of the gradient.

4.3.6.3 Two-Dimensional HMQC

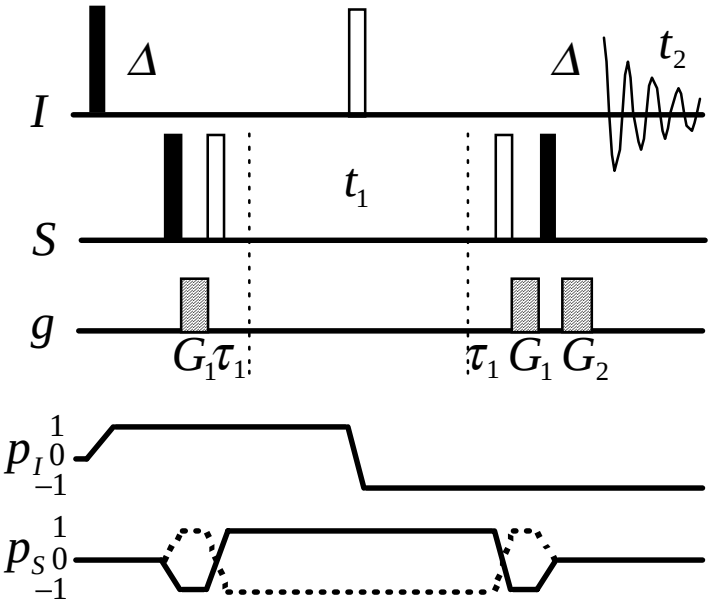

Figure 23. Pulse sequence for recording absorption mode HMQC spectra. The CTP for the *N*-type spectrum is shown as a solid line and that for the *P*-type spectrum is shown dashed.

There are several ways of implementing gradient selection into the HMQC experiment, one of which, which leads to absorption mode spectra, is shown in Fig. 23. The centrally placed *I* spin 180° pulse results in no net dephasing of the *I* spin part of the heteronuclear multiple quantum coherence by the two gradients G_1 *i.e.* the dephasing of the *I* spin coherence caused by the first is undone by the second. However, the *S* spin coherence experiences a net dephasing due to these two gradients and this coherence is subsequently refocused by G_2. Two 180° *S* spin pulses together with the delays τ_1 refocus shift evolution during the two gradients G_1. The centrally placed 180° *I* spin pulse refocuses chemical shift evolution of the *I* spins during the delays Δ and all of the gradient pulses (the last gradient is contained within the final delay, Δ). The refocusing condition is

$$\mp 2\gamma_s G_1 - \gamma_I G_2 = 0 \qquad [41]$$

where the + and – signs refer to the *P*- and *N*-type spectra respectively. The switch between recording these two types of spectra is made simply by reversing the sense of G_2. The *P*- and *N*-type spectra are recorded separately and then combined in the manner described in section 4.3.3 to give a frequency discriminated absorption mode spectrum.

In the case that *I* and *S* are proton and carbon-13 respectively, the gradients G_1 and G_2 are in the ratio 2 : ± 1. Proton magnetization not involved in heteronuclear multiple quantum coherence, *i.e.* magnetization from protons not coupled to carbon-13, is refocused after the second gradient G_1 but is then dephased by the final gradient G_2. Provided that the

gradient is strong enough these unwanted signals, and the t_1-noise associated with them, will be suppressed.

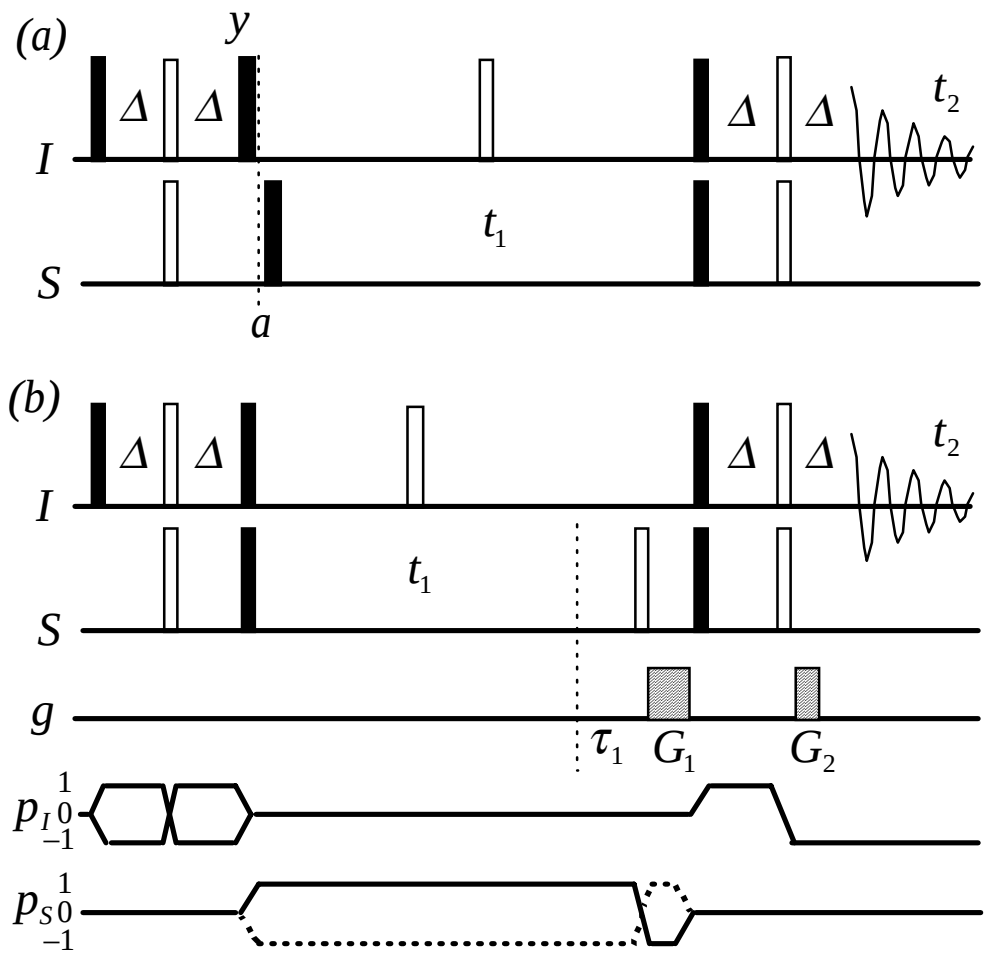

Figure 24. Pulse sequences for recording absorption mode HSQC spectra: (a) is the usual sequence, see text for a description of the significance of point *a*; (b) gives *P*- or *N*-type spectra which can be recombined to give an absorption mode spectrum.

The basic pulse sequence for the HSQC experiment is shown in Fig. 24 (a). For a coupled two spin system the transfer can be described as proceeding via the spin ordered state $2I_zS_z$ which exists at point *a* in the sequence. In the absence of significant relaxation magnetization from uncoupled *I* spins is present at this point as I_y. Thus, a field gradient applied at point *a* will dephase the unwanted magnetization and leave the wanted term unaffected. The main practical difficulty with this approach is that the uncoupled magnetization is only along *y* at point *a* provided all of the pulses are perfect; if the pulses are imperfect there will be some *z* magnetization present which will not be eliminated by the gradient. In the case of observing proton - carbon-13 or proton - nitrogen-15 HSQC spectra from natural abundance samples, the magnetization from uncoupled protons is very much larger than the wanted magnetization, so even very small imperfections in the pulses can give rise to unacceptably large residual signals. However, for globally labelled samples the degree of suppression has been shown to be sufficient, especially if some minimal phase cycling or other procedures are used in addition. Indeed, such an approach has been

used successfully as part of a number of three- and four-dimensional experiments applied to globally carbon-13 and nitrogen-15 labelled proteins (*vide infra*).

The key to obtaining the best suppression of the uncoupled magnetization is to apply a gradient when transverse magnetization is present on the *S* spin. An example of the HSQC experiment utilising such a principle is given in Fig. 24 (b). Here, G_1 dephases the *S* spin magnetization present at the end of t_1, and after transfer to the *I* spins, refocusing is effected by G_2. An extra 180° pulse to *S* in conjunction with the extra delay τ_1 ensures that phase errors which accumulate during G_1 are refocused; G_2 is contained within an existing spin echo. The refocusing condition is

$$\mp \gamma_S G_1 - \gamma_I G_2 = 0 \qquad [42]$$

where the – and + signs refer to the *N*- and *P*-type spectra respectively. As before, an absorption mode spectrum is obtained by combining the *N*- and *P*-type spectra, which can be selected simply by reversing the sense of G_2.

The basic HMQC and HSQC sequences can be extended to give two- and three-dimensional experiments such as HMQC-NOESY and HMQC-TOCSY. The HSQC experiment is often used as a basic element in other two-dimensional experiments. For example, in proteins the proton - nitrogen-15 NOE is usually measured by recording a two-dimensional spectrum using a pulse sequence in which native nitrogen-15 magnetization is transferred to proton for observation. The difference between two such spectra recorded with and without pre-saturation of the entire proton spectrum reveals the NOE. Suppression of the water resonance in the control spectrum causes considerable difficulties, which are conveniently overcome by use of gradient pulses for selection.

4.3.6.5 Sensitivity Enhanced HSQC

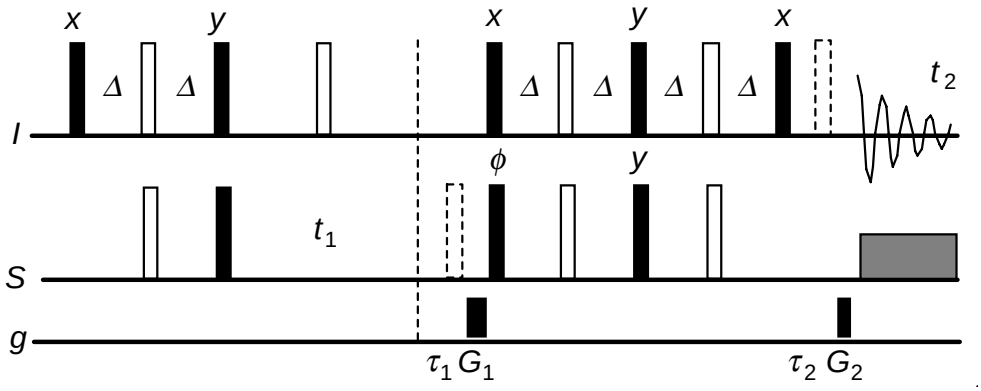

Figure 25. Pulse sequence for recoording sensitivity-enhanced HSQC spectra. In its original form the sequence is used without the gradients, the delays τ_1 and τ_2 and the 180° pulses shown dashed. In the Kay modification these optional elements are included; see text for discussion. The phase ϕ is $\pm x$.

The pulse sequence of Fig 25. is a modification of the basic HSQC

sequence which, when compared to that sequence, gives a signal-to-noise ratio which is higher by a factor of $\sqrt{2}$. The sequence achieves this by transferring to the I spins both the x and the y components of the S spin magnetization present at the end of t_1. The conventional HSQC experiment only transfers *one* of these components and so results in a weaker signal overall.

The way in which this sequence works can be determined by a quick analysis using product operators; we shall assume that the delay Δ is set to $1/(4J)$. At the end of t_1 the x component of the magnetization, $2I_zS_x$, is transferred by the first pair of 90° pulses to heteronuclear multiple quantum, $2I_yS_x$. The subsequent spin echo refocuses this term and then the next pair of 90° pulses transfers the coherence to anti-phase on the I spins: $2I_yS_z$. This anti-phase term evolves into in-phase along x, I_x, during the final spin echo. The final pulse has no effect on this state. Thus the x component is transferred from S to I.

At the end of t_1 the y component of the magnetization, $2I_zS_y$, is transferred by the first pair of 90° pulses to the anti-phase state, $2I_yS_z$. This re-phases during the subsequent spin echo to the in-phase state I_x. The next 90° pulse to I rotates this to I_z where it remains for the rest of the sequence until the final I spin 90° pulse which turns it to the observable, I_y. Note that the x-component is transferred to I_x and the y-component to I_y *i.e.* there is a 90° phase shift in the observed signal.

If one component (for example the x-component) present at the end of t_1 is transferred the resulting modulation in t_1 is one of amplitude, for example varying as $\cos(\Omega_S t_1)$. The perpendicular component (y) will also be amplitude modulated, but as it is 90° out of phase with the x-component the modulation is of the form $\sin(\Omega_S t_1)$. In the sensitivity-enhanced experiment both of these components are transferred, and what is more the transferred signals appear along perpendicular axes. The overall result of this is that the observed signal is *phase modulated* with respect to t_1. Formally the observed signal varies as $\cos(\Omega_S t_1) + \mathrm{i}\sin(\Omega_S t_1) = \exp(\mathrm{i}\Omega_S t_1)$, where the complex i in the combination accounts for the phase shift between the two observed signals.

The first S spin 90° pulse after t_1 does not affect the x component of the magnetization, but does affect the y-component. If the phase of this pulse is altered from x to $-x$, therefore, the sign of the transferred y-component will be altered whereas the transferred x-component is unaffected. Thus, by changing the phase of this pulse the observed modulation can be altered to $\cos(\Omega_S t_1) - \mathrm{i}\sin(\Omega_S t_1) = \exp(-\mathrm{i}\Omega_S t_1)$.

In effect the experiment allows us to record phase modulated data and to choose if the phase modulation is of the form that will lead to a P-type spectrum or an N-type spectrum. These two spectra can be combined together in precisely the manner described in section 4.3.3 to give an absorption mode spectrum; this is essentially the data processing proposed for this sensitivity-enhanced experiment.

If we consider the coherence transfer pathway brought about by this sensitivity-enhanced sequence we conclude that, as the data is phase modulated, a single coherence order must have been selected in during t_1. If the phase of the S spin pulse is chose such that P-type data is obtained then we conclude that the coherence order selected in t_1 is -1 whereas if N-type

data is obtained the coherence order selected is +1. We could add gradient pulses to select either of these two pathways; suitable modifications are shown in the sequence shown in Fig. 25. The relative sense of the two gradients will determine which of the *P*- or *N*-type modulation is selected.

The key point is, then, that as the *original* experiment selects inherently just one out of the two pathways the addition of gradient selection, which can only select one pathway at a time, will not result in any loss of signal. Thus, the sensitivity-enhanced experiment with gradient selection gives, in theory, identical signal-to-noise ratio as obtained without gradients. This is a rather unusual as, as we have seen, coherence selection with gradients usually leads to a loss in signal.

The detailed argument concerning the sensitivity of these experiments can be found elsewhere (see section 4.3.4 and reference quoted there). In summary we conclude that the sensitivity-enhanced experiment, with or without gradients, has a signal-to-noise ratio which is greater by a factor of $\sqrt{2}$ than that of the equivalent phase cycled experiment. Compared to a gradient experiment in which separate *P*- and *N*-type spectra are recorded the signal-to-noise ratio is enhanced by a factor of 2.

The sequence of pulses used to transfer both the components of magnetization can be added to many heteronuclear experiments, thus giving the benefits of both improved sensitivity and, if required, gradient selection. The resulting sequences are, however, considerably longer than the originals so there is the possibility that the potential sensitivity gain will be reduced as a consequence of losing signal due to relaxation.

4.3.6.6 Three-Dimensional HN(CO)CA

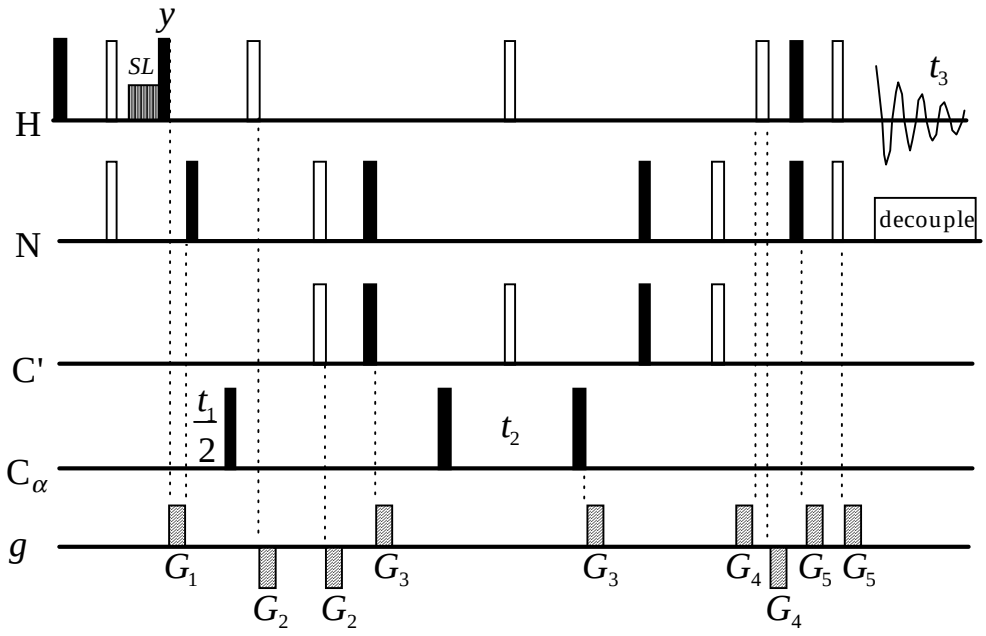

Figure 26. An HN(CO)CA experiment with gradients.

Figure 26 shows a pulse sequence used by Bax and Pochapsky to record constant time three-dimensional HN(CO)CA spectra of globally labelled

proteins.[63] In this sequence, gradients are used in several different roles. The gradient G_1 is used to dephase magnetization from protons not coupled to nitrogen-15, as was described above in connection with the HSQC experiment (section 4.3.6.4 and Fig. 24 (a)). As was described above, this kind of gradient selection fails in the presence of pulse imperfections. However, in this case the use of a period of spin locking prior to the second proton 90° pulse, combined with the fact that the sample is globally labelled in both nitrogen-15 and carbon-13, results in a degree of suppression that is more than adequate. The two gradients G_2 combine to select only that magnetization which has been refocused by the second 180° nitrogen pulse. Likewise the two gradients G_3 select magnetization which is correctly refocused by the 180° pulse to the carbonyl carbons placed in the centre of t_2. In addition, these gradients dephase any nitrogen magnetization present. The two gradients G_4 serve to eliminate any magnetization which is created by the second to last proton 180° pulse, and the final pair of gradients G_5, like G_2 and G_3, select the proton magnetization which is correctly refocused by the final proton 180° pulse. These uses of gradient pulses in conjunction with different types of spin echoes have been described in the section above. The polarity of the various gradient pulses is chosen so as to maximise the dephasing of uncoupled proton magnetization, and hence give the best suppression.

The most important feature of this pulse sequence is that the gradients are applied either when the required magnetization is along *z* or as part of refocusing schemes using 180° pulses. Thus, in contrast with all of the experiments described in this section, there is *no loss of signal* associated with the use of gradients. In addition, as no gradients are associated with the evolution times, absorption mode spectra are obtained without further manipulation of the data.

4.3.6.7 Four-Dimensional HCANNH

Boucher *et al.* have described a four-dimensional HCANNH experiment, used for recording spectra of globally nitrogen-15, carbon-13 labelled proteins, which combines gradient selection with limited phase cycling. The sequence is shown in Fig. 27. A single pair of gradients is used to select the final nitrogen to proton transfer step and a two step phase cycle of the first 90° pulse to C_α is used to select the transfer from C_α to N. A period of spin locking of the proton signal just prior to the first transfer to C_α is used to improve the water suppression. The $^{13}C_\alpha$ and ^{15}N shifts are monitored during constant time periods, and the gradient G_1 is included in the second of these. As has been described above, placing a gradient in a constant time period does not give rise to any extra phase errors due to the evolution of offsets during the gradient. The refocusing gradient G_2 is placed within an existing spin echo. The refocusing condition is

$$\pm \gamma_N G_1 - \gamma_H G_2 = 0\,, \qquad [43]$$

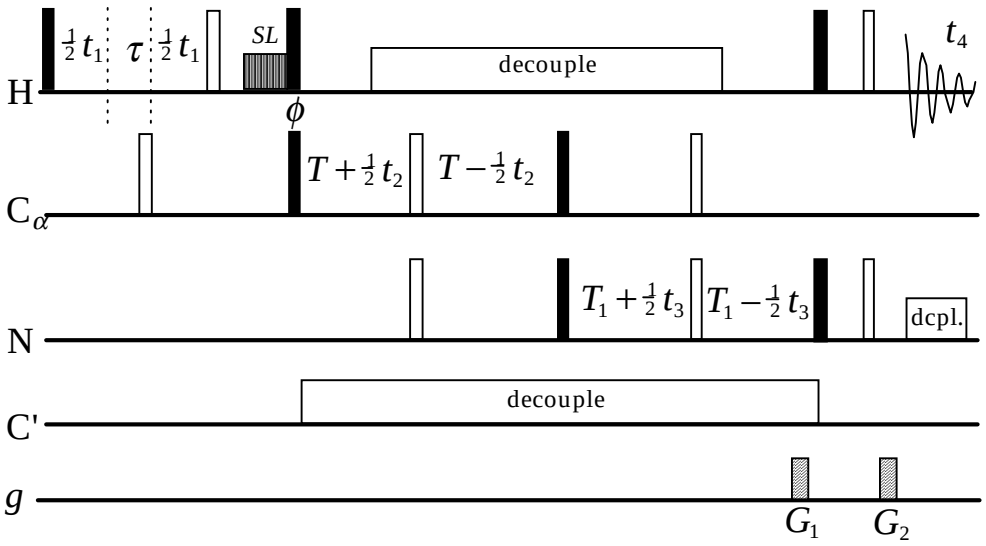

Figure 27. The HCANNH experiment with one step of gradient selection.

where γN and γH are the gyromagnetic ratios of nitrogen-15 and proton respectively; the change between *P*- and *N*-type data is made simply by reversing the sense of one of the gradients. Absorption mode spectra in the F_1 and F_2 domains are obtained using the SHR-TPPI method. Separate *P*- and *N*-type data sets are recorded and then combined in the manner described above so as to give absorption mode lineshapes in F_3. The experiment thus shows a signal-to-noise ratio which is $\sqrt{2}$ poorer than an equivalent phase cycled experiment.

4.3.7 Zero-Quantum Dephasing and Purge Pulses

Both *z*-magnetization and homonuclear zero-quantum coherence have coherence order 0, and thus neither are dephased by the application of a gradient pulse. Selection of coherence order zero is achieved simply by applying a gradient pulse which is long enough to dephase all other coherences; no refocusing is used. In the vast majority of experiments it is the *z*-magnetization which is required and the zero-quantum coherence that is selected at the same time is something of a nuisance.

A number of methods have been developed to suppress contributions to the spectrum from zero-quantum coherence. Most of these utilise the property that zero-quantum coherence evolves in time, whereas *z*-magnetization does not. Thus if several experiments in which the zero-quantum has been allowed to evolve for different times are co-added, cancellation of zero-quantum contributions to the spectrum will occur. Like phase cycling, such a method is time consuming and relies on a difference procedure; it is thus subject to the same criticisms as can be levelled at phase cycling. However, it has been shown that if a field gradient is combined with a period of spin-locking the coherences which give rise to these zero-quantum coherences can be dephased. Such a process is conveniently considered as a modified purging pulse.

4.3.7.1 Purging Pulses

A purging pulse consists of a relatively long period of spin-locking, taken here to be applied along the *x*-axis. Magnetization not aligned along *x* will precess about the spin-locking field and, because this field is inevitably inhomogeneous, such magnetization will dephase. The effect is thus to purge all magnetization except that aligned along *x*. However, in a coupled spin system certain anti-phase states aligned perpendicular to the spin-lock axis are also preserved. For a two spin system (with spins *k* and *l*), the operators preserved under spin-locking are I_{kx}, I_{lx} and the anti-phase state $2I_{ky}I_{lz} - 2I_{kz}I_{ly}$. Thus, in a coupled spin system, the purging effect of the spin-locking pulse is less than perfect.

The reason why these anti-phase terms are preserved can best be seen by transforming to a tilted co-ordinate system whose *z*-axis is aligned with the *effective* field seen by each spin. For the case of a strong B_1 field placed close to resonance the effective field seen by each spin is along *x*, and so the operators are transformed to the tilted frame simply by rotating them by –90° about *y*

$$I_{kx} \xrightarrow{-\pi/2 I_{ky}} I_{kz}^{\mathrm{T}} \qquad I_{lx} \xrightarrow{-\pi/2 I_{ly}} I_{lz}^{\mathrm{T}} \qquad [44]$$

$$2I_{ky}I_{lz} - 2I_{kz}I_{ly} \xrightarrow{-\pi/2(I_{ky}+I_{ly})} 2I_{ky}^{\mathrm{T}}I_{lx}^{\mathrm{T}} - 2I_{kx}^{\mathrm{T}}I_{ly}^{\mathrm{T}} \quad . \qquad [45]$$

Operators in the tilted frame are denoted with a superscript T. In this frame the *x*-magnetization has become *z*, and as this is parallel with the effective field, it clearly does not dephase. The anti-phase magnetization along *y* has become $2I_{ky}^{\mathrm{T}}I_{lx}^{\mathrm{T}} - 2I_{kx}^{\mathrm{T}}I_{ly}^{\mathrm{T}}$, which is recognised as *zero-quantum coherence in the tilted frame*. Like zero-quantum coherence in the normal frame, this coherence does not dephase in a strong spin-locking field. There is thus a connection between the inability of a field gradient to dephase zero-quantum coherence and the preservation of certain anti-phase terms during a purging pulse.

Zero-quantum coherence in the tilted frame evolves with time at a frequency, $\Omega_{\mathrm{ZQ}}^{\mathrm{T}}$, given by

$$\Omega_{\mathrm{ZQ}}^{\mathrm{T}} = \left| \sqrt{(\Omega_k^2 + \omega_1^2)} - \sqrt{(\Omega_l^2 + \omega_1^2)} \right| \qquad [46]$$

where Ω_i is the offset from the transmitter of spin *i* and ω_1 is the B_1 field strength. If a field gradient is applied during the spin-locking period the zero quantum frequency is modified to

$$\Omega_{\mathrm{ZQ}}^{\mathrm{T}}(r) = \left| \sqrt{(\Omega_k + \gamma B_{\mathrm{g}}(r) + \varpi_1)^2} - \sqrt{(\Omega_l + \gamma B_{\mathrm{g}}(r) + \varpi_1)^2} \right| \quad . \qquad [47]$$

This frequency can, under certain circumstances, become spatially dependent and thus the zero-quantum coherence in the tilted frame will dephase. This is in contrast to the case of zero-quantum coherence in the laboratory frame which is not dephased by a gradient pulse.

The principles of this dephasing procedure are discussed in detail elsewhere (*J. Magn. Reson. Ser. A* **105**, 167-183 (1993)). Here, we note the following features. (a) The optimum dephasing is obtained when the extra offset induced by the gradient at the edges of the sample, $\gamma B_g(r_{max})$, is of the order of ω_1. (b) The rate of dephasing is proportional to the zero-quantum frequency in the absence of a gradient, $\Omega_k - \Omega_l$. (c) The gradient must be switched on and off adiabatically. (d) The zero-quantum coherences may also be dephased using the inherent inhomogeneity of the radio-frequency field produced by typical NMR probes, but in such a case the optimum dephasing rate is obtained by spin locking off-resonance so that $\tan^{-1} \omega_1/\Omega_{k,l} \approx 54°$. (e) Dephasing in an inhomogeneous B_1 field can be accelerated by the use of special composite pulse sequences.

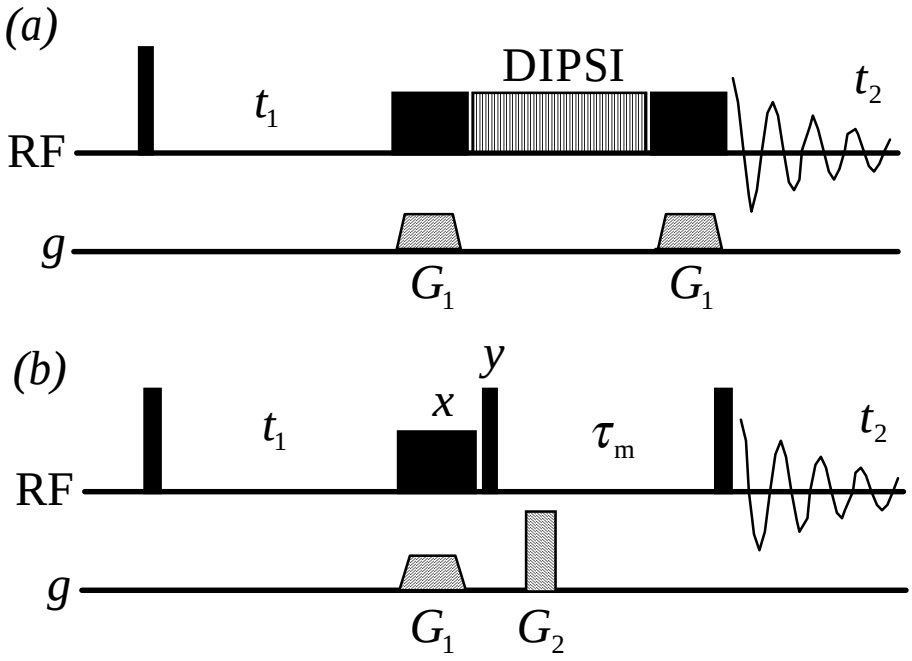

Figure 28 Pulse sequences employing zero-quantum dephasing by a combination of spin-locking and a B_0 gradient pulse: (a) for TOCSY and (b) for NOESY.

The combination of spin-locking with a gradient pulse allows the implementation of essentially perfect purging pulses. Such a pulse could be used in a two-dimensional TOCSY experiment whose pulse sequence is shown in Fig. 28 (a). The period of isotropic mixing transfers in-phase magnetization (say along *x*) between coupled spins, giving rise to cross-peaks which are absorptive and in-phase in both dimensions. However, the mixing sequence also both transfers and generates anti-phase magnetization along *y*, which gives rise to undesirable dispersive anti-phase contributions in the spectrum. In the sequence of Fig. 24 (a) these anti-phase contributions are eliminated by the use of a purging pulse as described here. Of course, at the same time all magnetization other than *x* is also eliminated, giving a near perfect TOCSY spectrum without the need for phase cycling or other difference measures.

These purging pulses can be used to generate pure *z*-magnetization without contamination from zero-quantum coherence by following them with a 90°(*y*) pulse, as is shown in the NOESY sequence in Fig. 28 (b). Zero-quantum coherences present during the mixing time of a NOESY experiment give rise to troublesome dispersive contributions in the spectra, which can be eliminated by the use of this sequence.

4.3.8 Conclusions

Pulsed-field gradients appear to offer a solution to many of the difficulties associated with phase cycling, in particular they promise higher quality spectra and the freedom to chose the experiment time solely on the basis of the required resolution and sensitivity are attractive features. However, these improvements are not unconditional. When gradient selection is used, attention has to be paid to their effect on sensitivity and lineshapes, and dealing with these issues usually results in a more complex pulse sequence. Indeed it seems that the potential loss in sensitivity when using gradient selection is the most serious drawback of such experiments. Nevertheless, in a significant number of cases the potential gains, seen in the broadest sense, seem to outweigh the losses.

4.4 Key References

Coherence Order, Coherence Transfer Pathways and Phase Cycling

G. Bodenhausen, H. Kogler and R. R. Ernst, *J. Magn. Reson.* **58**, 370 (1984).

A. D. Bain, *J. Magn. Reson.* **56**, 418 (1984).

R. R. Ernst, G. Bodenhausen and A. Wokaun, *Principles of Nuclear Magnetic Resonance in One and Two Dimensions* (Oxford University Press, Oxford, 1987).

J. Keeler, *Multinuclear Magnetic Resonance in Liquids and Solids - Chemical Applications* edited by P. Granger and R. K. Harris (Kluwer, Dordrecht, 1990)

Phase Sensitive Two-Dimensional NMR

J. Keeler and D. Neuhaus, *J. Magn. Reson.* **63**, 454-472 (1985).

D. J. States, R. A. Haberkorn and D. J. Ruben, *J. Magn. Reson.* **48**, 286 (1982).

D. Marion and K. Wüthrich, *Biochem. Biophys. Res. Commun.* **113**, 967 (1983).

Sensitivity of Two-Dimensional NMR

M. H. Levitt, G. Bodenhausen and R. R. Ernst, *J. Magn. Reson.* **58**, 462 (1984).

Original Gradient Experiments

A. A. Maudsley, A. Wokaun and R. R. Ernst, *Chem. Phys. Lett.* **55**, 9-14 (1978).

R. E. Hurd, *J. Magn. Reson.* **87**, 422-428 (1990).

Review of Gradient Methods (September 1993)

J. Keeler in *Methods in Enzymology, Volume 239 part C*, edited by T. L. James and N. J. Oppenheimer. Academic Press, San Diego, 1994.

Sensitivity-Enhanced Methods

J. Cavanagh and M. Rance, *J. Magn. Reson.* **88**, 72-85 (1990).

A. G. Palmer III, J. Cavanagh, P. E. Wright and M. Rance, *J. Magn. Reson.* **93**, 151-170 (1991).

L. E. Kay, P. Keifer and T. Saarinen, *J. Am. Chem. Soc.* **114**, 10663-10665 (1992).